

Spectra of the ψ and T_c Systems
in a Consistent Quark Model with
Fine and Hyperfine Corrections

Nishith Mukerji

A Thesis
in
The Department
of
Physics

Presented in Partial Fulfillment of the Requirements
for the degree of Doctor of Philosophy at
Concordia University
Montréal, Québec, Canada

August 1984

© Nishith Mukerji, 1984

ABSTRACT

Spectra of the ψ and T Systems
in a Consistent Quark Model with
Fine and Hyperfine Corrections

Nishith Mukerji, Ph.D.
Concordia University, 1984

Masses of all mesons up to $n = 4$ in the ψ and T systems are calculated using a consistent quark phenomenological model which comprises a harmonic oscillator potential perturbed by an unknown anharmonic term, with fine and hyperfine corrections. The parameter set for the Upsilon sector is derived from that of the Charmonium sector so that, in effect, the same parameter set is being used for both systems. The results are in good agreement with available experimental values. Predictions are made for many states for which experimental values are yet to come.

DEDICATION

This thesis is dedicated to Dr. C.S. Kalman, my thesis supervisor, whose unfailing inspiration, guidance and assistance were always proffered with generosity and patience.

ACKNOWLEDGEMENT

I would like to thank the Physics Department, and particularly the Graduate Program Director, Dr. S.K. Misra for the continued support and advice I have received during the years of this research.

I would like to thank my two colleagues in research, Ian D'Souza and David Pfeffer, for the encouragement they extended to me whenever the going got rough and for their unstinted help whenever I required it.

v

TABLE OF CONTENTS

	Page
Introduction	1
Chapter I	
1.1 Positronium and Mesons	7
1.2 Significance of the J/ψ Meson	10
1.3 The Colour Postulate	12
1.4 Quark Confinement and QCD	16
Chapter II	
2.1 Confinement Potential	21
2.2 DGG Model	21
2.3 Success of DGG	26
2.4 The Isgur-Karl Model (I-K)	29
2.5 The Successes of the I-K Model	31
2.6 Inconsistencies in the I-K Model	39
Chapter III	
3.1 The Isgur-Karl Hamiltonian	41
3.2 The Anharmonic Potential U	42
3.3 The Consistent Quark Model	45

	Page
Chapter IV	
4.1 Baryons to Mesons	50
4.2 The Meson Hamiltonian	51
4.3 The Harmonic Oscillator Potential	53
4.4 The Anharmonic Potential (Mesons)	54
Chapter V	
5.1 The Spin Dependent Terms	61
5.2 Explicit Expressions for Hyperfine and Spin-Orbit Terms	63
Chapter VI	
6.1 Publications	74
6.2 Application of the Isgur-Karl Model to Mesons	74
6.3 ψ and T Systems in a Consistent Quark Model	77
6.4 Full Calculations for ψ and T Systems	78
6.5 Results	78
6.6 Discussion of Results	83
Conclusion	89
References and Footnotes	91
Appendices	94

LIST OF ILLUSTRATIONS

	Page
1. Comparison of the Energy Levels of Charmonium and Positronium	8
2. Comparison of the Charmonium Spectrum with Those of Other Potentials	13
3. Pair Production of Quark and Antiquark	20
4. Qualitative Picture of Potential as a Function of $q\bar{q}$ Separation	22
5. Comparison of Predicted and Observed Spectrum of Negative Parity Baryons	33
6. Harmonic Oscillators in a Strange Baryon	36
7. Forbidden Decay of $\Lambda^{5/2} \rightarrow \bar{K}N, \bar{K}^*N$	37
8. Pattern of Splitting of Low-Lying Supermultiplets by U Term Perturbation	44
9. Contact and Tensor Forces of Hyperfine Interaction	61
10. Quark and Antiquark Coupling in a Meson with Gluon Transfer	111
11. Inverse Propogator of Quark-Antiquark	113
12. Graphical Representation of B-S Scattering Amplitude in a Two-quark, Two-antiquark Scattering Process	114

LIST OF TABLES

	Page
1. Mass and Mixture Compositions of some Baryons with Comparisons to Independent Calculations of HLC and FP	35
2. Masses of the States of the ψ System, in GeV	86
3. Masses of the States of the T System in GeV	87

LIST OF APPENDICES

Appendix	Page
A. Sample Calculation of U Term Matrix Element	94
B. Sample Calculation of Contact Term Matrix Element	96
C. Sample Calculation of Tensor Term Matrix Element	97
D. Sample Calculation of Spin-Orbit Term Matrix Element	101
E. First Publication : "Application of the Isgur-Karl Model to the Low-Lying S States of Charmonium	103
F. Second Publication : ψ and T Systems in a Consistent Quark Model	105
G. Formulation of spin-related expressions.	110

INTRODUCTION

The search for the fundamental building blocks of nature has, at significant times, yielded even more 'elementary' particles, conclusively establishing that one can never be certain that what we currently regard as the basic ingredients of all existent matter may not themselves be shown to be constructed of yet finer ingredients at a later date. The so-called 90 'elements' of an earlier time were found to be composites of 3 yet smaller 'elements', the neutron, the proton and the electron. And now it is postulated that each neutron and proton is built up of 3 still tinier 'elements' called quarks. Do quarks really exist, or is this postulate merely a convenient model which, by and large, fits the facts, with little experimental evidence to support their individual existence? To date no quark has been isolated experimentally. But a bare 50 years ago, when Pauli first postulated the existence of the neutrino, that too was deemed a figment of imagination until its experimental discovery 20 years later. We shall later refer to the confining potential which appears to prohibit the existence of a free quark, but it is appropriate here to mention the earliest experimental evidence for the existence of quarks.

Rutherford's scattering experiments yielded the picture of an atom comprised mostly of empty space with a hard core nucleus at the center. When the angular distribution, momenta and energies of scattered α -particles were studied, detailed

calculations were made on the scattering pattern that should evolve if the entire positive charge of an atom was concentrated in a hard core nucleus. The computed and observed scattering patterns matched with remarkable consistency. The new image of the atom was born.

In 1968¹ somewhat similar results were obtained when high energy electron beams were aimed at proton targets. The scattering pattern suggests that the proton as a whole is not a single scattering point but that there is a multiplicity of scattering points within the proton which scattered the electrons through large angles. The assumption of concentrated points of charge within the proton and the consequent calculation of energies of the scattered beam and its angular distribution have been largely borne out by experimental observations.

Just as the nuclear model of the atom explained much that was known but not understood until then, so the quark model has helped to explain the multitude of short-lived particles that were created by the high energy accelerators. The nuclear model exhibited that all the known "elements" were built from three basic particles - the neutron, the proton and the electron. Similarly the quark model infers that each of the hundreds of high energy particles is a different composite of a few basic sub-atomic particles, the quarks. At first it was thought that there were three such basic sub-atomic particles or flavours of quarks, the up, down and strange quarks. In the mid-seventies the

existence of the fourth flavour, the charmed quark, which had been strongly predicted, was confirmed. Since then, a fifth flavour of quark, the beauty quark, has been discovered, and the existence of a sixth flavour of quark, the truth quark, is, in its turn, strongly predicted.

There are four types of forces known to exist in nature: gravitational force, electromagnetic force, strong force and weak force. Each force is mediated or transmitted by its own type of particle. The well known photon mediates the electromagnetic force. Quarks are subjected to all four types of forces, but it is the strong force that predominates between quarks, and the mediating particle is the gluon.

Particles subjected to the strong force are known as hadrons, of which we have two principal types: baryons and mesons. In the quark model, the baryons, of which protons and neutrons are common examples, are each composed of three quarks. The mesons, such as pions and kaons, are each composed of a quark and an antiquark, and it is the bound state of a quark and an antiquark which lent credence to the existence of quarks, as we shall elaborate in Chapter I.

The object of this research is to study the energy levels of two mesons: the ψ meson and the T . The first is a bound state of a charmed quark and antiquark, the second a bound state of a beauty quark and antiquark.

The potential that governs the interactions between quarks is not, as yet, well known. Therefore, it will be our endeavour to study the spectra of the ψ and T mesons in

4.

the light of a specific potential model. It is hoped that the success which we claim for the model will help to bring us a little closer to a knowledge of the true nature of the forces binding quarks.

The specific phenomenological model used is a harmonic oscillator model perturbed by an unknown anharmonic potential U which incorporates an attractive potential at short range (a Coulomb like piece derived from QCD) and deviations from the harmonic oscillator interaction at large quark separation. Further to that, the model includes corrections for the spin-spin interaction between quarks (Hyperfine) and spin-orbit effects (Fine).

The organisation of the thesis is as follows. The first three chapters deal with the groundwork on which the present research is based. Chapter I seeks to establish that quarks are real physical entities: the energy levels of Charmonium and positronium are compared, the colour hypothesis is briefly explained together with the theoretical and experimental support it has, and the problem of quark confinement is introduced. Chapter II deals with two models of the confinement potential, the general model proposed by de Rujula, Georgi and Glashow (DDG), and the specific harmonic oscillator model proposed by Isgur and Karl (I-K) which is based on the DGG model. The success of each model is discussed and the inconsistencies of the I-K model mentioned. Chapter III outlines the I-K model in greater detail and focuses attention on the anharmonic potential U . This chapter also introduces

the consistent quark model which sought to rectify the inconsistencies of the I-K model and, more importantly, proposed a technique developed by Kalman, Hall and Misra whereby the parameters used to determine the energy levels of one baryon could be effectively used to obtain the levels of any other baryon.

Chapters IV to VI deal with the current research. Chapter IV shows how the framework of the consistent quark model can be used to determine the energy levels of mesons. The meson Hamiltonian is presented, followed by the harmonic oscillator wave functions upto $n = 4$ which were worked out specifically for this problem. The anharmonic potential is then derived in detail, showing in particular how the 5 parameters necessary for the energy levels of the Charmonium system can be adapted by quartic approximation for the corresponding levels of the Upsilon system. This is followed by the explicit expressions which were worked out for each of the energy matrix elements, both mixed and unmixed, in terms of the 5 parameters defined. A sample calculation of a matrix element is given as an appendix. Chapter V deals with the spin-dependent terms. It is to be read in conjunction with Appendix G which gives an outline of the derivation of the expressions of the spin-dependent terms from Quantum Chromodynamics (QCD), firstly for the hyperfine interactions (both contact and tensor), and secondly for the two parts of the spin-orbit interaction between the quark and antiquark of the meson. In Chapter V

these expressions are used to compute the expectation values of the spin-related terms using 3 additional parameters. A sample calculation of each type of interaction is presented as an appendix. Chapter VI presents the results of the calculation of the energy levels of the two systems of equal quark-anti-quark mesons, together with a brief discussion of them.

The work was done in three phases. The first phase, the work for which comprised the first publication of this research, obtained the energy levels of the S-states of Charmonium using the Isgur-Karl approach. The second phase (incorporated in the second publication) computed the energy levels of both the Charmonium and Upsilon systems upto $n = 2$ using the consistent quark model. The third phase (as yet unpublished) extended this work upto $n = 4$. Copies of the two publications are included as appendices.

CHAPTER I.

1.1 Positronium and Mesons

The notion that quarks were physical realities gained considerable support when a study was made of the comparison between the energy levels of positronium and mesons. There was a striking similarity. Positronium is a bound state of an electron and a positron. The force that binds them is Coulombic. Since electrons and positrons are spin $\frac{1}{2}$ fermions, a single electron and a single positron can couple their spins to yield a total spin of 0 in the singlet state or 1 in the triplet state. These spin states obtain in each of several states of relative orbital momentum $L:0,1,2,3,\dots$ in the S,P, D,F,... states respectively. Combining spin with orbital angular momentum, we obtain the total angular momentum $J = L + S$ in a multiplicity of $2S + 1$ states. In the ground state ($L = 0$) we obtain 1S_0 and 3S_1 ; in the $L = 1$ state 1P_1 , 3P_0 , 3P_1 , 3P_2 ; in the $L = 2$ state 1D_2 , 3D_1 , 3D_2 , 3D_3 and so on. The spectrum of positronium has precise experimental energies for each of these levels. If mesons display an energy spectrum similar to that of positronium, there is a strong suggestion that the meson is comprised of two interacting particles which are mutually attractive. (Fig.1 shows a comparison of the energy levels of the J/ψ meson and positronium. Although all the levels are not represented, enough is displayed to indicate the similarity).

The quark theory states that the mesons that display energy levels similar to those of positronium are similar indeed in quark content to positronium. Such a meson

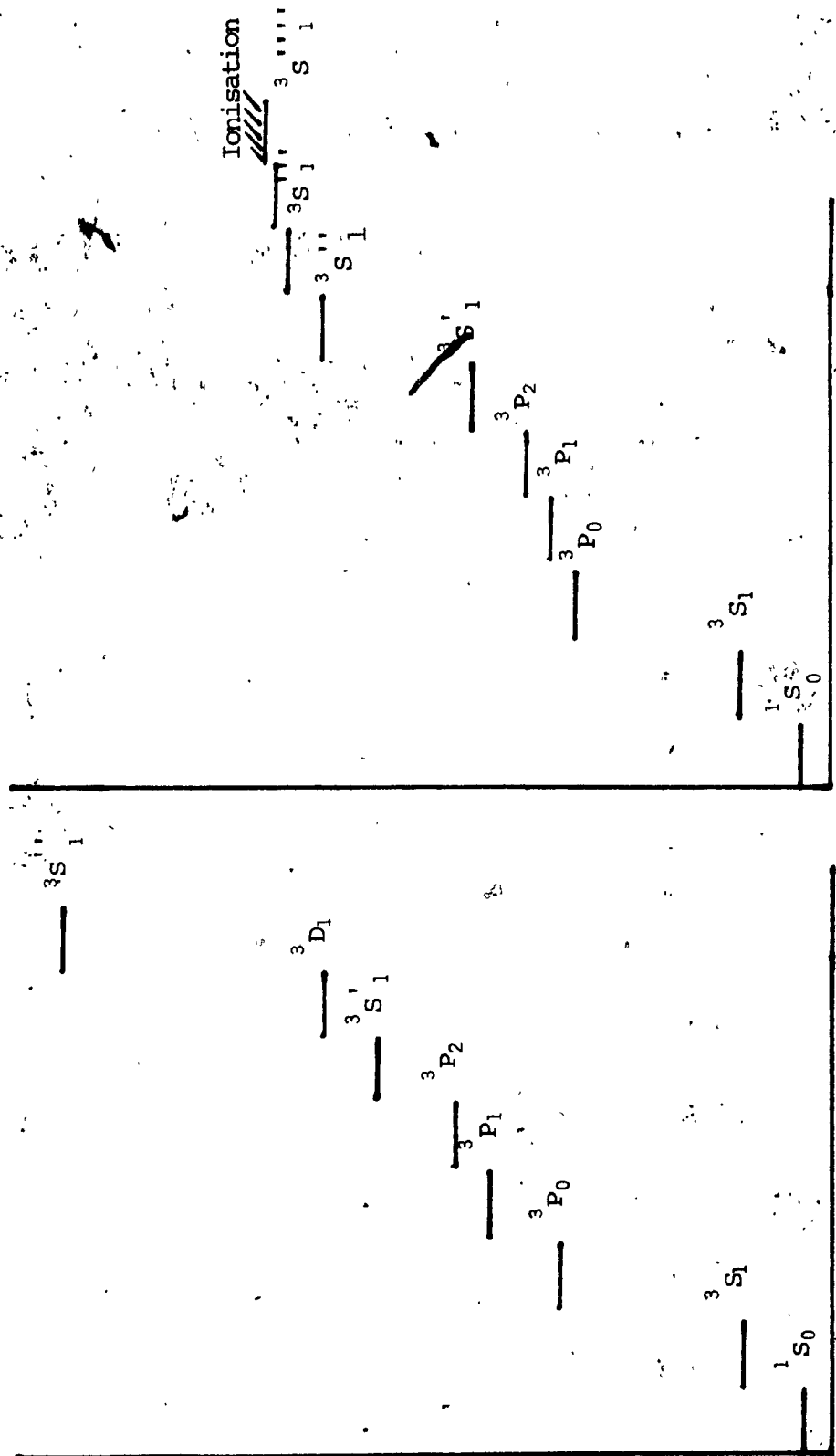


Fig. 1

Comparison of the Energy Levels of Charmonium and Positronium

comprises a quark and an antiquark of the same flavour - the quantum numbers are either identical or exact opposites of one another. For example, a charm quark has the same spin but opposite charge to a charm antiquark. So, just as in positronium, we have two equal mass but oppositely charged particles, mutually attractive, revolving around each other in a bound state, both in the ground state and at higher energy levels of excitation. (As we shall see later, in the quark model, the 'opposite charge' which causes the mutual attraction is more than a simple electric charge). In the realm of quarkonium, if energy levels exist analogical to those of positronium, we would have particles corresponding to each of the levels of positronium.

Such particles do indeed exist, but many more are known to exist in quarkonium than in positronium since, while an electron can only combine with its own antiparticle, the positron, each flavour of quark can combine with the anti-quark of its own flavour as well as with that of every other flavour. Consider, at first, only two flavours of quarks - the up and down quarks. Taking all possible combinations of quark with antiquark we obtain 4 particles - viz. $u\bar{d}$, $d\bar{u}$, $(u\bar{u} + d\bar{d})/\sqrt{2}$, $(u\bar{u} - d\bar{d})/\sqrt{2}$ - for both $J = 0$ (pseudoscalar mesons) as well as $J = 1$ (vector mesons). Particles corresponding to each of these low levels have been experimentally confirmed to exist. At the lowest level, the 1S_0 state, we have the well known pi mesons or pions and the η , and at the triplet state we have the ω and ρ resonances. If we now

include the third quark flavour, the strange quark, the combination of three quarks with three antiquarks yields nine mesons.

1.2 Significance of the J/ψ Meson

Until the mid-seventies, although the similarity in the spectra of positronium and mesons was noted, it was necessarily an incomplete comparison because no mesons had been discovered corresponding to the higher energy levels of positronium. Even the literature gave no prominence to the comparison. Any experimental attempt to create higher excitations of the u, d, and s quarks rapidly lead to the decay of the mesons into smaller particles. And then, in November 1974, a dramatic event occurred in the world of particle physics - the discovery of the J/ψ meson. It had a large mass (3097MeV) and its most remarkable property was its extremely narrow width ($\Gamma = 70\text{KeV}$) which was a factor 1000 smaller than a typical hadronic width. This implied a long lifetime, a stability not encountered in new particles. Why was this discovery so momentous? The new particle was heavy, yet relatively stable. Heavy particles generally have many channels of strong decay open to them. Yet this particle would only decay by weak interaction. It was suspected that a new quantum number was being conserved which suppressed the strong decay. A few years earlier (1970), Glashow et al² had predicted the existence of a fourth flavour of quark when they observed the suppression of strangeness changing neutral currents in the decay $K_L \rightarrow \mu^+ \mu^-$. The new particle was

considered to be the bound state of this fourth flavour of quark - the charmed quark. Within 10 days the first excited state, the ψ' , was discovered, to be soon followed by the unveiling of a whole family of new particles. The energy spectrum of Charmonium, the name given to the $c\bar{c}$ bound state, was sufficiently broad to make the comparison with positronium more complete. The similarity in the spectra was remarkable (Fig.1), and gave convincing evidence that the meson was a bound state of two mutually attractive particles. The quark[†] was no longer considered a possibility, it was a fact. In 1977 the validity of the quark model was further strengthened with the discovery of a much heavier meson, the T , which is deemed to be the bound state of a beauty quark and antiquark. There appears to be a symmetry observed in nature which the Weinberg-Salam³ model deals with. Every quark appears to have a 'partner': the up quark has the down quark, the strange quark has the charm quark. This symmetry requirement has strongly predicted the discovery of the beauty quark's 'partner' - the truth quark.

However, despite the similarity stressed above, there is a significant difference between the quarkonium spectrum and that of positronium. Since the force between the electron and the positron is Coulombic, the energy levels are widely spaced in the lower regions but rapidly crowd together at higher levels, after which ionisation is achieved if further energy is fed into the system, thus liberating the electron and the positron from each other. No analogous effect is

achieved with quarks. As energy is pumped in, the quarkonium jumps to almost equally spaced higher energy levels, the pattern being different to the Coulombic potential, more closely resembling the harmonic oscillator potential. Figure 2 displays the spectrum of Charmonium beside hypothetical spectra drawn from three different potentials: Coulombic, harmonic oscillator and linear. The resemblance to both the linear and harmonic oscillator potentials is greater than that to the Coulombic at the higher excitation levels. Moreover, as yet there has been no equivalent to ionisation in quarkonia. Pumping in of greater amounts of energy does not separate the quark from the antiquark, instead leading to the creation of further quark-antiquark pairs (or new mesons) as the energy exceeds the threshold of strong pair production.

1.3 The Colour Postulate

Quarks are spin $\frac{1}{2}$ fermions like the proton and the neutron. They obey Fermi-Dirac statistics and are subject to Pauli's exclusion principle that prohibits such particles from having identical quantum numbers. No two identical quarks can be in the same state in any hadron. In the case of mesons the question of violating this principle does not arise since quark and antiquark are not identical particles. But in the case of baryons, particles are known to exist with the same quantum numbers of spin and flavour (charge, isospin, strangeness, charm and baryon numbers) for each of the quarks they contain. We may cite, as examples, the particles Δ^{++} (uuu), Δ^- (ddd) and Ω^- (sss). There are three identical

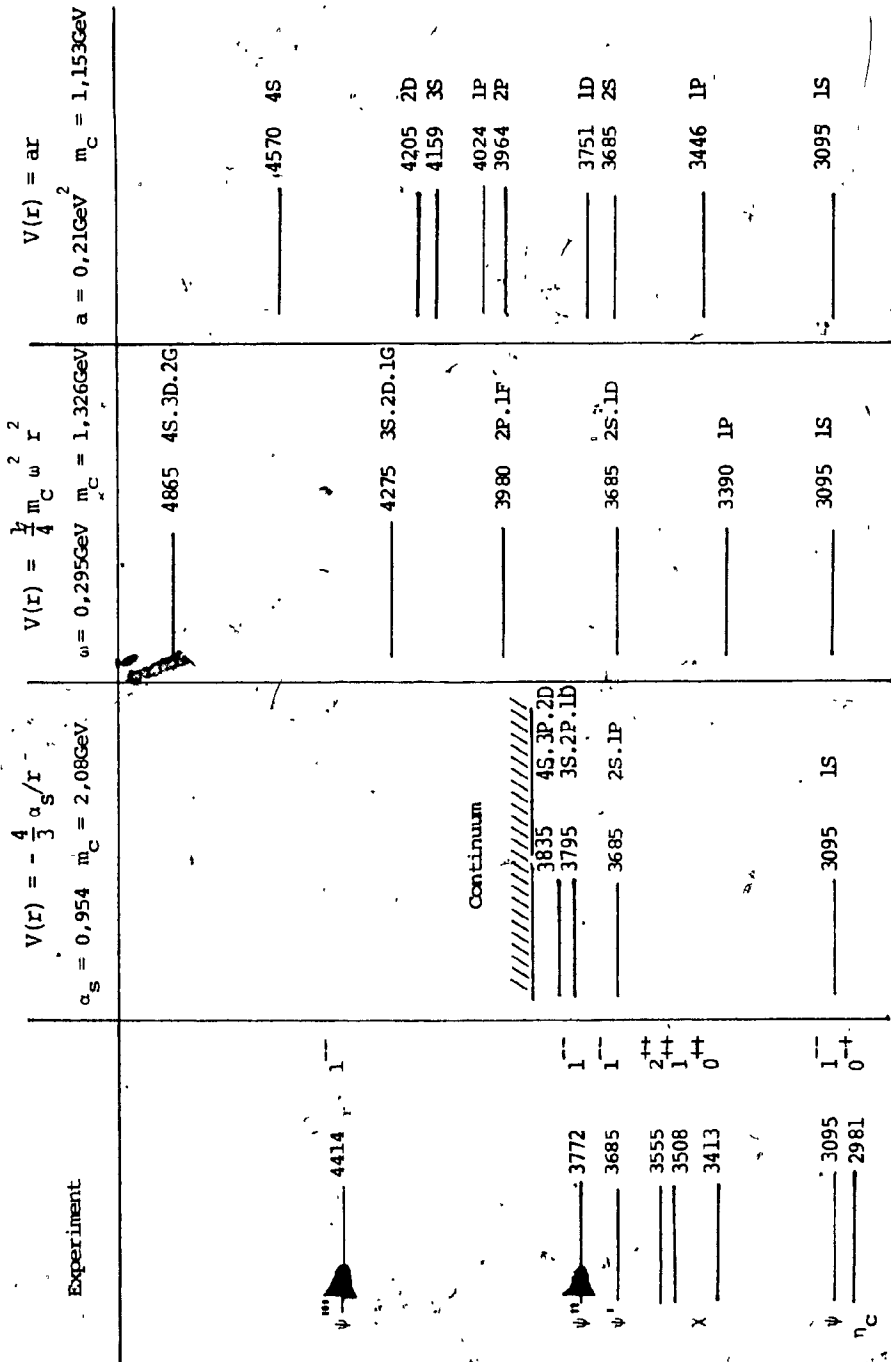


Fig. 2

Comparison of the C armonium Spectrum with Those of Other Potentials

quarks in each of these particles. When the baryon is in a spin $3/2$ state, the three quarks are aligned ($↑↑↑$) and the exclusion principle is clearly and substantially violated. Even when the baryon is in a spin $1/2$ state, at least two of the quarks have the same quantum numbers ($↑↑↑$) and the principle is still violated. It was postulated that quarks have another degree of freedom which was arbitrarily given the name colour. Every quark comes in one of three colours, red, blue or green. Antiquarks come in anticcolours, antired, antiblue and antigreen. When the three colours combine antisymmetrically, the result is colourless, when a colour combines with its own anticcolour, we achieve the same effect. All existing particles are colourless. Colour is an exact symmetry. Flavour is not. Quarks of different flavours, such as an up quark and a strange quark, differ in many respects: mass, charge, and in other quantum numbers. But like-flavour quarks of different colours, such as red and blue charmed quarks, are identical in every respect (mass, charge, etc.) save in colour.

The colour hypothesis solved two obvious problems faced in the quark model. The first related to the difficulty about Pauli's exclusion principle. If each quark in a baryon had a different colour, otherwise identical, aligned quarks as in Ω^- (sss) had differing colour quantum numbers, so there was no violation of the exclusion principle. The second related to the question of why no particles were found in nature with quark contents qq , $qqqq$, $qqq\bar{q}$ or

otherwise. All existing particles were comprised of either three quarks, qqq , or a quark and an antiquark, $q\bar{q}$. The colour postulate had a simple answer. Nature required that existing particles be colourless. With only three colours and three anticolours to choose from, there was no other way to make combinations of white except with groups of three quarks, each with a different colour (colour singlet), or a coupling of one colour with its own anticolour in groups of two.⁵

Experimental support for the colour postulate was quite considerable. In the annihilation of electrons and positrons, the ratio of the decay to hadrons and the decay to muon pairs (below charm threshold)

$$R = \frac{\sigma(e^+e^- \rightarrow \text{hadrons})}{\sigma(e^+e^- \rightarrow \mu^+\mu^-)} \quad (1.1)$$

theoretically worked out to $2/3$ without the colour postulate and to 2 if we allowed for the three colours as the postulate required. Experimentally this ratio was between 2 and 2.5. The width of the decay of neutral pions to 2 photons is given by the use of the formalism of Partially Conserved Axial Current (PCAC) to be

$$\Gamma(\pi^0 \rightarrow 2\gamma) = \left[\frac{m_\pi^3}{32\pi F_\pi} \right] \left(\frac{\alpha}{\pi} \right) \left(\frac{n}{3} \right)^2 = 7.87 \left(\frac{n}{3} \right)^2 \text{ eV} \quad (1.2)$$

where $F_\pi = 0.96 m_\pi$ is the pion decay constant and n is the number of colours. For the no-colour situation the width would be one-ninth of what it is with three colours. The

experimental value is 7.95 ± 0.55 eV which provides excellent agreement to the value computed with $n = 3$. In the process of hadrons to lepton pairs (the Drell-Yan process $pp \rightarrow \mu^+ \mu^- + \dots$), the lepton pair is the annihilation product of a massive photon produced when a quark in one proton annihilates with an antiquark of the same flavour in another proton. The cross-section of this decay would have been a factor one-third of what it is if no colour existed. Finally, when the heavy τ lepton decays, the three decay modes are:

$$\tau \longrightarrow e^- + \bar{\nu}_e + \nu_\tau, \quad (1.3)$$

$$\tau \longrightarrow \mu^- + \bar{\nu}_\mu + \nu_\tau, \quad (1.4)$$

$$\text{and } \tau \longrightarrow \text{hadrons} + \nu_\tau \quad (1.5)$$

The branching ratio of these three modes would have been 1:1:1 without colour. But with colour, since the quarks of the hadrons in (1.5) come in three colours, the branching ratio is 1:1:3 in line with experiment.

1.4 Quark Confinement and QCD

Several theories have been advanced as to the nature of the forces that bind quarks. What is it that inhibits the liberation of a quark? Is it simply that accelerators are as yet inadequately powerful to shatter a meson or baryon into its quark components, or is there a law in nature that prohibits the existence of a free quark altogether? This question has yet to be answered conclusively. But with the acceptance of the colour postulate, a new look has been taken at the strong force and the laws that govern it. The theory

formulated on the basis of the colour force, Quantum Chromo Dynamics (QCD), is similar to Quantum Electro Dynamics (QED), yet there are significant differences.

Forces in QED are mediated by electrically chargeless photons between electrically charged particles. Similarly, forces in QCD are mediated by gluons between strong interacting particles such as quarks. These gluons are electrically neutral but they possess colour charges. Since there are 3 colours and 3 anticolours, there can be 9 possible combinations. One of these, $(R\bar{R} + G\bar{G} + B\bar{B}) / \sqrt{3}$ is effectively colourless, but the other 8 are coloured gluons. Unlike the neutral photons which do not interact with one another, colour-charged gluons can couple with one another to form glueballs.

The problem of quark confinement can be viewed as analogous to what happens in QED around an electrically charged particle. An electron surrounds itself with a multitude of electron-positron pairs which polarize the vacuum around it and thereby screen the bare charge of the electron. At close proximity to the electron, this screening is absent, so that the potential rises, it may be said, infinitely. However, as the distance from the central electron increases, the potential falls off as the inverse of the distance due to the screening effect of the polarized vacuum. In the same manner, the colour-charged quark colour-polarizes the vacuum around it by surrounding itself with quark-antiquark pairs. As in the case of the electron this has a screening effect

which shields the bare colour-charge of the quark. But in this case the forces are mediated by gluons which are themselves colour-charged. A field therefore acts as a source of itself. This is not such a novel hypothesis as it may first appear. In Einstein's theory of gravitation, forces are mediated by gravitons which themselves generate gravity. The gluon colour field is similar to the quark which generated it, and, at increasing distance from the quark, the field intensifies rather than weakens. This is an anti-shielding effect which is considerably more pronounced than the shielding effect of the quark-antiquark pairs that are generated by the original central quark.

The theories that govern the formalism of these two models (QED and QCD) are the Abelian and Non-Abelian gauge theories. The electron is governed by the Abelian gauge theory where the long range field of the electron is proportional to its charge quantum number, but the field itself carries no quantum number. The quark is governed by the Non-Abelian gauge theory where, due to the gluons themselves carrying colour charges, the fields themselves have quantum numbers. The result is that force fields binding quarks do not fall off as Coulombic fields do, but increase with separation.

In Rutherford's experiments, the particles inside an atom were probed by alpha particles. Similarly, the particles inside a meson have been probed by high energy electrons. But to a probe which has relatively low energy,

the quark-antiquark pair moves in concert and appears to be strongly bound together. This is because the probe only approaches the pair at a distance and lacks the energy to obtain access to the interior. A much higher energy probe can get within a quark-antiquark pair, although for a very short time, and it "sees" the quarks as discrete particles, not bound. Low energy probes can be likened to low frequency photons which are typical in the infra-red region of light, whereas the high energy probes can be likened to the ultra-violet photons. That is why the low energy probes which observe only the strongly bound state of the quarks are said to study its infra-red slavery, whereas the high energy probes study its ultra-violet freedom. To be more technical, the low energy probes have a wavelength that vastly exceeds the inter-quark spacing and hence observes them only in tandem, strongly bound, whereas the high energy probes have a wavelength which is more comparable with the inter-quark separation and hence provide sufficiently high resolution to observe the quarks more 'interiorly' and find them relatively free.

What inhibits the quark from freeing itself, even if vast amounts of energy are fed into the system? If the hypothesis of anti-screening effect is correct, then the force between two quarks increases with increased separation. It is sometimes hypothesized that the force increases linearly so that at infinite distance the force is infinite. (In Fig. 2 the energy levels due to a strictly linear potential were

shown, for comparison, beside the energy levels of Charmonium. The levels are not very dissimilar). With such a potential the lines of force connecting a quark and an anti-quark would become parallel lines. If energy is continued to be pumped in to separate them further, it will soon exceed the threshold energy for strong pair production and the meson will effectively split into two mesons, so that, instead of freeing the quark, we have only pair produced another meson (Fig.3).

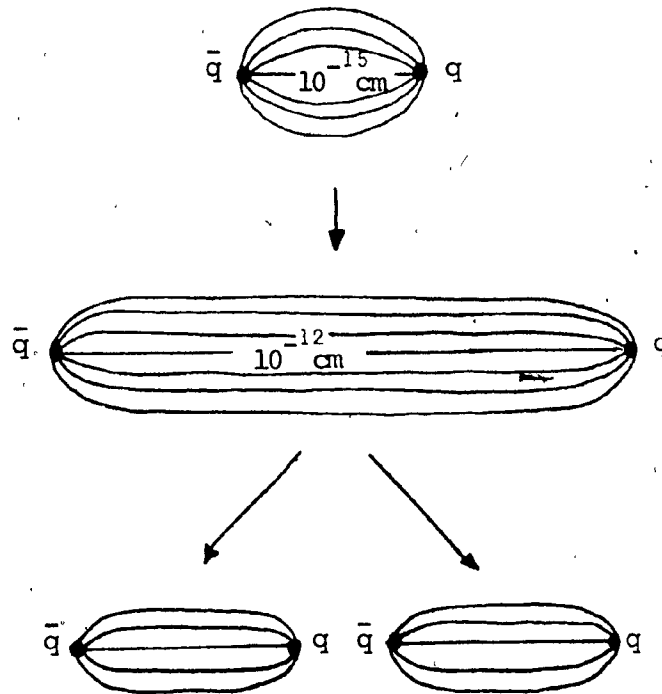


Fig. 3

Pair Production of Quark and Antiquark

In the next chapter we can look a little more closely at some specific potentials in the light of quark confinement.

CHAPTER II.

2.1 Confinement Potential

It should be clear from the discussions in the previous chapter that forces binding quarks are relatively weak when the quarks are in close proximity to one another and that the forces are relatively strong as the separation increases. In hadrons studied by high energy probes the forces are low enough to be mediated by one gluon exchange and are essentially Coulombic in nature. But at large quark separation, the potential tends to increase linearly. Figure 4⁴ gives a qualitative picture of the potential as a function of $q - \bar{q}$ distance r . The full lines show the Coulombic (short range) and linear (long range) parts of the potential. The problem is to obtain a potential that would accommodate both the short range and long range requirements. The problem was dealt with by Isgur and Karl⁶ who proposed a harmonic oscillator model perturbed by an anharmonic term with hyperfine corrections. They based their model on a more general Hamiltonian put forward by De Rujula, Georgi and Glashow (DGG)⁷.

2.2 DGG Model

Essentially, the DGG model does not provide a specific potential for the quark binding forces. It does specify that the same forces mediate between different types of quarks - i.e. the Hamiltonian is flavour independent. To put it differently, the energy of a system of bound quarks may be computed by the same Hamiltonian whether the quarks are up, down, strange or otherwise. For a given system the differences

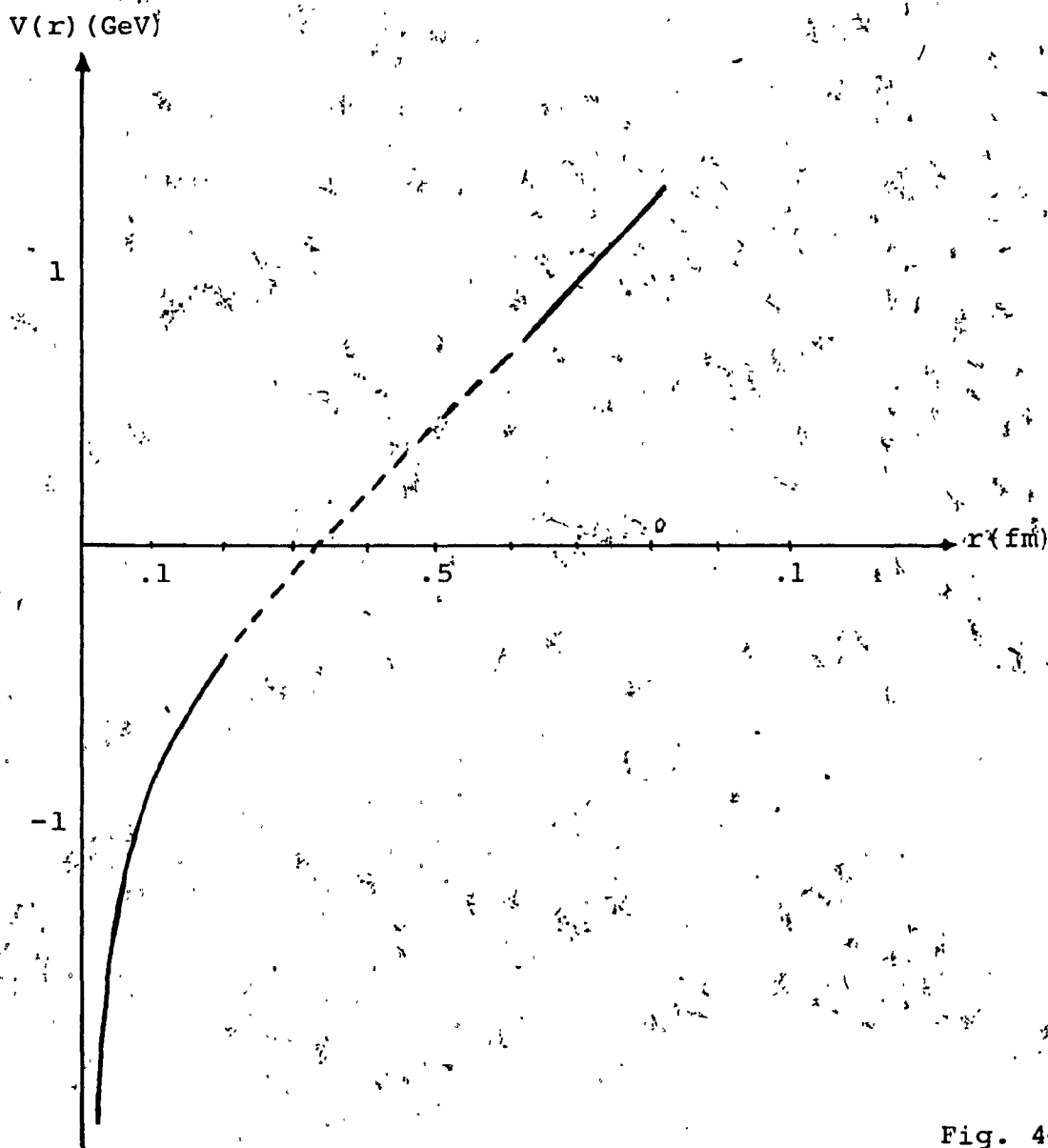


Fig. 4

Qualitative Picture of Potential as a Function
of $q\bar{q}$ Separation

in energy would arise only due to the mass difference of the individual quarks, and due to the separation of the quarks.

The Hamiltonian is

$$H = L(\vec{r}_1, \vec{r}_2, \dots) + \sum_i (m_i + \vec{p}_i^2 / 2m_i + \dots) + \sum_{i>j} (\alpha Q_i Q_j + K \lambda_{ij}) \quad (2.1)$$

L is the universal interaction responsible for quark binding. The nature of the binding is not specified. Particular quark models with specific potentials can be fitted in to complete the Hamiltonian. Here m_i are the masses of the individual quarks interacting, $\vec{p}_i^2 / 2m_i$ are the kinetic energies of the quarks, and other terms within the parenthesis (represented here by a series of dots) would provide the relativistic corrections should they be required. (Since this research deals specifically with heavy quarks, it has been deemed justifiable to ignore relativistic corrections). The Q_i are the electric charges of the quarks, K is the expectation value for the dot product of the λ matrices resulting from colour charges. Since there are eight coloured gluons there are eight such matrices. Colour averaging has been computed for baryons and mesons separately. The results are

$$K = \left\langle \frac{\lambda_i}{2} \cdot \frac{\lambda_j}{2} \right\rangle_{qq} = -2/3 \text{ (baryons)}$$

$$K = \left\langle \frac{\lambda_i}{2} \cdot \frac{-\lambda_j^*}{2} \right\rangle_{q\bar{q}} = -4/3 \text{ (mesons)} \quad (2.2)$$

The factors α and α_s are the fine structure constants of ordinary electromagnetic interactions and strong interactions respectively. α_s is not a 'constant' in the strict sense - it has a dependence on the separation of quarks, ranging from a small value when the quarks are in close proximity to large values as separation increases. It is more correctly called a running coupling constant. It is given by the expression

$$\alpha_s = \alpha_0 \left(1 - \frac{2}{3} f \frac{\alpha_0}{4\pi} \ln \frac{\Lambda^2}{Q^2} + \frac{11}{4\pi} \alpha_0 \ln \frac{\Lambda^2}{Q^2} + \dots \right) \quad (2.3)$$

where $\alpha_0 = g^2/4\pi$, f is the number of flavours, Λ is the ultraviolet cut off, $\Lambda \gg m$, $Q \sim O(1/r)$. The positive third term of equation (2.3) results in the anti-screening effect with increasing separation that was discussed in Chapter I.

\vec{S}_{ij} is the Breit interaction between quarks i and j . In the case of mesons it is the interaction between quark and antiquark.

$$\vec{S}_{ij} = \frac{1}{r} + \frac{1}{2m_i m_j} \left[\frac{\vec{p}_i \cdot \vec{p}_j}{r} + \frac{\vec{r} \cdot (\vec{r} \cdot \vec{p}_i) \vec{p}_j}{r^3} \right] \quad (\text{Darwin term})$$

$$- \frac{\pi}{2} \delta^3(r) \left[\frac{1}{m_i^2} + \frac{1}{m_j^2} \right] \quad (\text{Zitterbewegung})$$

$$- \frac{1}{m_i m_j} \left\{ \frac{8\pi}{3} \vec{S}_i \cdot \vec{S}_j \delta^3(r) + \frac{1}{r} \left[3(\vec{S}_i \cdot \vec{r})(\vec{S}_j \cdot \vec{r}) \right. \right.$$

$$\begin{aligned}
& - \left. \left[\vec{s}_i \cdot \vec{s}_j \right] \right\} \quad (\text{spin-spin}) \\
& - \frac{1}{2r^3} \left\{ \frac{1}{m_i^2} \vec{r} \times \vec{p}_i \cdot \vec{s}_i - \frac{1}{m_j^2} \vec{r} \times \vec{p}_j \cdot \vec{s}_j \right. \\
& \left. + \frac{1}{m_i m_j} \left[2 \vec{r} \times \vec{p}_i \cdot \vec{s}_j - 2 \vec{r} \times \vec{p}_j \cdot \vec{s}_i \right] \right\} \quad (\text{spin-orbit}) \\
& + \dots \quad (2.4)
\end{aligned}$$

where, again, the series of dots at the end of equation (2.4) denotes the neglected relativistic corrections. The present research is concerned with charmonium spectroscopy and the corresponding b - quark spectroscopy - viz. the Upsilon. As such, we have, everywhere, $m_i = m_j$.

Equation (2.4) is typical in Q.E.D. for Coulomb potentials. Quark confinement does not appear to have the same potential for all separations. At large separations the potential tends to increase with linear dependence but its true nature is not yet known with certainty. However, at short separations, in the region of ultraviolet freedom, experimental evidence indicates that forces are governed by one - gluon exchanges and that the potential is typically Coulombic - i.e. with a $1/r$ dependence. That justifies use of the Breit interaction which incorporates the Fermi contact term and the tensor terms of Q.E.D.

To summarize, the DGG model assumes

- (i) A non-relativistic SU(6) picture;
- (ii) long-range flavour and spin independent confining forces;

- (iii) SU(3) breaking only via quark masses;
- (iv) asymptotic freedom for the quark-gluon interactions which permits a short-range, spin and flavour dependent force arising from the non-relativistic reduction of one-gluon exchange between quarks.
- (v) the term L incorporates the (presumed) colour confining potential but no explicit form for these confining forces is assumed.

2.3 Success of DGG

The significant success of the DGG model was to provide a reliable method of breaking the SU(3) symmetry of quark masses. As will be outlined in the following paragraphs, with the use of first order perturbation in quark masses, they computed the mass ratio between the up (or down) quark and the strange quark. They worked out this ratio by two different approaches and came up with consistent values.

In the Hamiltonian presented in (2.1) if the first two terms are listed as H_0 , then we have

$$H_0 = \sum L(\vec{r}_1, \vec{r}_2, \dots) + \sum_i (m_u + \frac{\vec{p}_i^2}{2m_u}) \quad (2.5)$$

where m_i has been replaced by m_u , the mass of the up (or down) quark. The third term of equation (2.1) is listed as V

$$V = \sum_{i>j} (\alpha Q_i Q_j + K \alpha_s) \vec{S}_{ij} + \sum_i \Delta m_i + \frac{\vec{p}_i^2}{2} \left(\frac{1}{m_i} - \frac{1}{m_u} \right) \quad (2.6)$$

so that the Hamiltonian now reads

$$H = H_0 + V \quad (2.7)$$

The eigenstates of H_0 are degenerate $SU(6)$ supermultiplets; and first order perturbation theory in V introduces the splitting due to the different masses of the quarks within the supermultiplets.

The mass perturbation term has the form

$$\begin{aligned}
 M = M_0 + \sum_i \left[\Delta m_i + a \left(\frac{1}{m_i} - \frac{1}{m_u} \right) \right. \\
 \left. + \sum_{i>j} (\alpha Q_i Q_j - \frac{2}{3} \alpha_s) \left[b - \frac{c}{m_i m_j} - d \left(\frac{1}{m_i^2} + \frac{1}{m_j^2} \right. \right. \right. \\
 \left. \left. + \frac{16 \vec{S}_i \cdot \vec{S}_j}{3 m_i m_j} \right) \right] \quad (2.8)
 \end{aligned}$$

where, by using a wave function $\psi_0(r_1, r_2, r_3)$ which is an eigenstate of H_0 and therefore must be symmetric in position and anti-symmetric in colour, we have $H_0 |\psi_0\rangle = M_0 |\psi_0\rangle$, and we define

$$\Delta m_i = m_i - m_u$$

$$a = \frac{1}{2} \langle \psi_0 | \vec{p}_i^2 | \psi_0 \rangle$$

$$b = \langle \psi_0 | (1/|r_{12}|) | \psi_0 \rangle$$

$$c = \frac{1}{2} \langle \psi_0 | \frac{\vec{r}_{12}^2 \vec{p}_1 \cdot \vec{p}_2 + \vec{r}_{12} \cdot (\vec{r}_{12} \cdot \vec{p}_1) \vec{p}_2}{|\vec{r}_{12}|^3} | \psi_0 \rangle$$

$$d = \frac{\pi}{2} \langle \psi_0 | \delta^3(\vec{r}_{12}) | \psi_0 \rangle \quad (2.9)$$

The mass of the nucleon N and of the Δ particle, each of which is comprised of three quarks of the same mass, differ only due to the spin alignment. They are both Dirac particles: the Δ which is from the decuplet has spin $3/2$ and has a higher

energy than the nucleon which is from the octet and has spin $\frac{1}{2}$. In computing the mass of the two particles using equation (2.8), the splitting occurs only in the last term:

$$\frac{32}{9} \frac{\alpha_s^d}{m_u^2} \sum_{i>j} \langle \vec{S}_i \cdot \vec{S}_j \rangle$$

For the N particle $\langle \vec{S}_i \cdot \vec{S}_j \rangle = -3/4$ whereas for the Δ particle $\langle \vec{S}_i \cdot \vec{S}_j \rangle = +3/4$ (2.10)

It follows that the mass difference of the two particles

$$m(\Delta-N) = \frac{16}{3} \frac{\alpha_s^d}{m_u} \quad (2.11)$$

A similar computation can now be repeated with the Σ and Λ particles, each of which is a baryon with one strange quark. The Σ has quark composition uds and is an isotriplet whereas the Λ is a singlet with quarks uds. The computation yields the mass difference.

$$m(\Sigma-\Lambda) = \frac{32}{9} \frac{\alpha_s^d}{m_u^2} \left(1 - \frac{m_u}{m_s}\right) \quad (2.12)$$

Substituting the relation (2.11) we obtain

$$m(\Sigma-\Lambda) = \frac{2}{3} \left(1 - \frac{m_u}{m_s}\right) m(\Delta-N) \quad (2.13)$$

The mass difference of $(\Sigma-\Lambda)$ and $(\Delta-N)$ are known experimentally. Inserting these in (2.13), we get

$$\frac{m_u}{m_s} = 0.600 \quad (2.14)$$

The above calculation was accomplished by utilising the known mass difference of strange baryons on one side of (2.13)

and of non-strange baryons on the other. The process can be repeated entirely with the strange baryons Σ^* , Σ and Λ . This computation yields

$$\frac{m_u}{m_s} = \frac{2(\Sigma^* - \Sigma)}{2\Sigma^* + \Sigma - 3\Lambda} \approx 0.621 \quad (2.15)$$

The close agreement between the ratios (2.14) and (2.15) is significant. It is a measure of the success of the DGG model. The mass perturbation approach neatly avoids the portions of the Hamiltonian which are unspecified - viz the quark binding forces - and yields a consistent ratio of the two flavours of quarks. Subsequent calculations by Isgur and Karl⁶ have shown that this ratio was reliable and reasonably accurate.

2.4 The Isgur - Karl Model (I-K)

The general base provided by the DGG model has been successfully built on by Isgur and Karl. They studied a large number of baryon resonance data which significantly match the calculations based on the model constructed by them.⁶ Stated simply, they have, in effect, completed the DGG Hamiltonian by using a harmonic oscillator potential which is perturbed by an anharmonic potential U with hyperfine corrections. The model explains the baryon data with remarkable success. The extent of the success will be outlined later.

The choice of a harmonic oscillator potential as the confinement potential of quarks in baryons stems from the

fact that the analytic expressions for the eigenfunctions are tractable and yield fairly accurate estimates of energy levels.⁸ Calculation expediency is not by itself adequate justification for using a harmonic oscillator potential, but its success in fitting the I-K model to a considerable amount of experimental baryon data offers its own justification.

Isgur has explained his preference for dealing with baryons instead of mesons to test the I-K model. He states⁹ that with respect to $I = 1$ -P wave mesons there are only two that are well established - viz $A_2(1320)2^{++}$ and $B(1230)1^{++}$. By contrast, there are 20 well established P wave baryon resonances, each in general having at least several well-measured decay amplitudes. Isgur points out, furthermore, that a non-relativistic model is not entirely satisfactory for $I = 0$ mesons due to certain effects which stem from quark - antiquark annihilation channels. There is another advantage in testing the model with baryons. According to Isgur and Karl the L.S spin-orbit forces can be neglected in calculating the mass spectrum of baryons. The L.S forces arise from two sources - viz from the one gluon exchange which forms part of the Breit interaction and from the Lorentz scalar confining potential via Thomas precession. Isgur contends that although the calculation of the contribution due to the one-gluon exchange potential is not trivial, it is reasonable to assume that the two contributions mutually tend to cancel each other. In support of his contention he points out that empirical evidence, at least in baryons, do

indicate that the spin-orbit forces are minimal.

Isgur's reasons for testing the model with baryon data were expressed in 1978. Subsequent to that, considerable experimental data on mesons has been made available by Particle Data Group (P.D.G.). The objective of the present research is to show that the Consistent Quark Model of Kalman and Hall,^{10,11} a model developed from the Isgur-Karl model, can successfully be applied to mesons, in particular the Charmonium and Upsilon systems. The recent meson data furnished by P.D.G. has made the test on mesons feasible. For the Charmonium spectrum: in the S wave in the spin zero region we have two states available - viz. η_c and η_c' , in the spin one region we have three states - viz. ψ , ψ' , and ψ'' , in the P wave level there are three states for which data is available. For the Upsilon spectrum there are four states available in the S wave - viz. T , T' , T'' and T''' ; three states are available in the P wave and three more in the P' wave. It can hardly be contended any longer that experimental data is insufficient to test the model on mesons. Isgur's objection to using a non-relativistic model may apply more validly to light mesons like pions, not to heavy mesons like J/ψ and T .

2.5 The Successes of the I-K Model

Four significant successes of the I-K model are outlined below:

- (i) The accurate prediction of baryon masses and mixing composition;
- (ii) The voluminous correct predictions of baryon decay rates;
- (iii) The explanation of the decay mode of $\Sigma^{5/2}$ and other

strange particles; and

(iv) The explanation of the mass inversion of the Σ and Λ particles as they are excited above the ground state.

A few brief remarks on the above 4 points are appropriate.

2.5.1 Mass and Mixing

The mass predictions made by the I-K model cover a wide range of baryons, both in the ground state and in the excited states. It will suffice to point out the striking accuracy of the predictions as they are matched by experimental data by displaying in Fig. 5 a few of the predictions of strange and non-strange negative parity baryons.⁶ The measure of the success must include the fact that the model has used only a few parameters, at most seven. By contrast, other models¹² use a great many parameters to predict relatively few masses - in one case as many as 19 parameters were used to predict of the order of 120 masses. (In the present research on mesons we have used 8 parameters in the Charmonium system and only one more - viz. the mass of the b quark - in the Upsilon system).

Negative parity baryons below charm threshold are arranged in 70-plet SU(6) mixed symmetry states. The two possible spin states of quarks give rise to SU(2) symmetry for the spin whereas the three flavours - up, down, and strange - lead to SU(3) symmetry for flavours. The combination is the familiar SU(6) symmetry. Mixed symmetry in SU(6) results from the following four combinations of spin with flavour: symmetric in spin with mixed symmetry in flavour or vice versa, antisymmetric in flavour with mixed symmetry in

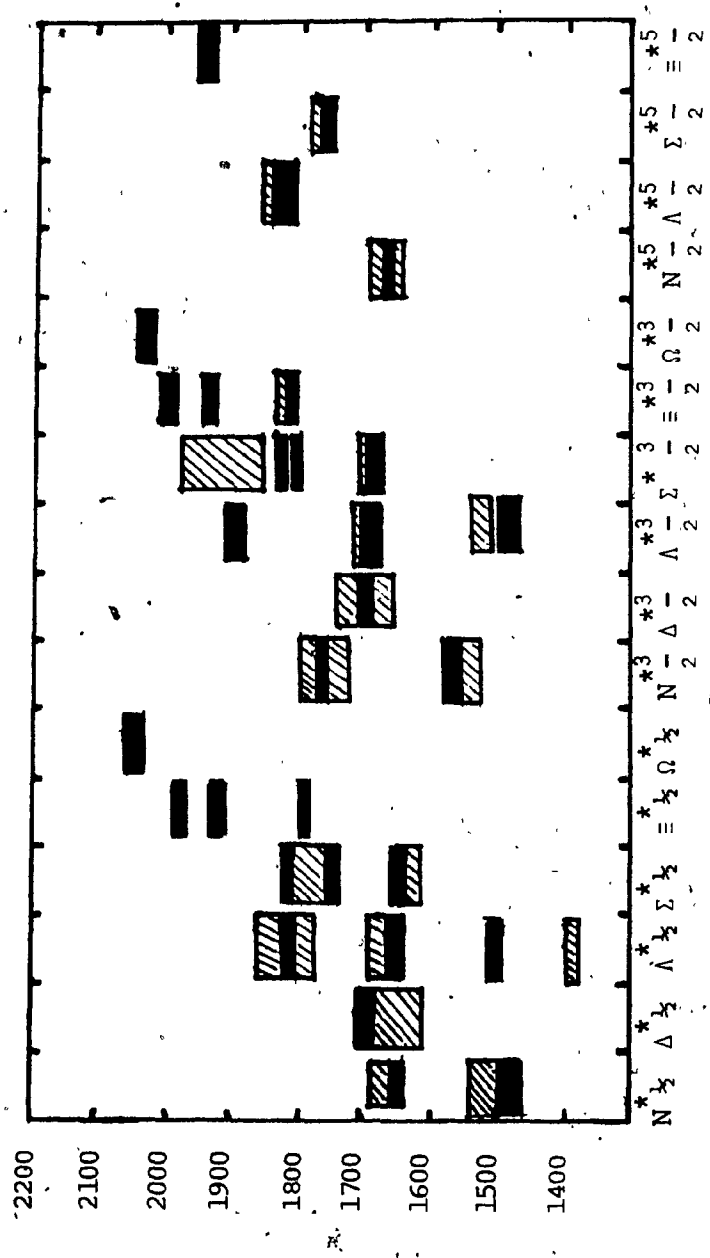


Fig. 5

Comparison of Predicted and Observed Spectrum of Negative Parity Baryons

spin, and mixed symmetry in spin with mixed symmetry in flavour. The four categories of mixed symmetry are symbolized in the notation

$$2_1 \quad 2_8 \quad 4_8 \quad 2_{10}$$

where the superscript refers to the number of possibilities in spin states and the subscript to the number of possibilities in flavour states. A baryon can, in fact, exist in more than one of these mixture combinations. The I-K model has computed the mixture combinations of many baryons as it has computed their masses. Both mass and mixture composition of a few baryons are presented in Table 1. Independent measured compositions by Hey, Litchfield, and Cashmore (HLC)¹³ and by Faiman and Plane (FP)¹³ are also presented for comparison. The close agreement between the I-K mixture predictions on the one hand and the measured composition of HLC and FP on the other bear out the accuracy of the I-K model.

2.5.2 Decay Rates

The noteworthy success of the I-K model in predicting baryon masses would not be complete if it were not followed by an equally striking success in explaining decay rates. To quote Isgur⁹ "A dynamical model for hadron structure is being tested in a quite limited way when it is compared only with spectroscopic data: once a state is predicted at a given mass it is next necessary to decide whether the internal structure attributed to the state by the model will give rise to its observed width and branching ratios. It is not very convincing, for example, to correctly predict the masses of

Table 1

Predicted Masses and Compositions of Negative-Parity
Baryons - Isgur and Karl. (HLC and FP see reference 13).

State	Predicted Mass (MeV)	Predicted (**) and measured Compositions				
		2_1	2_8	4_8	2_{10}	
$N^{*\frac{1}{2}-}$	1490	**		+0.85	+0.53	
		HLC		+0.85	+0.53	
		FP		+0.73	+0.68	
$N^{*\frac{3}{2}-}$	1655	**		+0.53	-0.85	
		HLC		+0.53	-0.85	
		FP		+0.68	-0.73	
$\Lambda^{*\frac{1}{2}-}$	1490	**	+0.90	+0.43	+0.06	
		HLC	+0.85	+0.46	+0.25	
		FP	+0.79	+0.61	-0.04	
$\Lambda^{*\frac{3}{2}-}$	1650	**	-0.39	+0.75	+0.58	
		HLC	-0.30	+0.04	+0.95	
		FP	-0.44	+0.63	+0.64	
$\Lambda^{*\frac{5}{2}-}$	1800	**	-0.18	+0.50	-0.85	
		HLC	-0.43	+0.89	-0.17	
		FP	-0.41	+0.49	-0.77	
$N^{*\frac{3}{2}-}$	1535	**		+0.99	-0.11	
		HLC		+0.98	-0.18	
		FP		+0.97	-0.26	
$\Sigma^{*\frac{3}{2}-}$	1675	**		+0.96	-0.11	-0.26
		HLC		+0.89	-0.38	+0.26
		FP		+0.88	+0.07	-0.46

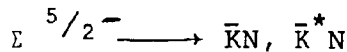
the $N^{*1/2}(1515)$ and $N^{*1/2}(1690)$ but to fail to predict that, despite phase space factors and comparable widths, the $N\eta$ decay mode is dominant in the first and negligible in the second."

Using the I-K model, Isgur and Koniuk¹⁴ have explained the decay rates and branching ratios of a remarkably large number of baryons, each from a great many excited states. Several of the decay rates have not yet been seen experimentally, but the vast majority of them have been matched with good accuracy by known decay rates.

A significant achievement of the I-K model is the fact that it is the only model which predicts both masses and decay rates of baryons, and that too with such good agreement with experiment.

2.5.3 The Decay Mode of $\Sigma^{5/2^-}$

It is experimentally known that the dominant decay mode of $\Sigma^{5/2^-}$ is



However, the decay $\Lambda^{5/2^-} \longrightarrow \bar{K}N, \bar{K}^*N$ appears to be forbidden by nature. The I-K model explanation of this preference is simple and reasonable. To understand it we must look a little more closely at the two oscillators that exist in each baryon.

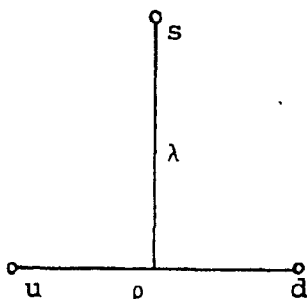


Fig. 6

Harmonic Oscillators in a Strange Baryon

In baryons such as Σ and Λ which are $S = -1$ (one strange quark) there are two equal mass quarks (u and d) and one heavier quark (s quark). The I-K model links the two equal mass quarks in one oscillator, the ρ oscillator, while the heavier quark by itself links with the other two together in the second oscillator, the λ oscillator (Fig.6). When the baryon is excited with one unit of angular momentum ($L = 1$) either the ρ oscillator is excited so that the u and d quarks oscillate against each other while the s quark sits still as a spectator (ρ mode), or the λ oscillator is excited in which case the heavier s quark oscillates alone against the u and d quarks moving in conjunction (λ mode).

In the harmonic oscillator model, the ρ mode excited particle is $\Lambda^{5/2^-}$ and the λ mode excited particle is $\Sigma^{5/2^-}$. When a baryon returns to the ground state, the decay must carry away the unit of angular momentum that caused the excitation.

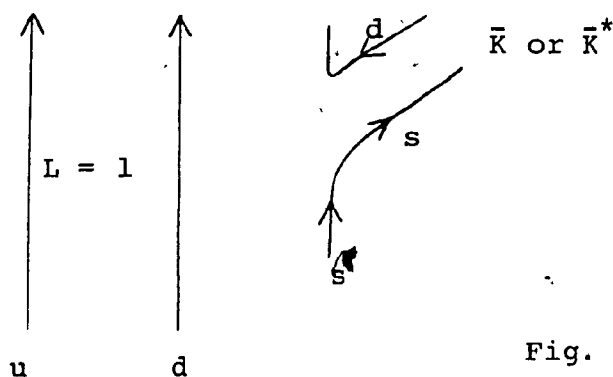


Fig. 7

Forbidden Decay of $\Lambda^{5/2^-} \rightarrow \bar{K}N, \bar{K}^*N$

For the baryon $\Lambda^{5/2^-}$ to decay to a nucleon, the s quark must be replaced by a u or d quark and this replacement must be accompanied by the removal of the angular momentum. However, since $\Lambda^{5/2^-}$ has a ρ mode excitation, the angular momentum lies betwixt the u and d quarks which are oscillating with the excitation (Fig.7). The replacement of the s quark does nothing to remove this excitation, hence the baryon remains excited even after the "decay". This explanation shows why the decay $\Lambda^{5/2^-} \longrightarrow \bar{K}N, \bar{K}^*N$ is forbidden by nature. No such impediment forbids the decay of the $\Sigma^{5/2^-}$. This baryon has its excitation in the λ mode. The decay of the λ oscillator very simply removes both the angular momentum and the s quark, and returns the baryon to its ground state.

2.5.4 The Mass Inversion of Σ and Λ

In the ground state the mass of the Σ particle is 1193 MeV while that of Λ is 1116 MeV. This is normal since, although each baryon comprises of quarks u, d and s, the Σ being an isotriplet state has a higher energy than the Λ which is a singlet. However, as the particles are excited, the Λ particle acquires a higher mass than the Σ . Thus $\Lambda^{5/2^-}$ has a mass of 1830 MeV compared to $\Sigma^{5/2^-}$ having a mass of 1765 MeV. This inversion of mass is neatly explained by the oscillator model as shown by Isgur and Karl.

The frequency of the harmonic oscillator is given by

$$\omega = \left(\frac{3K}{m}\right)^{1/2} \quad (2.16)$$

In the ground state neither the ρ nor λ oscillators are excited and the mass of the Σ exceeds the mass of the Λ as

indicated. But with excitation the mass increases by quanta of $\hbar\omega$. However, the frequency of an oscillator in the ρ mode (ω_ρ) exceeds that of an oscillator in the λ mode (ω_λ) because the mass of the λ oscillator is heavier than that of the ρ oscillator. Therefore, the excited levels of Λ which oscillates in the ρ mode increase by greater jumps than that of the Σ which oscillates in the λ mode. Consequently, the mass of $\Lambda^{5/2^-}$ exceeds that of $\Sigma^{5/2^-}$. This explanation of the mass inversion has been termed¹⁰ as one of the major triumphs of the I-K model.

2.6 Inconsistencies in the I-K Model

In dealing with the anharmonic potential U , the Isgur-Karl model for baryons considers the masses of the three lightest quarks - u , d and s - in the $SU(3)$ limit - viz. $m_u = m_d = m_s$. As a consequence, when the same values of parameters are used to compute masses for positive parity baryons as well as for negative parity baryons, the mass difference of $\Lambda^{5/2^-}$ and $\Sigma^{5/2^-}$ is reduced from 50 MeV to 15 MeV which is inconsistent with experiment. By introducing a technique developed by Kalman, Hall and Misra¹⁵ which takes into consideration the mass difference between strange and non-strange quarks, Kalman and Hall¹⁰ re-evaluated the parameters. On that basis, the mass difference between $\Lambda^{5/2^-}$ and $\Sigma^{5/2^-}$ is restored to consistency with experiment. Furthermore, a substantial refinement of the I-K model by Kalman and Hall¹⁰ is to use the parameters obtained for the anharmonic part of the potential for one baryon (by fitting to known energy levels

of that baryon) to compute the corresponding parameters for a different baryon by constructing quadratic approximations about the parameters of the first baryon. This technique, the details of which will be given in Chapter IV, has been fruitfully utilised in this research in the case of mesons to use the parameters obtained from fittings in the Charmonium system to compute the corresponding parameters in the Upsilon system.

CHAPTER III.

3.1 The Isgur-Karl Hamiltonian

In their work on baryons, Isgur and Karl have used a Hamiltonian of the form

$$H = \sum_{i=1}^3 m_i + H_0 + H_{\text{hyp}} \quad (3.1)$$

where m_i are the masses of the constituent quarks,

$$H_0 = \sum \frac{\vec{p}_i^2}{2m_i} + \sum_{i<j} v_{\text{conf}}^{ij} - \frac{[\sum \vec{p}_i]^2}{[2\sum m_i]} \quad (3.2)$$

and

$$H_{\text{hyp}} = \sum_{i<j} \frac{2\alpha_s}{3m_i m_j} \left\{ \frac{8\pi}{3} \delta^3(\vec{r}_{ij}) (\vec{s}_i \cdot \vec{s}_j) + \frac{1}{r_{ij}^3} \left[\frac{3(\vec{s}_i \cdot \vec{r}_{ij})(\vec{s}_j \cdot \vec{r}_{ij})}{r_{ij}^2} - \vec{s}_i \cdot \vec{s}_j \right] \right\} \quad (3.3)$$

where \vec{r}_{ij} is the separation between a pair of quarks.

$$v_{\text{conf}}^{ij} = \frac{1}{2} k r_{ij}^2 + U(r_{ij}) \quad (3.4)$$

where $U(r_{ij})$ is some unknown anharmonic potential which incorporates an attractive potential at short range (a Coulomb type piece derived from QCD) and deviations from the harmonic oscillator form at large range.

It must be noted that the spin-orbit forces in the Breit interaction have been entirely neglected in keeping

with Isgur and Karl's contention that the two parts of the spin orbit term tend to mutually cancel (Chapter II). Therefore, equation (3.3) represents the whole of the spin-spin interaction. The first term is the Fermi contact term which operates between quarks when they are in a state of zero angular momentum, while the second term is the tensor force which operates when the angular momentum is non-zero. These terms will be dealt with in greater detail in Chapter V, along with sample calculations.

3.2 The Anharmonic Potential U

Isgur justified the use of the harmonic oscillator potential in these words:⁹ "Since we have a three-body problem, and since this problem cannot in general be exactly solved, we do perturbation theory around the one soluble case: a harmonic confining potential. This choice turns out to generate a quite reasonable set of basis states; numerical studies have shown that the low lying states of many potentials (for example, linear plus Coulomb) can be approximated by wave functions of the harmonic oscillator form."

In QCD, the short range potential between two quarks is clearly Coulombic. With increasing separation the potential tends to be linear. We may combine the two potentials to obtain

$$V(r_{ij}) = -\alpha_s/r_{ij} + ar_{ij} \quad (3.5)$$

where α_s is the quark-gluon fine structure constant and r_{ij}

is the separation in quark pairs.

Gromes and Stamatescu¹⁷, using a harmonic oscillator basis, wrote the potential as

$$\begin{aligned} V(r) &= \frac{1}{2} \mu \omega^2 r^2 + \left[V(r) - \frac{1}{2} \mu \omega^2 r^2 \right] \\ &= V_0(r) + U(r) \end{aligned} \quad (3.6)$$

where μ is the reduced mass, and $U(r)$ is treated perturbatively. They point out that if $V(r)$ is purely linear

$$V(r) = a r \quad (3.7)$$

then the approximation is quite good. In our case we have a linear plus Coulomb potential. They remark that the approximation is still good if the linear term predominates.

Isgur and Karl⁹ noted that it was the U term which broke the degeneracy of the $N = 2$ level multiplets. Using the harmonic oscillator potential there is no degeneracy at the ground state $[56, 0^+]$ and in the negative parity $[70, 1^-]$ at $N = 1$ level, but at $N = 2$ the oscillator potential has five $SU(6)$ multiplets degenerate. This is contrary to experimental data for $N = 2$ positive parity multiplets. However, when the U term perturbation on oscillator potential is used, we obtain five distinctly spaced levels, breaking the degeneracy as shown in Fig. 8.

The actual computation of the U term perturbation was as follows:

Three constants a , b , and c were explicitly defined in terms of Gaussian moments of the potential:

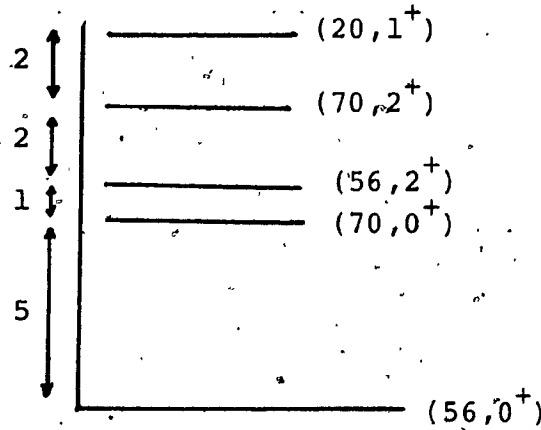


Fig. 8

Pattern of Splitting of Low-Lying Supermultiplets by U Term Perturbation

$$\begin{aligned}
 a &= \frac{3\alpha}{\pi^{3/2}} \int d^3\rho U(\sqrt{2\rho}) \left(e^{-\alpha^2 \rho^2} \right) \\
 b &= \frac{3\alpha}{\pi^{3/2}} \int d^3\rho U(\sqrt{2\rho}) \left(e^{-\alpha^2 \rho^2} \right) \rho^2 \\
 c &= \frac{3\alpha}{\pi^{3/2}} \int d^3\rho U(\sqrt{2\rho}) \left(e^{-\alpha^2 \rho^2} \right) \rho^4
 \end{aligned} \tag{3.8}$$

where α was defined as

$$\alpha = (3Km)^{1/4} \tag{3.9}$$

Expectation values are taken with the U operator on harmonic oscillator wave functions

$$\langle \psi | U(\sqrt{2\rho}) | \psi \rangle \tag{3.10}$$

and with the integrand still unsolved because of the unknown nature of U, the energy is computed in terms of the integrals a, b and c.

The masses of the $N = 2$ multiplets were expressed in terms of the results of the above computation as follows:⁹

$$E[56,0^+] = E_0 + 2\Omega - \Delta \quad (3.11)$$

$$E[70,0^+] = E_0 + 2\Omega - \frac{1}{2}\Delta \quad (3.12)$$

$$E[56,2^+] = E_0 + 2\Omega - \frac{2}{5}\Delta \quad (3.13)$$

$$E[70,2^+] = E_0 + 2\Omega - \frac{1}{5}\Delta \quad (3.14)$$

$$E[20,1^+] = E_0 + 2\Omega \quad (3.15)$$

where $E_0 = 3m + 3\omega + a$; $\Omega = \omega - \frac{1}{2}a - \frac{1}{3}b$; $\Delta = -\frac{5}{4}a + \frac{5}{3}b - \frac{1}{3}c$

$$(3.16)$$

and

$$\omega = (3K/m)^{\frac{1}{2}} \quad (3.17)$$

As emphasized by Isgur and Karl,⁹ the pattern of splitting is actually independent of the form of U . The negative sign given to Δ was deliberately assigned in order to make the level of $[20,1^+]$ the highest and $[56,0^+]$ the lowest, but since the energy differences are expressed in terms of the moments a , b and c , the explicit form of U is neatly avoided. Thus, while the perturbative effect of U splits the degeneracy at $N = 2$, the unknown nature of U itself does not hinder the splitting.

3.3 The Consistent Quark Model

The inconsistency of the Isgur-Karl model (Chapter II) was to use different values for the parameters for computing

the energy levels of the ground state, the first excited positive parity state, and the negative parity P states of baryons separately.⁶ As pointed out by Kalman and Hall¹⁰ and by Kalman,¹¹ the fault lay in computing the U term in the SU(3) limit of $m_u = m_d = m_s$. The consistent quark model (Kalman and Hall¹⁰) resolves this inconsistency by allowing for quark mass differences. The significance of this adjustment needs to be emphasized. When determining the energy levels of baryons of unequal quark masses, a problem which is going to be progressively more engaging as higher energy accelerators produce heavier particles with combinations of all six quarks and antiquarks, one will require several experimentally determined particle masses to fit to in order to obtain parameter values. Yet, with few energy levels known, the same difficulty will arise as was faced by Isgur and Karl with respect to mesons in 1978 - viz. too many parameters and too few known masses. However, if the same parameter set is used for both positive and negative parity particles, a substantially larger volume of known data becomes progressively available.

The second major contribution of the consistent quark model is to enable one to use the parameters obtained by fitting to levels of one baryon in computing the levels of a second baryon. What is significant in this contribution is that it emphasizes the flavour independence of the model inasmuch as the two baryons may have very different quark content. Kalman and Pfeffer used the model successfully to

compute the energy levels, firstly of baryons containing one charmed quark, and then of baryons containing one beauty quark, in both cases using the selfsame set of parameters that was developed for baryons containing neither charm nor beauty quark. This technique involves the computation of the parameters of the U term.

The constants of the U term - viz. a, b and c - were defined in (3.8). Let these parameters be redefined as being those of the first baryon:

$$\begin{aligned} a(1) &= a \\ b(1) &= b \\ c(1) &= c \end{aligned} \quad (3.18)$$

The corresponding parameters for the second baryon are defined as:

$$\begin{aligned} a(s) &= \frac{3\alpha^3 s^{3/2}}{\pi^{3/2}} \int d^3 \rho U(\sqrt{2}\rho) \exp(-s\alpha^2 \rho^2) \\ b(s) &= \frac{3\alpha^5 s^{5/2}}{\pi^{3/2}} \int d^3 \rho U(\sqrt{2}\rho) \exp(-s\alpha^2 \rho^2) \rho^2 \\ c(s) &= \frac{3\alpha^7 s^{7/2}}{\pi^{3/2}} \int d^3 \rho U(\sqrt{2}\rho) \exp(-s\alpha^2 \rho^2) \rho^4 \end{aligned} \quad (3.19)$$

The factor s is the link between α of baryon #1 to α of baryon #2:

$$(\alpha')^2 = \alpha^2 s \quad (3.20)$$

From the definition of α in (3.9) it is simple to show from (3.20) that for baryons containing quarks of equal masses

$$s = \left(\frac{m'}{m}\right)^{\frac{1}{2}} \quad (3.21)$$

where m and m' are the masses of the quarks in baryons 1 and 2 respectively. The corresponding expressions for baryons of unequal mass quarks are slightly more complicated but are unnecessary for formulation in meson spectra of the Charmonium type which we are primarily concerned with.

For baryons, Isgur and Karl⁶ obtain

$$L = 0, E(S) = 3m + 3\omega + a$$

$$L = 1, E(P) = 3m + 4\omega + \frac{a}{2} + \frac{b}{3}$$

$$L = 2, E(S') = 3m + 5\omega + \frac{5a}{4} - b + \frac{c}{3} \quad (3.22)$$

and, using $\omega = 250\text{MeV}$ and $m = m_u = m_d = 350\text{MeV}$ (Isgur and Karl⁶), we obtain

$$a(1) = -650\text{MeV}, b(1) = -405\text{MeV}, \text{ and } c(1) = -908\text{MeV} \quad (3.23)$$

By constructing quadratic approximations about $s = 1$ for $a(s)$, $b(s)$, and $c(s)$ we find from (3.22) and (3.23) that

$$a(s) = A + Bs + Cs^2$$

$$b(s) = \frac{1}{2}(3A + Bs - Cs^2)$$

$$c(s) = \frac{1}{4}(15A + 3Bs - Cs^2) \quad (3.24)$$

$$\text{where } A = -170, B = -390, \text{ and } C = -90\text{MeV} \quad (3.25)$$

*These parameters were obtained by Kalman, Hall and

Misra¹⁵ using the original parameters of Isgur and Karl. Subsequently, Kalman and Hall¹⁰, and Kalman¹¹, worked out a uniform parameter set which was used to compute both the positive and negative parity states. (The technique of quadratic approximation will be fully explained in the next chapter, although in this research the approximation is quartic).

We now have the explicit expressions for the parameters of the U term for any baryon in terms of the corresponding parameters of any other baryon, the dependence being solely on the ratio of the quark masses of the two baryons. This feature of the consistent quark model further emphasizes the flavour independence of the DGG and I-K models on which the consistent quark model is based.

CHAPTER IV.

4.1 Baryons to Mesons

The consistent quark model, as developed in outline in the last chapter, was used by Kalman, Hall and Misra¹⁵ and by Kalman and Misra¹⁹ to examine baryonia. The present research has been on applying the model to mesons: in particular to the Charmonium and Upsilon systems.

It was suggested by Isgur in 1978 that the low-lying energy states of mesons could be computed in the I-K model from a baryonic perspective - i.e. by using baryon parameters as a starting point and obtaining corresponding meson parameters from them. This approach was attempted by Kalman and Barbari.²⁰ While the results conclusively showed that the same forces occur in both mesons and baryons, the mass predictions were not very accurate. The present research deals with mesons ab initio: based on the consistent quark model, the low-lying energy states of Charmonium are computed using a harmonic-oscillator confining potential perturbed by the unknown anharmonic potential U with fine and hyperfine corrections. In the case of baryons, Isgur and Karl⁹ neglected spin-orbit effects, as has been explained in Chapter II, due to the tendency of the two spin-orbit terms to mutually cancel. This suggestion is considered in detail by Schnitzer.²¹ He notes that the sum of the two spin-orbit terms depends on $\langle r \rangle_{\text{hadron}}$: "Since $\langle r \rangle_{\text{baryon}}$ is somewhat larger than $\langle r \rangle_{\text{qq}}$, one understands why the coefficient of $\vec{L} \cdot \vec{S}$ is absent in the Isgur-Karl model of baryons, is weakly

attractive for ordinary mesons, and is more strongly attractive for Charmonium." In view of Schnitzer's findings spin-orbit effects have been included in the meson Hamiltonian.

After computing the energy levels of Charmonium, the consistent quark model is used to evaluate the energies of the low-lying levels of beautyonium (Upsilon).

4.2 The Meson Hamiltonian

Each of the two systems investigated, ψ and T , has an equal mass quark and antiquark. The Hamiltonian has the form

$$H = 2m_Q + (H_0 + H_{\text{hyp}} + H_{\text{SO}}) \sum_{\alpha} \Lambda_1^{\alpha} (-\Lambda_2^{*\alpha}), \quad (4.1)$$

where m_Q is the mass of the c quark (antiquark) for the ψ system and of the b quark (antiquark) for the T system.

$$H_0 = \sum \frac{\vec{p}_i^2}{2m_Q} + V - \frac{\left[\sum_i \vec{p}_i \right]^2}{4m_Q} \quad (4.2)$$

$$H_{\text{hyp}} = \frac{4\alpha_s}{3m_Q^2} \left\{ \frac{8\pi}{3} (\vec{S}_1 \cdot \vec{S}_2) \delta^3(\vec{r}) + \frac{1}{r^3} \left[\frac{3(\vec{S}_1 \cdot \vec{r})(\vec{S}_2 \cdot \vec{r})}{r^2} - \vec{S}_1 \cdot \vec{S}_2 \right] \right\}, \quad (4.3)$$

where r is the interquark distance and \vec{p} , \vec{S}_1 , \vec{S}_2 and $\Lambda^{\alpha} (-\Lambda^{*\alpha})$ are the momenta, spins, and colour vectors of the quark (antiquark), and α_s is the running coupling constant.

$$H_{\text{so}} = H_{\text{so}(1G)} + H_{\text{so}(HO)} , \quad (4.4)$$

$$H_{\text{so}(1G)} = \frac{4\alpha_s}{3m_Q^2 r^3} \left[(\vec{S}_1 \cdot \vec{r} \times \vec{p}_1 - \vec{S}_2 \cdot \vec{r} \times \vec{p}_2 - 2\vec{S}_1 \cdot \vec{r} \times \vec{p}_2 + 2\vec{S}_2 \cdot \vec{r} \times \vec{p}_1) \right] , \quad (4.5)$$

which can also be written as

$$H_{\text{so}(1G)} = \frac{2\alpha_s}{m_Q^2 r^3} \vec{L} \cdot \vec{S} \quad (4.6)$$

where $\vec{S} = \vec{S}_1 + \vec{S}_2$ is the total quark intrinsic spin and \vec{L} is the relative orbital angular momentum of the quark-antiquark pair;

$$H_{\text{so}(HO)} = -\frac{1}{r} \frac{dV}{dr} \frac{\vec{L} \cdot \vec{S}}{m_Q} \quad (4.7)$$

which can also be written as

$$H_{\text{so}(HO)} = -\frac{2K}{m_Q} \vec{L} \cdot \vec{S} \quad (4.8)$$

where

$$K = \frac{\omega}{4} m_Q \quad (4.9)$$

and ω is the frequency of the single harmonic oscillator binding the quark and antiquark;

$$V = \frac{1}{2}kr^2 + U(r) , \quad (4.10)$$

where, by colour averaging,⁹ we have $2K = -\frac{4}{3} k$

where $U(r)$ is the unknown anharmonic potential which perturbs the harmonic oscillator potential.

4.3 The Harmonic-Oscillator Potential

The harmonic-oscillator wave functions for the low-lying meson states are as follows:

$$\psi_{000} = \frac{\beta^{3/2}}{\pi^{3/4}} \exp(-\frac{1}{2}\beta^2 r^2) \quad (4.11)$$

$$\psi_{11m} = \left(\frac{2}{3}\right)^{1/2} \frac{2\beta^{5/2}}{\pi^{1/4}} r \exp(-\frac{1}{2}\beta^2 r^2) Y_{1m}(\theta, \phi) \quad (4.12)$$

$$\psi_{200} = \left(\frac{2}{3}\right)^{1/2} \frac{\beta^{3/2}}{\pi^{3/4}} \left(\frac{3}{2} - \beta^2 r^2\right) \exp(-\frac{1}{2}\beta^2 r^2) \quad (4.13)$$

$$\psi_{22m} = \frac{4\beta^{7/2}}{\sqrt{15} \pi^{1/4}} r^2 \exp(-\frac{1}{2}\beta^2 r^2) Y_{2m}(\theta, \phi) \quad (4.14)$$

$$\psi_{31m} = \frac{4\beta^{5/2}}{\sqrt{15} \pi^{1/4}} r \left(\frac{5}{2} - \beta^2 r^2\right) \exp(-\frac{1}{2}\beta^2 r^2) Y_{1m}(\theta, \phi) \quad (4.15)$$

$$\psi_{33m} = 4\sqrt{\frac{2}{105}} \frac{\beta^{9/2}}{\pi^{1/4}} r^3 \exp(-\frac{1}{2}\beta^2 r^2) Y_{3m}(\theta, \phi) \quad (4.16)$$

$$\psi_{400} = 2\sqrt{\frac{2}{15}} \frac{\beta^{3/2}}{\pi^{3/4}} \left(\frac{15}{8} - \frac{5}{2}\beta^2 r^2 + \frac{\beta^4 r^4}{2}\right) \exp(-\frac{1}{2}\beta^2 r^2) \quad (4.17)$$

$$\psi_{42m} = 4\sqrt{\frac{2}{105}} \frac{\beta^{7/2}}{\pi^{1/4}} r^2 \left(\frac{7}{2} - \beta^2 r^2\right) \exp(-\frac{1}{2}\beta^2 r^2) Y_{2m}(\theta, \phi) \quad (4.18)$$

$$\psi_{44m} = \frac{8}{3\sqrt{105}} \frac{\beta^{11/2}}{\pi^{1/4}} r^4 \exp(-\frac{1}{2}\beta^2 r^2) Y_{4m}(\theta, \phi) \quad (4.19)$$

where

$$\beta = (Km_Q)^{1/2} \quad (4.20)$$

The contribution of the harmonic oscillator potential to the energy of each state is given by

$$E_0 = \left(n + \frac{3}{2}\right)\omega \quad (4.21)$$

4.4 The Anharmonic Potential (Mesons)

Calculation of the anharmonic part of the potential $U(r)$ for different values of β - i.e. for different mesons, each with its own flavour of quark-antiquark pair - have been discussed by Kalman, Hall and Misra.¹⁵

First, we define moments of $U(r)$ by setting

$$a(t) = \frac{\beta^3 t^{3/2}}{\pi^{3/2}} \int d^3 r U(r) \exp(-t\beta^2 r^2) \quad (4.22)$$

$$b(t) = \frac{\beta^5 t^{5/2}}{\pi^{3/2}} \int d^3 r U(r) \exp(-t\beta^2 r^2) r^2 \quad (4.23)$$

$$c(t) = \frac{\beta^7 t^{7/2}}{\pi^{3/2}} \int d^3 r U(r) \exp(-t\beta^2 r^2) r^4 \quad (4.24)$$

$$d(t) = \frac{\beta^9 t^{9/2}}{\pi^{3/2}} \int d^3 r U(r) \exp(-t\beta^2 r^2) r^6 \quad (4.25)$$

$$e(t) = \frac{\beta^{11} t^{11/2}}{\pi^{3/2}} \int d^3 r U(r) \exp(-t\beta^2 r^2) r^8 \quad (4.26)$$

For Charmonium we set $t = 1$ so that we have

$$\begin{aligned} a &= a(1) \\ b &= b(1) \\ c &= c(1) \\ d &= d(1) \\ e &= e(1) \end{aligned} \quad (4.27)$$

where a, b, c, d and e are five of the basic parameters needed to be set from experimental data. For the T system we construct quartic approximations about $t = 1$ for $a(t)$,

$b(t)$, $c(t)$, $d(t)$ and $e(t)$.

The technique of quartic approximation is as follows:

We define

$$f(t) = \frac{\beta^3}{\pi^{3/2}} \int d^3 r U(r) \exp(-t\beta^2 r^2) \quad (4.28)$$

so that we have $a(t) = t^{3/2} f(t)$ which we define as $g(t)$

$$a(t) = t^{3/2} f(t) = g(t) \quad (4.29)$$

It follows that

$$\begin{aligned} b(t) &= -t^{5/2} f'(t) \\ c(t) &= t^{7/2} f''(t) \\ d(t) &= -t^{9/2} f'''(t) \\ e(t) &= t^{11/2} f''''(t) \end{aligned} \quad (4.30)$$

and

$$\begin{aligned} f(1) &= a \\ f'(1) &= -b \\ f''(1) &= c \\ f'''(1) &= -d \\ f''''(1) &= e \end{aligned} \quad (4.31)$$

By further differentiation with respect to t we obtain

$$\begin{aligned} g'(t) &= \frac{3}{2} t^{1/2} f(t) + t^{3/2} f'(t) \\ g''(t) &= \frac{3}{4} t^{-1/2} f(t) + 3t^{1/2} f'(t) + t^{3/2} f''(t) \end{aligned}$$

$$\begin{aligned}
g'''(t) &= -\frac{3}{8} t^{-3/2} f(t) + \frac{9}{4} t^{-1/2} f'(t) + \frac{9}{2} t^{1/2} f''(t) \\
&\quad + t^{3/2} f'''(t) \\
g''''(t) &= \frac{9}{16} t^{-5/2} f(t) - \frac{3}{2} t^{-3/2} f'(t) + \frac{9}{2} t^{-1/2} f''(t) \\
&\quad + 6t^{1/2} f'''(t) + t^{3/2} f''''(t) \tag{4.32}
\end{aligned}$$

We now expand $g(t)$ in a Taylor series expansion around $t = 1$ up to the fifth term:

$$\begin{aligned}
g(t) &\doteq g(1) + (t-1)g'(1) + \frac{(t-1)^2}{2!} g''(1) + \frac{(t-1)^3}{3!} g'''(1) \\
&\quad + \frac{(t-1)^4}{4!} g''''(1) \tag{4.33}
\end{aligned}$$

Substituting $t = 1$ in (4.29), (4.30) and (4.32), and using (4.31) we obtain

$$\begin{aligned}
g(t) &\doteq a + (t-1) \left(\frac{3}{2}a-b \right) + \frac{(t-1)^2}{2} \left(\frac{3}{4}a-3b+c \right) \\
&\quad + \frac{(t-1)^3}{6} \left(-\frac{3}{8}a - \frac{9}{4}b + \frac{9}{2}c - d \right) \\
&\quad + \frac{(t-1)^4}{24} \left(\frac{9}{16}a + \frac{3}{2}b + \frac{9}{2}c - 6d + e \right) \tag{4.34}
\end{aligned}$$

After expanding and gathering like terms, we get

$$g(t) = A + Bt + Ct^2 + Dt^3 + Et^4 \tag{4.35}$$

where

$$A = -\frac{5}{128}a - \frac{b}{16} - \frac{c}{16} - \frac{d}{12} + \frac{e}{24}$$

$$B = \frac{15}{32}a + \frac{5}{8}b + \frac{c}{2} + \frac{d}{2} - \frac{e}{6}$$

$$C = \frac{45}{64}a - \frac{5}{8}c - d + \frac{e}{4}$$

$$D = -\frac{5}{32}a - \frac{5}{8}b + \frac{5}{6}d - \frac{e}{6}$$

$$E = \frac{3}{128}a + \frac{b}{16} + \frac{3}{16}c - \frac{d}{4} + \frac{e}{24} \quad (4.36)$$

By differentiating (4.35) with respect to t and once more using (4.29) and (4.30) we obtain

$$f(t) = t^{-3/2} (A + Bt + Ct^2 + Dt^3 + Et^4)$$

$$f'(t) = \frac{1}{2}t^{-5/2} (-3A - Bt + Ct^2 + 3Dt^3 + 5Et^4)$$

$$f''(t) = \frac{1}{4}t^{-7/2} (15A + 3Bt - Ct^2 + 3Dt^3 + 15Et^4)$$

$$f'''(t) = \frac{1}{8}t^{-9/2} (-105A - 15Bt + 3Ct^2 - 3Dt^3 + 15Et^4)$$

$$f''''(t) = \frac{1}{16}t^{-11/2} (945A + 105Bt - 15Ct^2 + 9Dt^3 - 15Et^4) \quad (4.37)$$

and finally, the quartic approximation

$$a(t) = A + Bt + Ct^2 + Dt^3 + Et^4$$

$$b(t) = \frac{1}{2}(3A + Bt - Ct^2 - 3Dt^3 - 5Et^4)$$

$$c(t) = \frac{1}{4}(15A + 3Bt - Ct^2 + 3Dt^3 + 15Et^4)$$

$$d(t) = \frac{1}{8}(105A + 15Bt - 3Ct^2 + 3Dt^3 - 15Et^4)$$

$$e(t) = \frac{1}{16}(945A + 105Bt - 15Ct^2 + 9Dt^3 - 15Et^4) \quad (4.38)$$

The values of A, B, C, D and E are obtained from a, b, c, d and e by setting $t = 1$ in (4.38). Thus the parameters for the T system are derived from those of the Charmonium system by setting

$$t = \left[\frac{m_b}{m_c} \right]^{1/2} \quad (4.39)$$

where m_b and m_c are the masses of the beauty quark (antiquark) and charm quark (antiquark) respectively.

It now follows from equations (4.1), (4.11) to (4.19), (4.21) and (4.22) to (4.26) that the total contribution to the energy excluding mixing, hyperfine, and spin-orbit effects is

$$E_0(S) = 2m_Q + \frac{3}{2}\omega + a(t) \quad (4.40)$$

$$E_0(P) = 2m_Q + \frac{5}{2}\omega + \frac{2}{3}b(t) \quad (4.41)$$

$$E_0(S') = 2m_Q + \frac{7}{2}\omega + \frac{3}{2}a(t) - 2b(t) + \frac{2}{3}c(t) \quad (4.42)$$

$$E_0(D) = 2m_Q + \frac{7}{2}\omega + \frac{4}{15}c(t) \quad (4.43)$$

$$E_0(P') = 2m_Q + \frac{9}{2}\omega + \frac{5}{3}b(t) - \frac{4}{3}c(t) + \frac{4}{15}d(t) \quad (4.44)$$

$$E_0(F) = 2m_Q + \frac{9}{2}\omega + \frac{8}{105}d(t) \quad (4.45)$$

$$E_0(S'') = 2m_Q + \frac{11}{2}\omega + \frac{15}{8}a(t) - 5b(t) + \frac{13}{3}c(t) - \frac{4}{3}d(t) + \frac{2}{15}e(t) \quad (4.46)$$

$$E_0(D') = 2m_Q + \frac{11}{2}\omega + \frac{14}{15}c(t) - \frac{8}{15}d(t) + \frac{8}{105}e(t) \quad (4.47)$$

$$E_0(G) = 2m_Q + \frac{11}{2}\omega + \frac{16}{945}e(t) \quad (4.48)$$

In evaluating the $U(r)$ anharmonic perturbation contribution for each of the equations (4.40) to (4.48) we have computed expectation values with each respective harmonic oscillator wave function of which a sample calculation is shown in Appendix A. These equations give us the diagonal elements of energy matrices before including the fine and hyperfine corrections. Off-diagonal contributions also occur from the mixing between different energy levels.

There are five mixing terms up to $n = 4$. They are as follows:

$$\langle S | U | S' \rangle = \langle S' | \tilde{U} | S \rangle = \sqrt{\frac{3}{2}}a(t) - \sqrt{\frac{2}{3}}b(t) \quad (4.49)$$

$$\begin{aligned} \langle S | U | S'' \rangle = \langle S'' | U | S \rangle &= \sqrt{\frac{15}{8}}a(t) - \sqrt{\frac{10}{3}}b(t) \\ &+ \sqrt{\frac{2}{15}}c(t) \end{aligned} \quad (4.50)$$

$$\begin{aligned} \langle S' | U | S'' \rangle = \langle S'' | U | S' \rangle &= \frac{3\sqrt{5}}{4}a(t) - \frac{3\sqrt{5}}{2}b(t) \\ &+ \frac{13}{3\sqrt{5}}c(t) - \frac{2}{3\sqrt{5}}d(t) \end{aligned} \quad (4.51)$$

$$\langle P' | U | P \rangle = \langle P | U | P' \rangle = \sqrt{\frac{10}{9}}b(t) - \sqrt{\frac{8}{45}}c(t) \quad (4.52)$$

$$\langle D' | U | D \rangle = \langle D | U | D' \rangle = \frac{4\sqrt{7}}{15\sqrt{2}}c(t) - \frac{4\sqrt{2}}{15\sqrt{7}}d(t) \quad (4.53)$$

This completes all the contributions of the anharmonic perturbation to the confinement potential up to $n = 4$.

CHAPTER V.

5.1 The Spin Dependent Terms

The last two terms of the Hamiltonian of the consistent quark model come from the spin-spin effects (hyperfine) and the spin-orbit effects (fine). These two terms are derived in QCD similar to their derivation in QED. We will look at a qualitative view of these two terms before outlining the main features of their mathematical formulation.

Each spinning quark in the meson is a miniature colour magnet or dipole. Two types of interactions stem from a pair of dipoles. The first of these is well known - the macroscopic effect of one magnet with another. This occurs when one magnet reacts to the external magnetic field of the other - $\vec{\mu}_i \cdot \vec{B}_{\text{external}}^j$ (Fig. 9)

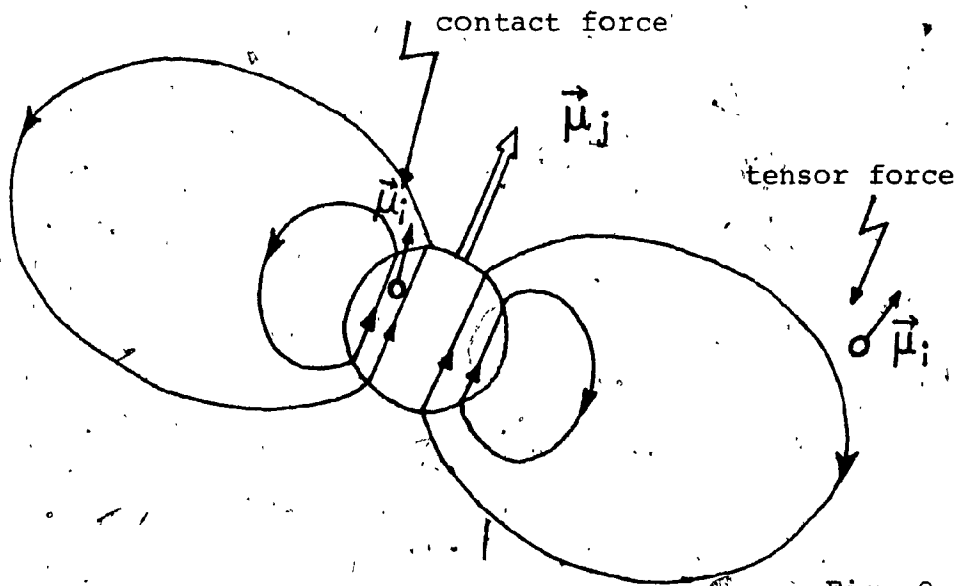


Fig. 9.

Contact and Tensor forces of Hyperfine Interaction,

In the diagram it is clear that colour magnet $\vec{\mu}_i$ reacts to this external force of colour magnet $\vec{\mu}_j$ only when it is at some distance away from it. This is the tensor part of the hyperfine interaction. It occurs when the quarks are not in a relative S wave.

The second type of dipole-dipole interaction occurs when they are in close proximity to one another - the Fermi contact term. In such a situation magnet $\vec{\mu}_i$ is reacting to the internal magnetic field of magnet $\vec{\mu}_j$ - the interaction being $\vec{\mu}_i \cdot \vec{B}_i^j$ internal. In the diagram this is illustrated with $\vec{\mu}_i$ in the left position. The contact force only occurs when the two quarks are in a relative S wave, in which situation the tensor force is non-existent. As an illustrative example of the contact force we may cite the 21 cm. line of the hydrogen atom. In the ground state it is in an S wave where tensor forces are absent: it is the contact force which yields the line when the atom decays from the triplet state to the singlet state.

The spin-orbit effect of the meson arises from the relative motion of one quark about the other in the rest frame of the second quark. Just as a charge carrying, spinning electron orbiting a charged nucleus in an atom is subjected to a torque $\vec{L} \cdot \vec{S}$ force, so a charge carrying, spinning quark orbiting a charged second quark is subjected to a similar torque force. In QCD this torque would arise due to one colour magnet (first quark) travelling within the chromoelectric field of the second quark. In the atom the

force is mediated between electron and nucleus by a photon, in a meson by a gluon.

The formulation of the spin-spin and spin-orbit portions of the Hamiltonian in equation (4.1) can be obtained conveniently if we proceed analogously from QED to QCD. Since this formulation is not an integral part of the work done in this research, it is shown in Appendix G. The explicit expressions which are used in the calculation of spin-dependent terms are obtained from the equations of Appendix G as shown below.

5.2 Explicit Expressions for Hyperfine and Spin-Orbit Terms

5.2.1 Contact Terms

Combining equations (G.33) and (G.34), and including the gluon coupling for colour wave functions $-(4/3)\alpha_s$ from equation (G.7), noting that $\vec{S}_1 = \frac{\vec{\sigma}_a}{2}$, $\vec{S}_2 = \frac{\vec{\sigma}_b}{2}$ and (for Charmonium and Upsilon) $m_a = m_b = m_Q$, we have, for the Fermi contact term

$$H_{\text{hyp}}^{\text{con}} = \frac{4\alpha_s}{3m_Q} \left(\frac{8\pi}{3} \vec{S}_1 \cdot \vec{S}_2 \delta^3(r) \right) \quad (5.1)$$

Since the contact force operates only between S-states, we compute the expectation values of the S-states with the operator (5.1) operating on the S-state harmonic oscillator

wave functions. A sample calculation for a contact term is given in Appendix B.

For simplicity, a factor δ_Q has been included in the expressions where

$$\delta_Q = \frac{4\alpha_s \beta^3}{3\sqrt{2}\pi m_Q^2} \quad (5.2)$$

the factor β having been defined in equation (4.20).

The Charmonium δ_c and the Upsilon δ_b are related by

$$\delta_b = \left(\frac{m_c}{m_b}\right)^{5/4} \delta_c \quad (5.3)$$

where m_c and m_b are the masses of the charm and beauty quarks respectively.

The contact term has a radial part and a spin part. For the $S = 1$ triplet state, the expectation value of the spin part is

$$\langle {}^3S_1 | \vec{S}_1 \cdot \vec{S}_2 | {}^3S_1 \rangle = \frac{1}{4} \quad (5.4)$$

and for the $S = 0$ singlet state, the expectation value of the spin part is

$$\langle {}^1S_0 | \vec{S}_1 \cdot \vec{S}_2 | {}^1S_0 \rangle = -\frac{3}{4} \quad (5.5)$$

The expressions for the contact terms are:

$$\langle S | H_{\text{cont}} | S \rangle = \frac{2}{3} \delta_Q \langle |\vec{S}_1 \cdot \vec{S}_2| \rangle \quad (5.6)$$

$$\langle S' | H_{\text{cont}} | S' \rangle = 2 \delta_Q \langle |\vec{S}_1 \cdot \vec{S}_2| \rangle \quad (5.7)$$

$$\langle S'' | H_{\text{cont}} | S'' \rangle = 5/2 \delta_Q \langle |\vec{S}_1 \cdot \vec{S}_2| \rangle \quad (5.8)$$

with the following mixtures between different S-states:

$$\langle S | H_{\text{cont}} | S' \rangle = \langle S' | H_{\text{cont}} | S \rangle = \frac{8}{\sqrt{3}} \delta_Q \langle |\vec{S}_1 \cdot \vec{S}_2| \rangle \quad (5.9)$$

$$\langle S | H_{\text{cont}} | S'' \rangle = \langle S'' | H_{\text{cont}} | S \rangle = \frac{4\sqrt{15}}{3} \delta_Q \langle |\vec{S}_1 \cdot \vec{S}_2| \rangle \quad (5.10)$$

$$\langle S' | H_{\text{cont}} | S'' \rangle = \langle S'' | H_{\text{cont}} | S' \rangle = \frac{4\sqrt{5}}{\sqrt{2}} \delta_Q \langle |\vec{S}_1 \cdot \vec{S}_2| \rangle \quad (5.11)$$

5.2.2 Tensor Terms

The tensor term arises for all non-S-states. Mixing of tensors occurs between all even parity states or between all odd parity states. There is no mixing between odd and even parity states.

The tensor operator is obtained from equations (G.38) and (G.39). Inserting the one-gluon Coulomb type potential from (G.30) in (G.38), again noting that $\vec{S}_1 = \frac{\vec{\sigma}_a}{2}$, $\vec{S}_2 = \frac{\vec{\sigma}_b}{2}$, $m_a = m_b = m_Q$, and including the one gluon colour coupling from (G.7) we obtain the tensor operator

$$H_{\text{hyp}}^{\text{tens}} = \frac{4\alpha_s}{3m_Q r^3} \left\{ \frac{3(\vec{S}_1 \cdot \vec{r})(\vec{S}_2 \cdot \vec{r})}{r^2} - \vec{S}_1 \cdot \vec{S}_2 \right\} \quad (5.12)$$

The tensor term has a non-zero contribution only for a vector potential, there is no contribution for a scalar potential.

To evaluate the tensor terms, following Isgur and Karl, we make use of the identity

$$\langle LSJ | \frac{3\vec{S}_1 \cdot \hat{r} \vec{S}_2 \cdot \hat{r} - \vec{S}_1 \cdot \vec{S}_2}{r^3} | L' S' J \rangle =$$

$$(-)^{(J-L-S')} [(2L+1)(2S+1)]^{1/2} W(LL'SS'; 2J)$$

$$\langle L || \frac{\sqrt{3}}{2r^3} \hat{r}_+ \hat{r}_+ || L' \rangle \langle S || \frac{\sqrt{3}}{2} S_{1-} S_{2-} || S' \rangle \quad (5.13)$$

where $\hat{r} = \sin \theta e^{i\phi}$, and

where W is the Racah coefficient and the last two factors are the reduced matrix elements of the tensors whose components are displayed.

A sample calculation of a tensor term is shown in Appendix C. The expectation values of the unmixed tensor terms are:

$$\langle {}^1P_1 | H_{\text{tens}} | {}^1P_1 \rangle = 0 \quad (5.14)$$

$$\langle {}^3P_0 | H_{\text{tens}} | {}^3P_0 \rangle = -\frac{4\sqrt{2}}{3} \delta_Q \quad (5.15)$$

$$\langle {}^3P_1 | H_{\text{tens}} | {}^3P_1 \rangle = \frac{2\sqrt{2}}{3} \delta_Q \quad (5.16)$$

$$\langle {}^3P_2 | H_{\text{tens}} | {}^3P_2 \rangle = -\frac{2\sqrt{2}}{15} \delta_Q \quad (5.17)$$

$$\langle {}^1D_2 | H_{\text{tens}} | {}^1D_2 \rangle = 0 \quad (5.18)$$

$$\langle {}^3D_1 | H_{\text{tens}} | {}^3D_1 \rangle = -\frac{4\sqrt{2}}{15} \delta_Q \quad (5.19)$$

$$\langle {}^3D_2 | H_{\text{tens}} | {}^3D_2 \rangle = +\frac{4\sqrt{2}}{15} \delta_Q \quad (5.20)$$

$$\langle {}^3D_3 | H_{\text{tens}} | {}^3D_3 \rangle = -\frac{8\sqrt{2}}{105} \delta_Q \quad (5.21)$$

$$\langle {}^3P'_0 | H_{\text{tens}} | {}^3P'_0 \rangle = -\frac{26\sqrt{2}}{15} \delta_Q \quad (5.22)$$

$$\langle {}^3P'_1 | H_{\text{tens}} | {}^3P'_1 \rangle = \frac{13\sqrt{2}}{15} \delta_Q \quad (5.23)$$

$$\langle {}^3P'_2 | H_{\text{tens}} | {}^3P'_2 \rangle = -\frac{13\sqrt{2}}{75} \delta_Q \quad (5.24)$$

$$\langle {}^3F_2 | H_{\text{tens}} | {}^3F_2 \rangle = \frac{64\sqrt{2}}{525} \delta_Q \quad (5.25)$$

$$\langle {}^3F_3 | H_{\text{tens}} | {}^3F_3 \rangle = \frac{16\sqrt{2}}{105} \delta_Q \quad (5.26)$$

$$\langle {}^3F_4 | H_{\text{tens}} | {}^3F_4 \rangle = -\frac{16\sqrt{2}}{315} \delta_Q \quad (5.27)$$

$$\langle {}^3D'_1 | H_{\text{tens}} | {}^3D'_1 \rangle = -\frac{34\sqrt{2}}{105} \delta_Q \quad (5.28)$$

$$\langle {}^3D'_2 | H_{\text{tens}} | {}^3D'_2 \rangle = +\frac{34\sqrt{2}}{105} \delta_Q \quad (5.29)$$

$$\langle {}^3D'_3 | H_{\text{tens}} | {}^3D'_3 \rangle = -\frac{68\sqrt{2}}{735} \delta_Q \quad (5.30)$$

$$\langle {}^3G_3 | H_{\text{tens}} | {}^3G_3 \rangle = -\frac{32\sqrt{2}}{441} \delta_Q \quad (5.31)$$

$$\langle {}^3G_4 | H_{\text{tens}} | {}^3G_4 \rangle = \frac{32\sqrt{2}}{315} \delta_Q \quad (5.32)$$

$$\langle {}^3G_5 | H_{\text{tens}} | {}^3G_5 \rangle = - \frac{128\sqrt{2}}{315} \delta_Q \quad (5.33)$$

In addition to the above terms we have the following mixed tensor terms:

$$\langle {}^3D_1 | H_{\text{tens}} | {}^3S_1 \rangle = \langle {}^3S_1 | H_{\text{tens}} | {}^3D_1 \rangle = \frac{4}{15} \delta_Q \quad (5.34)$$

$$\langle {}^3D_1 | H_{\text{tens}} | {}^3S'_1 \rangle = \langle {}^3S'_1 | H_{\text{tens}} | {}^3D_1 \rangle = \frac{2\sqrt{2}}{3\sqrt{5}} \delta_Q \quad (5.35)$$

$$\langle {}^3P_0 | H_{\text{tens}} | {}^3P'_0 \rangle = \langle {}^3P'_0 | H_{\text{tens}} | {}^3P_0 \rangle = - \frac{4}{\sqrt{5}} \delta_Q \quad (5.36)$$

$$\langle {}^3P_1 | H_{\text{tens}} | {}^3P'_1 \rangle = \langle {}^3P'_1 | H_{\text{tens}} | {}^3P_1 \rangle = \frac{2}{\sqrt{5}} \delta_Q \quad (5.37)$$

$$\langle {}^3P_2 | H_{\text{tens}} | {}^3P'_2 \rangle = \langle {}^3P'_2 | H_{\text{tens}} | {}^3P_2 \rangle = - \frac{2}{5\sqrt{5}} \delta_Q \quad (5.38)$$

$$\langle {}^3P'_2 | H_{\text{tens}} | {}^3F_2 \rangle = \langle {}^3F_2 | H_{\text{tens}} | {}^3P'_2 \rangle = \frac{4\sqrt{42}}{175} \delta_Q \quad (5.39)$$

$$\langle {}^3P_2 | H_{\text{tens}} | {}^3F_2 \rangle = \langle {}^3F_2 | H_{\text{tens}} | {}^3P_2 \rangle = \frac{8\sqrt{3}}{5\sqrt{35}} \delta_Q \quad (5.40)$$

$$\langle {}^3D_1 | H_{\text{tens}} | {}^3D'_1 \rangle = \langle {}^3D'_1 | H_{\text{tens}} | {}^3D_1 \rangle = - \frac{4}{5\sqrt{7}} \delta_Q \quad (5.41)$$

$$\langle {}^3D_2 | H_{\text{tens}} | {}^3D'_2 \rangle = \langle {}^3D'_2 | H_{\text{tens}} | {}^3D_2 \rangle = + \frac{4}{5\sqrt{7}} \delta_Q \quad (5.42)$$

$$\langle {}^3D_3 | H_{\text{tens}} | {}^3D'_3 \rangle = \langle {}^3D'_3 | H_{\text{tens}} | {}^3D_3 \rangle = - \frac{8}{35\sqrt{7}} \delta_Q \quad (5.43)$$

$$\langle {}^3S'_1 | H_{\text{tens}} | {}^3D_1 \rangle = \langle {}^3D_1 | H_{\text{tens}} | {}^3S'_1 \rangle = \frac{\sqrt{2}}{\sqrt{5}} \delta_Q \quad (5.44)$$

$$\langle {}^3 S'_1 | H_{\text{tens}} | {}^3 D'_1 \rangle = \langle {}^3 D'_1 | H_{\text{tens}} | {}^3 S'_1 \rangle = \frac{23}{1577} \delta_Q \quad (5.45)$$

$$\langle {}^3 S'_1 | H_{\text{tens}} | {}^3 D'_1 \rangle = \langle {}^3 D'_1 | H_{\text{tens}} | {}^3 S'_1 \rangle = \frac{6}{735} \delta_Q \quad (5.46)$$

$$\langle {}^3 S_1 | H_{\text{tens}} | {}^3 D'_1 \rangle = \langle {}^3 D'_1 | H_{\text{tens}} | {}^3 S_1 \rangle = \frac{2\sqrt{10}}{\sqrt{21}} \delta_Q \quad (5.47)$$

$$\langle {}^3 D'_3 | H_{\text{tens}} | {}^3 G_3 \rangle = \langle {}^3 G_3 | H_{\text{tens}} | {}^3 D'_3 \rangle = \frac{32\sqrt{3}}{735} \delta_Q \quad (5.48)$$

$$\langle {}^3 D_3 | H_{\text{tens}} | {}^3 G_3 \rangle = \langle {}^3 G_3 | H_{\text{tens}} | {}^3 D_3 \rangle = \frac{32\sqrt{6}}{10577} \delta_Q \quad (5.49)$$

5.2.3 Spin-Orbit Terms

Spin-orbit terms come from two sources: the one-gluon exchange potential as reduced by Thomas precession, and the harmonic-oscillator potential. For the one-gluon exchange we use the potential from equation (G.30) and insert it in equation (G.36). The result is

$$H_{\text{SO}(1G)} = \frac{2\alpha_s}{m_Q^2 r^3} \vec{L} \cdot \vec{S} \quad (5.50)$$

And for the harmonic oscillator potential we use

$$V_{\text{HO}} = -\frac{4}{3} (\frac{1}{2} k r^2) = K r^2 \quad (5.51)$$

where the factor $-\frac{4}{3}$ comes from colour averaging for mesons shown in equation (2.2). Inserting equation (5.51) in equation (G.37) we obtain

$$H_{SO}(HO) = -\frac{2K}{m_Q^2} \vec{L} \cdot \vec{S} \quad (5.52)$$

where

$$K = \frac{\omega}{4} m_Q^2 \quad (5.53)$$

Expectation values for the spin-orbit terms are computed with the combined operator

$$H_{SO} = \left\{ \frac{2\alpha_s}{m_Q^2 r^3} - \frac{2K}{m_Q^2} \right\} \vec{L} \cdot \vec{S} \quad (5.54)$$

For the calculation we note the relation

$$\begin{aligned} \langle LSJM | \vec{L} \cdot \vec{S} | L'SJM' \rangle &= \frac{1}{2} [J(J+1) - L(L+1) \\ &\quad - S(S+1)] \delta_{JJ'} \delta_{LL'} \delta_{MM'} \end{aligned} \quad (5.55)$$

A sample calculation of a spin-orbit term is shown in Appendix D. The unmixed spin-orbit terms are:

$$\langle {}^1P_1 | H_{SO} | {}^1P_1 \rangle = 0. \quad (5.56)$$

$$\langle {}^3P_0 | H_{SO} | {}^3P_0 \rangle = -4\sqrt{2} \delta_Q + \frac{\omega_Q^2}{m_Q} \quad (5.57)$$

$$\langle {}^3P_1 | H_{SO} | {}^3P_1 \rangle = -2\sqrt{2} \delta_Q + \frac{\omega_Q^2}{2m_Q} \quad (5.58)$$

$$\langle {}^3P_2 | H_{SO} | {}^3P_2 \rangle = + 2\sqrt{2} \delta_Q - \frac{\omega_Q^2}{2m_Q} \quad (5.59)$$

$$\langle {}^1D_2 | H_{SO} | {}^1D_2 \rangle = 0 \quad (5.60)$$

$$\langle {}^3D_1 | H_{SO} | {}^3D_1 \rangle = - \frac{12\sqrt{2}}{5} \delta_Q + \frac{3\omega_Q^2}{2m_Q} \quad (5.61)$$

$$\langle {}^3D_2 | H_{SO} | {}^3D_2 \rangle = - \frac{4\sqrt{2}}{5} \delta_Q + \frac{\omega_Q^2}{2m_Q} \quad (5.62)$$

$$\langle {}^3D_3 | H_{SO} | {}^3D_3 \rangle = \frac{8\sqrt{2}}{5} \delta_Q - \frac{\omega_Q^2}{m_Q} \quad (5.63)$$

$$\langle {}^3P'_0 | H_{SO} | {}^3P'_0 \rangle = - \frac{26\sqrt{2}}{5} \delta_Q + \frac{\omega_Q^2}{m_Q} \quad (5.64)$$

$$\langle {}^3P'_1 | H_{SO} | {}^3P'_1 \rangle = - \frac{13\sqrt{2}}{5} \delta_Q + \frac{\omega_Q^2}{2m_Q} \quad (5.65)$$

$$\langle {}^3P'_2 | H_{SO} | {}^3P'_2 \rangle = + \frac{13\sqrt{2}}{5} \delta_Q - \frac{\omega_Q^2}{2m_Q} \quad (5.66)$$

$$\langle {}^3F_2 | H_{SO} | {}^3F_2 \rangle = - \frac{64\sqrt{2}}{35} \delta_Q + \frac{2\omega_Q^2}{m_Q} \quad (5.67)$$

$$\langle {}^3F_3 | H_{SO} | {}^3F_3 \rangle = - \frac{16\sqrt{2}}{35} \delta_Q + \frac{\omega_Q^2}{2m_Q} \quad (5.68)$$

$$\langle {}^3F_4 | H_{SO} | {}^3F_4 \rangle = \frac{48\sqrt{2}}{35} \delta_Q - \frac{3\omega_Q^2}{2m_Q} \quad (5.69)$$

$$\langle {}^3D'_1 | H_{SO} | {}^3D'_1 \rangle = - \frac{102\sqrt{2}}{35} \delta_Q + \frac{3\omega_Q^2}{2m_Q} \quad (5.70)$$

$$\langle {}^3D'_2 | H_{SO} | {}^3D'_2 \rangle = -\frac{34\sqrt{2}}{35} \delta_Q + \frac{\omega_Q^2}{2m_Q} \quad (5.71)$$

$$\langle {}^3D'_3 | H_{SO} | {}^3D'_3 \rangle = \frac{68\sqrt{2}}{35} \delta_Q - \frac{\omega_Q^2}{m_Q} \quad (5.72)$$

$$\langle {}^3G_3 | H_{SO} | {}^3G_3 \rangle = -\frac{32\sqrt{2}}{21} \delta_Q + \frac{5\omega_Q^2}{2m_Q} \quad (5.73)$$

$$\langle {}^3G_4 | H_{SO} | {}^3G_4 \rangle = -\frac{32\sqrt{2}}{105} \delta_Q + \frac{\omega_Q^2}{2m_Q} \quad (5.74)$$

$$\langle {}^3G_5 | H_{SO} | {}^3G_5 \rangle = \frac{128\sqrt{2}}{105} \delta_Q - \frac{2\omega_Q^2}{m_Q} \quad (5.75)$$

and the mixed spin-orbit terms are:

$$\langle {}^3P_0 | H_{SO} | {}^3P'_0 \rangle = \langle {}^3P'_0 | H_{SO} | {}^3P_0 \rangle = -\frac{12}{\sqrt{5}} \delta_Q \quad (5.76)$$

$$\langle {}^3P_1 | H_{SO} | {}^3P'_1 \rangle = \langle {}^3P'_1 | H_{SO} | {}^3P_1 \rangle = -\frac{6}{\sqrt{5}} \delta_Q \quad (5.77)$$

$$\langle {}^3P_2 | H_{SO} | {}^3P'_2 \rangle = \langle {}^3P'_2 | H_{SO} | {}^3P_2 \rangle = +\frac{6}{\sqrt{5}} \delta_Q \quad (5.78)$$

$$\langle {}^3D_1 | H_{SO} | {}^3D'_1 \rangle = \langle {}^3D'_1 | H_{SO} | {}^3D_1 \rangle = -\frac{36}{5\sqrt{7}} \delta_Q \quad (5.79)$$

$$\langle {}^3D_2 | H_{SO} | {}^3D'_2 \rangle = \langle {}^3D'_2 | H_{SO} | {}^3D_2 \rangle = -\frac{12}{5\sqrt{7}} \delta_Q \quad (5.80)$$

$$\langle {}^3D_3 | H_{SO} | {}^3D'_3 \rangle = \langle {}^3D'_3 | H_{SO} | {}^3D_3 \rangle = \frac{24}{5\sqrt{7}} \delta_Q \quad (5.81)$$

This completes the list of all the expressions, both unmixed and mixed, for the hyperfine and spin-orbit contributions to the energy matrix elements in terms of the parameters δ_Q , m_Q and ω_Q .

CHAPTER VI.

6.1 Publications

Three papers were submitted for publication while this work was in progress covering the three phases of the application of the consistent quark model to quarkonia. Thus far two papers have been published and have been included in this thesis as Appendices E and F.

6.2 Application of the Isgur-Karl Model to Mesons

The first paper (Appendix E) covers the initial attempt to apply the Isgur-Karl model to mesons, in particular the low-lying S states of Charmonium. Essentially, it was an effort to show that the I-K model worked for mesons as well as it did for baryons.

In the S states of Charmonium we have four well-defined experimentally known masses - the ψ (3097MeV), ψ' (3685MeV), η_c (2984MeV) and η_c' (3592MeV). Since the expression for the unknown anharmonic potential is identical for ψ and η_c , as also for ψ' and η_c' , the splitting between ψ and η_c , and again between ψ' and η_c' , is caused only by the contact term of the hyperfine interaction. And since we are dealing with S states there are no tensor terms nor spin-orbit corrections. The Hamiltonian is therefore simply

$$H = 2m_c + \sum_{\alpha} \Lambda_1^{\alpha} (-\Lambda_2^{\alpha}) [H_{HO} + H_{con}] \quad (6.1)$$

where m_c is the mass of the charm quark, and where the harmonic-oscillator term H_{HO} includes the perturbation by

the anharmonic potential $U(r)$. The problem, therefore, was to determine three unknown parameters: E_0 , which was the degenerate energy for both ψ and η_c with the exclusion of the hyperfine term; E'_0 , which was the corresponding degenerate energy for ψ' and η'_c , and δ_m , a parameter which arises in the formulation of the contact term and was defined in equation (5.2). It is repeated for convenience.

$$\delta_m = \frac{4\alpha_s \beta^3}{3\sqrt{2\pi} m_c^2} \quad (6.2)$$

The two matrices were as follows:

For ψ and ψ'

$$\begin{bmatrix} E_0 + \frac{2\sqrt{2}}{3} \delta_m & \frac{2}{\sqrt{3}} \delta_m \\ \frac{2}{\sqrt{3}} \delta_m & E_0 + \sqrt{2} \delta_m \end{bmatrix} \quad (6.3)$$

For η_c and η'_c

$$\begin{bmatrix} E_0 - 2\sqrt{2} \delta_m & -2\sqrt{3} \delta_m \\ -2\sqrt{3} \delta_m & E'_0 - 3\sqrt{2} \delta_m \end{bmatrix} \quad (6.4)$$

After determining the three unknown parameters, one final calculation was made in the first phase. The parameter

δ_m is directly related to the corresponding parameter for baryons δ_b through the harmonic oscillator spring constant which is the same for both mesons and baryons. By setting up this relationship between the value of δ_m obtained in the research and the baryon parameters obtained earlier by Kalman,¹¹ the mass of the charm quark was computed. The relevant equations were:

$$\delta_b = \frac{4\alpha_s (m_u \omega)^{3/2}}{3\sqrt{2}\pi m_u^2} \quad (6.5)$$

$$\delta_m = (m_c/m_u)^{1/2} (\omega_c/\omega_u)^{3/2} \frac{\delta_b}{2\sqrt{2}} \quad (6.6)$$

where m_u is the mass of the up quark in baryons as obtained by Kalman.¹¹ The frequency of the harmonic oscillator ω is linked to the parameter β

$$\beta^2 = \frac{1}{2} m_c \omega_c^2 \quad (6.7)$$

and the frequency of the meson oscillator ω_c is linked with the frequency of the baryon oscillator

$$\omega_c = (4m_u/3m_c)^{1/2} \omega_u \quad (6.8)$$

The results of the calculation will be discussed later in this chapter.

6.3 ψ and T Systems in a Consistent Quark Model

The second phase of the research, presented in the second paper (Appendix F) had the following objectives:

- (a) To use exclusively meson parameters,
- (b) To determine the masses of all stable states of Charmonium upto $n = 2$,
- (c) To utilise the technique of Kalman, Hall and Misra¹⁵ to calculate the parameters of the Upsilon system from the corresponding ones of the Charmonium system in keeping with the consistent quark model as outlined in Section 3.3.
- (d) To use the parameters of the Upsilon system thus obtained to determine the masses of stable states of the Upsilon system upto $n = 2$. This phase only extended upto $n = 2$ because Charmonium has stable states only upto $n = 2$, and because the U-term expansion by Kalman and Hall¹⁰ which permitted the parameters of one meson to be transposed to those of another had only been done upto $n = 2$.

The use of the consistent quark model to obtain Upsilon energy levels essentially from Charmonium parameters tested the flavour independence of the model.

All the terms of the meson Hamiltonian (4.1) were computed for the various states. In the Charmonium sector there were six unknown parameters - $m_c, \omega_c, \delta_c, a, b, c$ - and seven experimentally known states - $\psi(3S_1), \psi(3S_1), \eta_c(1S_0), \eta_c(1S_0), \chi(3P_0), \chi(3P_1), \chi(3P_2)$. In the Upsilon system there were two experimentally known states - $T(3S_1)$ and $T(3S_1)$. All the experimentally unknown states were

predicted by the calculations using only one more parameter - m_b . The results will be discussed later in this chapter.

6.4 Full Calculations for ψ and T Systems

The third phase of the research was essentially to extend the work done in the second phase upto higher energy levels - $n = 4$. There were now nine unknown parameters altogether, eight of them in the Charmonium sector ($m_c, \omega_c, \delta_c, a, b, c, d, e$) and only one in the Upsilon sector - m_b .

In the Charmonium sector there was one more - $\psi''(S_1)$ - and in the Upsilon sector eight more - $T''(S_1), T'''(S_1), T^3_{P_0}, T^3_{P_1}, T^3_{P_2}, T^3_{P_0}, T^3_{P_1}, T^3_{P_2}$ - experimentally known states available. All experimentally unknown states upto G^3_5 were predicted. The results will be presented and discussed later in this chapter.

6.5 Results

The results of the first phase are given in Appendix E. By fitting to the known masses of ψ and ψ' , the masses of η_c and η'_c were predicted with good accuracy. Using baryon data from Kalman¹¹ and using equations (6.6) and (6.8) the mass of the charm quark was obtained as $m_c = 1450\text{MeV}$.

The results of the second phase are given in Table 1 of Appendix F. In the Charmonium sector, 6 unknown parameters - a, b, c, ω, δ and m_c - were found by brute force substitution which yielded the known experimental masses of $\psi, \psi', \eta_c, \eta'_c, \chi(3415)$ and $\chi(3510)$, and predictions were made for the masses of the states P^1_1, D^3_1, D^3_2 and D^3_3 . In the Upsilon sector, since there were only two experimentally known states,

the mass of the b quark, the only new parameter, was obtained as $m_b = 6188.6$ MeV, with which the computed masses for both T and T' had only 0.018 % deviation from experimental values.

The compositions of the states after mixing in the U term, the fine and hyperfine interactions are also given in Appendix F.

For the third phase there were eight positive parity states to fit to comprising both Charmonium and Upsilon systems ($\psi, \psi', \eta_c, \eta_c', T, T', T'', T'''$) and nine negative parity states ($^3P_0, ^3P_1, ^3P_2$ in the Charmonium sector, and $^3P_0, ^3P_1, ^3P_2, ^3P_0, ^3P_1, ^3P_2$ in the Upsilon sector). There were nine parameters to be obtained to fit to all the seventeen states. The first fit was made to the positive parity states. The parameters were slightly adjusted from those obtained in the second phase. The parameters obtained were: $m_c = 2681$ MeV, $\omega_c = 502$ MeV, $\delta_c = 38$ MeV, $a = -2943$ MeV, $b = -4500$ MeV, $c = -12040$ MeV, $d = -44900$ MeV, $e = -209795$ MeV, $m_b = 6282.1$ MeV.

However, this parameter set did not give good agreement with recent ²⁶ experimental values of negative parity states. To obtain a different set of parameters for better agreement with the negative parity states the approach was made by beginning with the Upsilon system and then working towards the Charmonium system, a switch which was equally valid in the consistent quark model. This change of approach was made because the difficulty in fitting was mainly with the T P states. For the positive parity fit, the Upsilon system

parameters, computed from the Charmonium parameters given in the last paragraph by using equations (4.38), (4.39) and (5.3), together with the relation

$$\omega_b = \frac{\omega_c}{t}, \quad (6.9)$$

were $\omega_b = 328$ MeV, $\delta_b = 13.1$ MeV, $a(t) = -2964$ MeV, $b(t) = -4277$ MeV, $c(t) = -10918$ MeV, $d(t) = -39711$ MeV, $e(t) = -19717$ MeV. To obtain the better fit in the negative parity states, relatively minor adjustments were made in the parameters: $b(t)$ was decreased by 7 MeV to -4284 MeV, $d(t)$ was decreased by 2 MeV to -39713 MeV, δ_b was changed to 11.5 MeV and m_b and m_c were altered to 5976 MeV and 2704 MeV respectively. Results obtained for both positive and negative parity states are given in Tables 2 and 3.

The composition of the states after mixing in the U term, fine and hyperfine interactions were as follows:

$$\begin{aligned} |\psi\rangle = & 0.9594 |^3S_1\rangle + .2634 |^3S_1'\rangle - .0567 |^3S_1''\rangle \\ & + .0522 |^3D_1\rangle + .0655 |^3D_1'\rangle \end{aligned} \quad (6.10)$$

$$\begin{aligned} |\psi'\rangle = & -.2470 |^3S_1\rangle + .9446 |^3S_1'\rangle + .2051 |^3S_1''\rangle \\ & + .0511 |^3D_1\rangle - .0453 |^3D_1'\rangle \end{aligned} \quad (6.11)$$

$$\begin{aligned} |\psi''\rangle = & -.0418 |^3S_1\rangle - .0752 |^3S_1'\rangle + .1121 |^3S_1''\rangle \\ & + .9585 |^3D_1\rangle + .2478 |^3D_1'\rangle \end{aligned} \quad (6.12)$$

$$|\eta_c\rangle = .9726 |^1S_0\rangle - .0897 |^1S_0'\rangle - .2143 |^1S_0''\rangle \quad (6.13)$$

$$|\eta_c'\rangle = .0999 |^1S_0\rangle + .9943 |^1S_0'\rangle + .0372 |^1S_0''\rangle \quad (6.14)$$

$$|^1P_{1c}\rangle = .9060 |^1P_1\rangle + .4233 |^1P_1'\rangle \quad (6.15)$$

$$|^3P_{0c}\rangle = .9802 |^3P_0\rangle + .1982 |^3P_0'\rangle \quad (6.16)$$

$$|^3P_{1c}\rangle = .9218 |^3P_1\rangle + .3876 |^3P_1'\rangle \quad (6.17)$$

$$|^3P_{2c}\rangle = .8876 |^3P_2\rangle + .4601 |^3P_2'\rangle - .0222 |^3F_2\rangle \quad (6.18)$$

$$|^1D_{1c}\rangle = .9399 |^1D_1\rangle + .3415 |^1D_1'\rangle \quad (6.19)$$

$$|^3D_{2c}\rangle = .9443 |^3D_2\rangle + .3292 |^3D_2'\rangle \quad (6.20)$$

$$|^3D_{3c}\rangle = .9278 |^3D_3\rangle + .3731 |^3D_3'\rangle + .0004 |^3G_3\rangle \quad (6.21)$$

$$|T\rangle = .9478 |^3S_1\rangle - .2919 |^3S_1'\rangle + .1258 |^3S_1''\rangle \\ - .0343 |^3D_1\rangle + .0062 |^3D_1'\rangle \quad (6.22)$$

$$|T'\rangle = .3173 |^3S_1\rangle + .8924 |^3S_1'\rangle - .2888 |^3S_1''\rangle \\ + .1386 |^3D_1\rangle + .0187 |^3D_1'\rangle \quad (6.23)$$

$$|T''\rangle = .0137 |^3S_1\rangle - .1440 |^3S_1'\rangle + .0118 |^3S_1''\rangle \\ + .9421 |^3D_1\rangle + .3023 |^3D_1'\rangle \quad (6.24)$$

$$\begin{aligned}
 |\gamma^{iii}\rangle = & -0.0292 |^3S_1\rangle + 0.3126 |^3S_1'\rangle + 0.9486 |^3S_1''\rangle \\
 & + 0.268 |^3D_1\rangle + 0.0272 |^3D_1'\rangle
 \end{aligned}
 \tag{6.25}$$

$$\begin{aligned}
 |\tau^{iv}\rangle = & -0.0727 |^3S_1\rangle + 0.0212 |^3S_1'\rangle - 0.0260 |^3S_1''\rangle \\
 & - 0.3022 |^3D_1\rangle + 0.9526 |^3D_1'\rangle
 \end{aligned}
 \tag{6.26}$$

$$|\eta_b\rangle = 0.9231 |^1S_0\rangle + 0.3730 |^1S_0'\rangle - 0.0932 |^1S_0''\rangle
 \tag{6.27}$$

$$|\eta_b'\rangle = 0.3788 |^1S_0\rangle + 0.8410 |^1S_0'\rangle - 0.3864 |^1S_0''\rangle
 \tag{6.28}$$

$$|\eta_b''\rangle = -0.0657 |^1S_0\rangle + 0.3920 |^1S_0'\rangle + 0.9176 |^1S_0''\rangle
 \tag{6.29}$$

$$|^1P_{1b}\rangle = 0.9722 |^1P_1\rangle + 0.2340 |^1P_1'\rangle
 \tag{6.30}$$

$$|^3P_0\rangle = 0.9999 |^3P_0\rangle + 0.0171 |^3P_0'\rangle
 \tag{6.31}$$

$$|^3P_{0b}\rangle = -0.0171 |^3P_0\rangle + 0.9999 |^3P_0'\rangle
 \tag{6.32}$$

$$|^3P_{1b}\rangle = 0.9821 |^3P_1\rangle + 0.1885 |^3P_1'\rangle
 \tag{6.33}$$

$$|^3P_{1b}'\rangle = -0.1885 |^3P_1\rangle + 0.9821 |^3P_1'\rangle
 \tag{6.34}$$

$$|^3P_{2b}\rangle = 0.9576 |^3P_2\rangle + 0.2874 |^3P_2'\rangle + 0.0194 |^3F_2\rangle
 \tag{6.35}$$

$$|^1D_{2b}\rangle = 0.9354 |^1D_1\rangle + 0.3536 |^1D_1'\rangle
 \tag{6.36}$$

$$|{}^1D_{2b}\rangle = -.3536 |{}^1D_1\rangle + .9354 |{}^1D_1'\rangle \quad (6.37)$$

$$|{}^3D_{2b}\rangle = .9390 |{}^3D_2\rangle + .3438 |{}^3D_2'\rangle \quad (6.38)$$

$$|{}^3D_{2b}\rangle = -.3438 |{}^3D_2\rangle + .9390 |{}^3D_2'\rangle \quad (6.39)$$

$$|{}^3D_{3b}\rangle = .9251 |{}^3D_3\rangle + .3797 |{}^3D_3'\rangle + .011 |{}^3G_3\rangle \quad (6.40)$$

$$|{}^3D_{3b}\rangle = -.3798 |{}^3D_3\rangle + .9247 |{}^3D_3'\rangle + .027 |{}^3G_3\rangle \quad (6.41)$$

$$|{}^3G_{3b}\rangle = .0006 |{}^3D_3\rangle - .0292 |{}^3D_3'\rangle + .9996 |{}^3G_3\rangle \quad (6.42)$$

6.6 Discussion of Results

The first phase of the research simply indicated that the Isgur-Karl model could be successfully transplanted from baryons to mesons. The % deviations obtained for the masses of η_c (0.63%) and η_c' (0.67%) were about the same as those obtained for baryons. (Kalman¹¹ obtained the masses of ground state baryons within a 0.7% deviation). The mass of the c quark obtained as 1450 MeV is about the same value as that used in Charmonium models. (For example, Kang²⁷ fixes $m_c = 1376$ MeV).

For the second phase, Table 1 of Appendix F shows that the % of seven of the Charmonium states is less than 0.03% which bears out very well that the consistent quark model can successfully be applied to mesons. The one exception is

the mass of the $^3 D_1$ state where there is a % deviation of 1.94%. But this state is just above threshold for disintegration by strong interaction pair-production into charmed mesons. So this state is not a valid test of the model since there are undoubtedly contributions to this mass from the strong decay of this state. However, the corresponding $^3 D_1$ state in the Upsilon system is below threshold for strong pair production. When this mass is experimentally obtained, it would be interesting to note whether or not the % deviation is well below 1.9%.

The second phase is also the first application in mesons of the major feature of the consistent quark model - viz. that the parameters obtained by working on one flavour of quarks can successfully be used to compute the masses of a different flavour of quarks. This feature underlines the flavour independence concept of the original DGG model on which the Isgur-Karl model and the consistent quark model are based.

Another interesting feature of the second phase results is the composition of the states in the Charmonium and Upsilon systems. In the Charmonium sector the states are essentially unmixed, but in the Upsilon sector both states contain almost equal mixtures of S and S' .

The third phase bears out that a great many states of both the Charmonium and Upsilon systems can be computed from relatively few parameters. Tables 2 and 3 show that generally there is good agreement between computed and experimental values.

The one disturbing feature of the third phase is that the parameters used for the positive parity states did not give good results for the negative parity states. Adjustments had to be made to the parameters to improve the P and P' states, after which the agreement between calculation and experiment was excellent. In this regard two points may be mentioned. Firstly, the adjustments to the parameters were relatively minor. Secondly, data on the negative parity states first became available only during the course of the research; it is difficult to assume that this initial data on the P states is firmly accepted. Subsequent experiments have occasionally been known to change earlier data. A more substantial test of the model will come when experiments within the next few years yield data to confirm or prove erroneous the vast number of predictions made in the higher energy levels of the Upsilon system. If forthcoming data does indicate that the predictions are incorrect, it would be proper to conclude that the model in its present form is limited in its accuracy to low energy levels only.

Table II Masses of the states of the ψ system in GeV

state	EXPERIMENT	CALCULATION
ψ	3.10	3.15
ψ'	3.69	3.71
ψ''	3.77	3.83
η_{c0}	2.98	2.98
η_{c1}	3.59	3.52
1P_1		3.50
3P_0	3.41	3.48
3P_1	3.51	3.52
3P_2	3.55	3.48
1D_2		3.77
3D_2		3.80
3D_3		3.71

Table III Masses of the States of T System in GeV

STATE	EXPERIMENT	CALCULATION
T	9.46	9.46
T	10.02	10.13
T''	10.35	10.23
T'''	10.58	10.61
T ^{iv}		10.83
η_b		9.32
η_b		10.10
η_b		10.56
1P_1		9.90
3P_0	9.86	9.85
3P_1	9.89	9.90
3P_2	9.91	9.91
1P_1		10.29
3P_0	10.23	10.17
3P_1	10.25	10.25
3P_2	10.27	10.33
1D_2		10.24
3D_2		10.24

Table III (continued)

STATE	EXPERIMENT	CALCULATION
³ D ₃		10.23
³ D ₂		10.88
³ D ₂		10.87
³ D ₃		10.91
¹ F ₃		10.41
³ F ₂		10.42
³ F ₃		10.42
³ F ₄		10.41
¹ G ₄		11.03
³ G ₃		11.04
³ G ₄		11.03
³ G ₅		11.01

CONCLUSION

This research has essayed to show that a specific combination of potentials does yield good results for the energy levels of mesons - viz. a harmonic oscillator potential, perturbed by an unknown anharmonic term with fine and hyperfine corrections. While it is contended that the fair accuracy of the results show that it is a good approximation of the true nature of quark binding forces in mesons as it was done earlier in baryons, it is presumptuous to say, as this point in time in the absence of sufficient experimental data, that the model has universal applicability.

This research was done in three phases. A few pertinent questions arise when a critical comparison is made between the results of the second and third phases. The later results, which include somewhat higher energy levels of the two meson systems, do not have the remarkable accuracy of the second phase: while the percentage deviation of the second phase averages less than 0.03%, that in the last phase has a mean of 0.7%, and it is in the Charmonium system that the deviations are higher. Another question relates to the use of the brute-force technique to obtain parameters. In the second phase there were 8 experimentally known values to fit to in order to obtain 7 parameters, in the third phase there were 18 available states with which to obtain 9 parameters. The hit-and-miss method of the brute-force technique becomes much more difficult to use successfully when the number of states multiplies, particularly when the higher states are sensitive to slight alterations of only 2 of

the 9 parameters. This problem was experienced during the research. But there is no mathematical tool yet devised to replace the brute-force technique in a search for parameters in a research problem of this nature.

This research has also tried to show the validity of the consistent quark model for mesons by underlining the flavour independence of the strong force. It is a significant triumph of the model if a single parameter set can be utilised to determine the energy levels of mesons of any flavour. Although in the third phase of the research slight modifications had to be made to the parameters to obtain better fits to the P-states of the Upsilon system, the results of both systems were essentially obtained from one parameter set. In this regard it should be mentioned that the very same parameters as obtained in this research were used fruitfully by D'Souza²⁸ to calculate energy levels of several mesons with mixed flavour quarks: in particular of the uc, dc, sc, ub, sb, cb and db systems. The fact that D'Souza obtained very good results for his problem further supports the validity of the parameters deduced in the present research.

Is the model good only for low-lying levels? Time will tell. When accelerators produce particles of the Upsilon system in the D, F, and G states, the accuracy of the 14 predictions made on the basis of the model will be tested. More detailed experimental data is required before one can definitely assess the applicability of the present model to compute energy levels of all mesons.

REFERENCES AND FOOTNOTES

1. W. Panofsky, In Proc. of International Symposium on High Energy Physics, Vienna (1968).
2. S. L. Glashow, J. Illiopoulos, L. Maiani, Phys. Rev. D2, 1285 (1970)
3. S. Weinberg, Phys. Rev. Lett. 19, 1264 (1967).
A. Salam Weak and Electromagnetic Interactions, Elementary Particle Theory. Edited by N. Svartholm (Almqvist, Wiksell), Stockholm (1968).
4. D. Flamm, F. Schoberl, Introduction to the Quark Model of Elementary Particles, Gordon and Breach, Science Publishers (1982).
5. Quark combinations of $q\bar{q}$ (mesons) and qqq (baryons) are not the only quark composites seen in nature. Particles which are multiples of the meson and baryon combinations such as $qqq\bar{q}$ and $qqqqqq$ also exist and are also colourless like the mesons and baryons.
6. N. Isgur and G. Karl, Phys. Lett 72B, 109 (1977); 74B, 353 (1978); Phys. Rev. D18, 4187 (1978); Phys. Rev. D19, 2653 (1979); Phys. Rev. D20, 1191 (1979).
7. A. De Rujula, H. Georgi, and S. L. Glashow, Phys. Rev. D12, 147 (1975).
8. A. J. G. Hey and R. L. Kelly, Phys. Rpt. (Section C of Phys. Lett.) 96, No. 2 and 3 (1983), 71-204, North Holland Publishing Company.

9. N. Isgur, Low Energy Hadron Physics with Chromodynamics, Lectures presented at XVI International School of Subnuclear Physics. Erice, August 1978 (unpublished).
10. C. S. Kalman and R. L. Hall, Phys. Rev. D25, 217 (1982).
11. C. S. Kalman, Phys. Rev. D26, 2326 (1982).
12. O. W. Greenberg and C. A. Nelson, Phys. Rpt. (Section C of Phys. Lett.) 32, No. 2 (1977) 69-121. North Holland Publishing Company.
13. A. J. G. Hey, P. J. Litchfield, and R. J. Cashmore, Nucl. Phys. B95 (1975); D. Faiman and D. E. Plane, ibid B50, 379 (1972).
14. N. Isgur and R. Koniuk, Phys. Rev. D21, 1868 (1980); Phys. Rev. Lett. 44, 845 (1980).
15. C. S. Kalman and R. L. Hall, and S. K. Misra, Phys. Rev. D21, 1908 (1980).
16. C. S. Kalman and R. L. Hall, Concordia University Reports CUQ/EPP 47 (1983)
17. D. Gromes and I. O. Stamatescu, Nucl. Phys. B112, 213 (1976).
18. C. S. Kalman and D. Pfeffer, Phys. Rev. D27, 1648 (1983); Phys. Rev. D28, 2324 (1983).
19. C. S. Kalman and S. K. Misra, Phys. Rev. D26, 233 (1982). (1982).
20. C. S. Kalman and S. Barbari, Phys. Rev. D28, 2321 (1983).

21. H. J. Schnitzer, Brandis University report, 1981 (unpublished).
22. H. A. Bethe and E. E. Salpeter, Quantum Mechanics of One- and Two - Electron Atoms, Academic, New York, (1959).
23. M. A. Strocio, Phys. Rpt. 22 C, 215 (1975).
24. G. Breit, Phys. Rev. 34, 553 (1929); Phys. Rev. 39, 616 (1932).
25. L. L. Foldy and S. A. Wouthuysen, Phys. Rev. 78, 29 (1950).
26. K. Berkelman, "Upsilon Spectroscopy at CESR" Lab of Nuclear Studies, Cornell University publication CLNS-83/564 (April, 1983) to be published in Phys. Repts. P. Haas et al. "Observation of Radiative Decays of the T (2S)" Lab of Nuclear Studies, Cornell University publication CLNS-83/591 (December, 1983).
27. J. S. Kang, Phys. Rev. D20, 2978 (1979).
28. I. D'Souza, "Unequal Mass Quarkonium Spectra in a Consistent Quark Model with Fine and Hyperfine Interactions", (Master of Science thesis) Physics Department, Concordia University, 1984.

APPENDIX A

Sample Calculation of a U-Term Matrix Element.

$$\langle S'' | U(r) | S'' \rangle$$

$$\psi_{400} = \sqrt{\frac{8}{15}} \left(\frac{4\beta^3}{\sqrt{\pi}} \right)^{1/2} \left(\frac{15}{8} - \frac{5}{2} \beta^2 r^2 + \frac{\beta^4 r^4}{2} \right) \exp(-\frac{1}{2} \beta^2 r^2) Y_0^0 \quad (\text{A.1})$$

where $Y_0^0 = (1/4\pi)^{1/2}$

$$\langle \psi_{400} | U(r) | \psi_{400} \rangle = \frac{1}{4\pi} \frac{8}{15} \frac{4\beta^3}{\sqrt{\pi}} \int_0^\infty \left(\frac{15}{8} - \frac{5}{2} \beta^2 r^2 + \frac{\beta^4 r^4}{2} \right) U(r) \exp(-\beta^2 r^2) dr$$

$$= \frac{8}{15} \frac{\beta^3}{\pi^{3/2}} \int_0^\infty \left(\frac{225}{64} - \frac{75}{8} \beta^2 r^2 + \frac{65}{8} \beta^4 r^4 - \frac{5}{2} \beta^6 r^6 + \frac{\beta^8 r^8}{4} \right) U(r) \exp(-\beta^2 r^2) dr$$

$$\begin{aligned} &= \frac{15}{8} \frac{\beta^3}{\pi^{3/2}} \int_0^\infty U(r) \exp(-\beta^2 r^2) dr \\ &\quad - \frac{5\beta}{\pi^{3/2}} \int_0^\infty U(r) \exp(-\beta^2 r^2) r^2 dr \\ &\quad + \frac{13}{3} \frac{\beta^7}{\pi^{3/2}} \int_0^\infty U(r) \exp(-\beta^2 r^2) r^4 dr \\ &\quad - \frac{4}{3} \frac{\beta^9}{\pi^{3/2}} \int_0^\infty U(r) \exp(-\beta^2 r^2) r^6 dr \\ &\quad + \frac{2}{15} \frac{\beta^{11}}{\pi^{3/2}} \int_0^\infty U(r) \exp(-\beta^2 r^2) r^8 dr \end{aligned} \quad (\text{A.2})$$

Using equations (4.22) to (4.26) and putting $t=1$, we get

$$\begin{aligned} \langle \psi_{400} | U(x) | \psi_{400} \rangle &= \frac{15}{8} a(1) - 5b(1) + \frac{13}{3} c(1) - \frac{4}{3} d(1) \\ &+ \frac{2}{15} e(1) \end{aligned} \quad (\text{A.3})$$

APPENDIX B

Sample Calculation of a Contact Term.

From equation (5.1),

$$H_{\text{hyp}}^{\text{con}} = \frac{4\alpha_s}{3m_Q^2} \left\{ \frac{8\pi}{3} \vec{s}_1 \cdot \vec{s}_2 \delta^3(r) \right\}$$

$$\psi_{400} = \sqrt{\frac{8}{15}} \left(\frac{4\beta^3}{\sqrt{\pi}} \right)^{1/2} \left(\frac{15}{8} - \frac{5}{2}\beta^2 r^2 + \frac{\beta^4 r^4}{2} \right) \exp(-\frac{1}{2}\beta^2 r^2) Y_0^0 \quad (\text{B.1})$$

where

$$Y_0^0 = (1/4\pi)^{1/2}$$

$$\langle S'' | H_{\text{cont}} | S'' \rangle = \frac{4\alpha_s}{3m_Q^2} \frac{8\pi}{3} \frac{1}{4\pi} \int_0^\infty \psi^* \delta^3(r_{12}) \psi dr (\vec{s}_1 \cdot \vec{s}_2) \quad (\text{B.2})$$

Only the first term of ψ_{400} contributes to the contact term.

$$\begin{aligned} \langle S'' | H_{\text{cont}} | S'' \rangle &= \frac{4\alpha_s}{3m_Q^2} \frac{8\pi}{3} \frac{1}{4\pi} \frac{8}{15} \frac{4\beta^3}{\sqrt{\pi}} \cdot \frac{225}{64} (\vec{s}_1 \cdot \vec{s}_2) \\ &= 5\sqrt{2} \left(\frac{4\alpha_s \beta^3}{3\sqrt{2}\pi m_Q^2} \right) \vec{s}_1 \cdot \vec{s}_2 \quad (\text{B.3}) \end{aligned}$$

Using the value of δ_Q from equation (5.2) we have

$$\langle S'' | H_{\text{cont}} | S'' \rangle = 5\sqrt{2} \delta_Q \vec{s}_1 \cdot \vec{s}_2 \quad (\text{B.4})$$

APPENDIX C

Sample Calculation of a Tensor Term. $\langle {}^3D_2 | H_{\text{tens}} | {}^3D_2 \rangle$

From equation (5.12)

$$H_{\text{hyp}}^{\text{tens}} = \frac{4\alpha_s}{3m_Q^2 r^3} \left\{ \frac{3(\vec{S}_1 \cdot \vec{r})(\vec{S}_2 \cdot \vec{r})}{r^2} - \vec{S}_1 \cdot \vec{S}_2 \right\}$$

From equation (4.18)

$$\psi_{42m} = 4\sqrt{\frac{2}{105}} \frac{\beta^{7/2}}{\pi^{1/4}} r^2 \left(\frac{7}{2} - \beta^2 r^2 \right) \exp(-\frac{1}{2}\beta^2 r^2) Y_{2m}(\theta, \phi)$$

From equation (4.14)

$$\psi_{22m} = \frac{4}{\sqrt{15}} \frac{\beta^{7/2}}{\pi^{1/4}} r^2 \exp(-\frac{1}{2}\beta^2 r^2) Y_{2m}(\theta, \phi)$$

Inserting the values of the spherical harmonics

$$\begin{aligned} \psi_{421} &= \sqrt{\frac{8}{105}} \left(\frac{4\beta^3}{\sqrt{\pi}} \right)^{1/2} \beta^2 r^2 \left(\frac{7}{2} - \beta^2 r^2 \right) \exp(-\frac{1}{2}\beta^2 r^2) \\ &\quad \times \left[-\frac{1}{2} \frac{15}{2\pi} \frac{1}{2} \sin\theta \cos\theta e^{i\phi} \right] \end{aligned} \quad (\text{C.1})$$

$$\begin{aligned} \psi_{421}^* &= \sqrt{\frac{8}{105}} \left(\frac{4\beta^3}{\sqrt{\pi}} \right)^{1/2} \beta^2 r^2 \left(\frac{7}{2} - \beta^2 r^2 \right) \exp(-\frac{1}{2}\beta^2 r^2) \\ &\quad \times \left[-\frac{1}{2} \frac{15}{2\pi} \frac{1}{2} \sin\theta \cos\theta e^{-i\phi} \right] \end{aligned} \quad (\text{C.2})$$

$$\begin{aligned} \psi_{22-1} &= \sqrt{\frac{4}{15}} \left(\frac{4\beta^3}{\sqrt{\pi}} \right)^{\frac{1}{2}} \beta^2 r^2 \exp(-\frac{1}{2}\beta^2 r^2) \\ &\times \left[\frac{1}{2} \frac{15}{2\pi} \frac{1}{2} \sin\theta \cos\theta e^{-i\phi} \right] \end{aligned} \quad (C.3)$$

We use the identity

$$\begin{aligned} &\langle LSJ | r^{-3} \{ (3\vec{S}_1 \cdot \hat{r})(\vec{S}_2 \cdot \hat{r}) - \vec{S}_1 \cdot \vec{S}_2 \} | L' S' J \rangle \\ &= (-)^{(J-L-S')} [(2L+1)(2S+1)]^{\frac{1}{2}} W(LL'SS'; 2J) \\ &\times \langle L || \frac{\sqrt{3}}{2r^3} \hat{r}_+ \hat{r}_+ || L' \rangle \langle S || \frac{\sqrt{3}}{2} S_{1-} S_{2-} || S' \rangle \end{aligned} \quad (C.4)$$

$$\begin{aligned} \langle \psi_{421} | \frac{\sqrt{3}}{2r^3} \hat{r}_+ \hat{r}_+ | \psi_{22-1} \rangle &= \frac{4}{\sqrt{15}} \sqrt{\frac{2}{7}} \left(\frac{4\beta^3}{\sqrt{\pi}} \right) \left(\frac{\sqrt{3}}{2} \right) \left(-\frac{1}{4} \right) \left(\frac{15}{2\pi} \right) \\ &\times \int_0^\infty \int_0^{2\pi} \int_0^\pi \frac{\beta^4 r^4}{r^3} \left(\frac{7}{2} - \beta^2 r^2 \right) \exp(-\beta^2 r^2) \sin^2 \theta \\ &\times \cos^2 \theta e^{-2i\phi} \sin^2 \theta e^{2i\phi} r^2 \sin \theta dr d\phi d\theta \end{aligned} \quad (C.5)$$

where we have noted that

$$\hat{r}_+ \hat{r}_+ = \sin^2 \theta e^{2i\phi} \quad (C.6)$$

$$\begin{aligned} \langle \psi_{421} | \frac{\sqrt{3}}{2r^3} \hat{r}_+ \hat{r}_+ | \psi_{22-1} \rangle &= -\sqrt{\frac{6}{7}} \frac{\beta^3}{\pi^{\frac{3}{2}}} \int_0^\infty \int_0^{2\pi} \int_0^\pi \beta^4 r^3 \\ &\times \left(\frac{7}{2} - \beta^2 r^2 \right) \sin^5 \theta \cos^2 \theta \exp(-\beta^2 r^2) dr d\phi d\theta \end{aligned} \quad (C.7)$$

The θ integration is

$$\int_0^\pi \sin^5 \theta \cos^2 \theta \, d\theta = \frac{16}{105} \quad (\text{C.8})$$

The ϕ integration yields 2π . (C.9)

The r integration is

$$\begin{aligned} & \int_0^\infty \frac{7}{2} \beta^4 r^3 \exp(-\beta^2 r^2) \, dr - \int_0^\infty \beta^6 r^5 \exp(-\beta^2 r^2) \, dr \\ &= \frac{7}{2} \beta^4 \left[\frac{\Gamma(2)}{2\beta^4} \right] - \beta^6 \left[\frac{\Gamma(3)}{2\beta^6} \right] = \frac{7}{4} - 1 = \frac{3}{4} \end{aligned} \quad (\text{C.10})$$

The first reduced tensor is the integral divided by the Clebsch-Gordon coefficient.

$$\text{C.G. Coefficient for } \langle 2-122 | 2221 \rangle = \frac{\sqrt{3}}{\sqrt{7}} \quad (\text{C.11})$$

First reduced tensor

$$\begin{aligned} &= -\frac{\sqrt{6}}{\sqrt{7}} \frac{\beta^3}{\pi^{3/2}} (2\pi) (16/105) (3/4) (\sqrt{7}/\sqrt{3}) \\ &= -\frac{8\sqrt{2}}{35} \frac{\beta^3}{\sqrt{\pi}} \end{aligned} \quad (\text{C.12})$$

For the spin term we have

$$\langle \chi_1^s | \frac{\sqrt{3}}{2} S_{1-} S_{2-} | \chi_{-1}^s \rangle = \frac{\sqrt{3}}{2} \quad (\text{C.13})$$

The C.G. Coefficient $\langle 1-122 | 1211 \rangle = \frac{3}{5}$
 The second reduced tensor is $\frac{\sqrt{3}}{2} \times \frac{\sqrt{5}}{\sqrt{3}} = \frac{\sqrt{5}}{2}$ (C.14)

$$[(2L + 1)(2S + 1)]^{\frac{1}{2}} = \sqrt{15} \quad (\text{C.15})$$

For $J = 2$, $(-1)^{(J-L-S)} = -1$ (C.16)

The Racah Coefficient $W(2211;22) = \frac{1}{10} \sqrt{\frac{7}{3}}$ (C.17)

The tensor term is

$$\begin{aligned} \langle {}^3D_2 | H_{\text{tens}} | {}^3D_2 \rangle &= \frac{4\alpha_S}{3m_Q} \left(\frac{-8\sqrt{2}}{35}, \frac{\beta^3}{\sqrt{\pi}} \right) (\sqrt{15}) (-1) \left(\frac{1}{10} \sqrt{\frac{7}{3}} \right) \\ &= \frac{4}{5\sqrt{7}} \left(\frac{4\alpha_S \beta^3}{3\sqrt{2\pi} m_Q^2} \right) \end{aligned} \quad (\text{C.18})$$

Using the value of δ_Q given in equation (5.2), we obtain

$$\langle {}^3D_2 | H_{\text{tens}} | {}^3D_2 \rangle = \frac{4}{5\sqrt{7}} \delta_Q \quad (\text{C.19})$$

APPENDIX D

Sample Calculation of a Spin-Orbit Term. $\langle {}^3F_2 | H_{SO} | {}^3F_2 \rangle$

From equation (5.54) we have

$$H_{SO} = \left\{ \frac{2\alpha_s}{m_Q^2 r^3} - \frac{2K}{m_Q^2} \right\} \hat{L} \cdot \hat{S}$$

From equation (4.16)

$$\psi_{33m} = 4 \sqrt{\frac{2}{105}} \frac{\beta^{9/2}}{\pi^{1/4}} r \exp(-\frac{1}{2}\beta^2 r^2) Y_{3m}(\theta, \phi)$$

$$\langle \psi_{33} | \frac{2\alpha_s}{m_Q^2 r^3} - \frac{2K}{m_Q^2} | \psi_{33} \rangle = \frac{8}{105} \frac{4\beta^3}{\sqrt{\pi}} \cdot \frac{2}{m_Q^2}$$

$$\times \left[\alpha_s \int_0^\infty \frac{\beta^6 r^6}{r^3} \exp(-\beta^2 r^2) r^2 dr - K \int_0^\infty \beta^6 r^6 \exp(-\beta^2 r^2) r^2 dr \right] \quad (D.1)$$

The first integral is

$$\alpha_s \beta^6 \int_0^\infty r^5 \exp(-\beta^2 r^2) dr = \alpha_s \beta^6 \left[\frac{\Gamma(3)}{2\beta^6} \right] = \alpha_s \quad (D.2)$$

The second integral is

$$K\beta^6 \int_0^\infty r^8 \exp(-\beta^2 r^2) dr = K\beta^6 \left[\frac{\Gamma(9/2)}{2\beta^9} \right] = \frac{K}{2\beta^3} \left(\frac{105\sqrt{\pi}}{16} \right) \quad (D.3)$$

$$\begin{aligned}
\langle \psi_{33} | \frac{2\alpha_s}{m_Q^2 r^3} - \frac{2K}{m_Q^2} | \psi_{33} \rangle &= \frac{4\beta^3}{m_Q^2 \sqrt{\pi}} \left(\frac{16}{105} \right) \left\{ \alpha_s - \left(\frac{105}{16} \right) \left(\frac{K\sqrt{\pi}}{2\beta^3} \right) \right\} \\
&= \frac{16\sqrt{2}}{35} \left(\frac{4\alpha_s \beta^3}{3\sqrt{2\pi} m_Q^2} \right) \left\{ 1 - \frac{35}{8\sqrt{2}} \frac{K}{m_Q^2} \left(\frac{3\sqrt{2\pi} m_Q^2}{4\alpha_s \beta^3} \right) \right\} \quad (D.4)
\end{aligned}$$

Using the value of δ_Q from equation (5.2) we obtain

$$\langle \psi_{33} | \frac{2\alpha_s}{m_Q^2 r^3} - \frac{2K}{m_Q^2} | \psi_{33} \rangle = \frac{16\sqrt{2}}{35} \delta_Q \left[1 - \frac{35}{8\sqrt{2}} \frac{K}{m_Q^2 \delta_Q} \right] \quad (D.5)$$

For the value of $\vec{L} \cdot \vec{S}$ we note that for the state 3F_2 , $L=3, S=1, J=2$. Hence,

$$\vec{L} \cdot \vec{S} = \frac{1}{2}(J^2 - L^2 - S^2) = -4 \quad (D.6)$$

Therefore we have

$$\begin{aligned}
\langle {}^3F_2 | H_{SO} | {}^3F_2 \rangle &= -4 \left(\frac{16\sqrt{2}}{35} \right) \delta_Q \left[1 - \frac{35K}{8\sqrt{2} m_Q^2 \delta_Q} \right] \\
&= -\frac{64\sqrt{2}}{35} \delta_Q + \frac{8K}{m_Q^2} \quad (D.7)
\end{aligned}$$

We now use the value of K from equation (4.9). Finally,

$$\langle {}^3F_2 | H_{SO} | {}^3F_2 \rangle = -\frac{64\sqrt{2}}{35} \delta_Q + \frac{2\omega^2}{m_Q} \quad (D.8)$$

APPENDIX E

PHYSICAL REVIEW D

VOLUME 26, NUMBER 11

1 DECEMBER 1982

Application of the Isgur-Karl model to the low-lying S states of charmonium

C. S. Kalman and N. Mukerji

Concordia University Elementary Particle Physics Group, 1455 de Maisonneuve Boulevard West,
Montreal, Quebec, Canada H3G 1M8

(Received 4 August 1982)

The low-lying S states of the charmonium system are used as a test case for the application of the Isgur-Karl model to mesons. Fitting exactly to the ψ and ψ' masses, the masses of the η_c and η_c' are obtained within 0.7% of the experimental values. The constituent mass of the c quark is predicted to be 1450 MeV.

Recently¹ the Isgur-Karl quark shell model, which has been highly successful in the treatment of the baryons, has been used to examine baryonia. A more interesting application is to the mesons. An ideal test case is the low-lying S states of charmonium since the basic features of the model can be summarized by three parameters and there are four known states. Also, by comparison with baryon data, the mass of the c quark can be obtained.

For a system of quarks in the S state, there are no spin-orbit or tensor hyperfine interactions. The Isgur-Karl Hamiltonian for charmonium in the S state then has the form

$$H = 2m_c - (H_0 + H_{np}) \sum_i \Lambda_i \Lambda_i^* \quad (1)$$

where m_c is the mass of the c quark, and

$$H_0 = \sum_i P_i^2 / 2m_c + \left(\sum_i P_i \right)^2 / 4m_c \quad (2)$$

$$H_{np} = \frac{3\pi\alpha_s}{9m_c^2} (\vec{S}_1 \cdot \vec{S}_2) \delta^{(3)}(r) \quad (3)$$

where F is the interquark distance and \vec{S} and Λ^* ($-\Lambda^*$) are the spins and color vectors of the quark (antiquark). Finally

$$V = \left[\frac{1}{2} kr^2 + U(r) \right] \quad (4)$$

where $U(r)$ is some unknown potential which incorporates an attractive potential at short range (a Coulomb-type piece derived from quantum chromodynamics) and deviations from the harmonic-oscillator interaction at large distances. Ignoring the hyperfine interaction, the mass of the ψ and η_c and of ψ' and η_c' are identical. The notation E_0 and E_0' will be used to indicate these energies. The corresponding harmonic-oscillator wave function for ψ and η_c is

$$\psi_{1s} = \frac{\beta^{3/2}}{\pi^{3/4}} \exp\left(-\frac{1}{2}\beta^2 r^2\right) \quad (5)$$

and for ψ' and η_c' is

$$\psi_{2s} = \left(\frac{2}{3}\right)^{1/2} \frac{\beta^{7/2}}{\pi^{3/4}} \left(\frac{3}{2}\beta^2 r^2 - 1\right) \exp\left(-\frac{1}{2}\beta^2 r^2\right) \quad (6)$$

The hyperfine interaction not only splits (ψ, η_c) and (ψ', η_c') but also (ψ, ψ') and (η_c, η_c'). Evaluating this interaction using Eqs. (3), (5), and (6) for ψ and ψ' yields the mixing matrix

$$\begin{pmatrix} E_0 + \frac{2\sqrt{2}}{3}\delta_M & \frac{2}{\sqrt{3}}\delta_M \\ \frac{2}{\sqrt{3}}\delta_M & E_0' + \sqrt{2}\delta_M \end{pmatrix} \quad (7)$$

and for η_c and η_c' ,

$$\begin{pmatrix} E_0 - 2\sqrt{2}\delta_M & -2\sqrt{3}\delta_M \\ -2\sqrt{3}\delta_M & E_0' - 3\sqrt{2}\delta_M \end{pmatrix} \quad (8)$$

where

$$\delta_M = 4\alpha_s \beta^3 / 3\sqrt{2}\pi m_c^2 \quad (9)$$

There are three parameters and four known masses. Fitting exactly to the mass of the ψ (3097 MeV) and ψ' (3685 MeV) yields a best fit to the η_c (3003 MeV, % change = 0.63) and η_c' (3568 MeV, % change = 0.67). The % change is compared to the experimental values² of η_c (2984 MeV) and η_c' (3592 MeV). These correspond to $E_0 = 3077$ MeV, $E_0' = 3652$ MeV, and $\delta_M = 22.4$. The parameter β in Eqs. (5), (6), and (9) is related to the frequency of the oscillator by the equation

$$\beta^2 = \frac{1}{2} m_c \omega_c \quad (10)$$

The parameter δ_M of Eqs. (7)–(9) is related to the parameter

$$\delta = 4\alpha_s (m_c \omega)^{3/2} / 3\sqrt{2}\pi m_c^2 \quad (11)$$

used in fits to baryon data⁴ as follows

$$\delta_M = (m_c/m_q)^{1/2} (\omega_c/\omega_q)^{3/2} (\delta/2\sqrt{2}) \quad (12)$$

assuming the quark-quark interaction is flavor independent and taking into account the different color factors occurring in the meson and baryon cases

$$\omega_c = (4m_u/3m_c)\omega_u \quad (13)$$

Using the values $\omega_u = 274$ MeV, $\delta = 265$ MeV, and $m_u = 385.7$ MeV derived in fits to baryon data¹ and the value $\delta_M = 22.4$ MeV obtained above, it follows from Eqs (12) and (13) that $m_c = 1450$ MeV.

This simple problem seems to indicate that the Isgur-Karl model can be successfully transplanted from the baryons to the mesons

The mass of the c quark obtained above as 1450

MeV is about the same value as that used in charmonium models. (For example, Kang³ fixes $m_c = 1376$ MeV.) Also, the % deviations obtained above for the masses of the η_c (0.63%) and η_c' (0.67%) are at the same level as obtained in the baryons (Kalman⁴ obtains masses of the ground-state baryons within a 0.7% deviation). Full-scale applications of the model to the ψ and Υ systems are planned to see if these positive indications work out in detail.

The authors are grateful to the Natural Sciences and Engineering Research Council of Canada for partial financial support (Grant No. A0358)

¹C. S. Kalman, R. L. Hall, and S. K. Misra, Phys. Rev. D **21**, 1908 (1980); C. S. Kalman and S. K. Misra, *ibid.* **26**, 233 (1982).

²N. Isgur and G. Karl, Phys. Rev. D **20**, 1191 (1979); C. S. Kalman and R. L. Hall, *ibid.* **25**, 217 (1982).

³F. C. Porter, Stanford Linear Accelerator Center Report No. SLAC-PUB-2796, 1981 (unpublished); C. Edwards *et al.*, Phys. Rev. Lett. **48**, 70 (1982).

⁴C. S. Kalman, Phys. Rev. D **26**, 2326 (1982).

⁵J. S. Kang, Phys. Rev. D **20**, 2978 (1979).

APPENDIX F

PHYSICAL REVIEW D

VOLUME 27, NUMBER 9

1 MAY 1983

ψ and Υ systems in a consistent quark model

C S Kalman and N Mukerji

Concordia University Elementary Particle Physics Group

1455 de Maisonneuve Boulevard West Montreal, Quebec Canada H3G 1M8

(Received 22 October 1982 revised manuscript received 10 January 1983)

The η_c , η_b , P , and D states of the Υ system as well as the missing 1P_1 , 1D_1 , and 3D states of the ψ system are calculated based on a parameter system obtained from the known masses of states of the charmonium system. The results are consistent with flavor independence of the potential however, the compositions of the states are found to differ in the ψ and Υ systems.

I INTRODUCTION

The general framework for models based on quantum chromodynamics (QCD) has been described by De Rujula, Georgi, and Glashow.¹ This consists of short-range $q-q$ (or $q-\bar{q}$) forces dominated by one-gluon exchange and at large distances a scalar confining potential. Within this framework Isgur and Karl^{2,3} introduced a model based on a harmonic-oscillator-confining potential to describe the spectra and decay couplings of the ground-state and low-lying excited baryon states, here each set of levels of alternating parity has been analyzed with a different parameter set. The effects of a Coulomb-type force derived from QCD and of deviations from the harmonic-oscillator form at large distances are incorporated in an interaction term $U(r_{ij})$. Kalman and Hall⁴ and Kalman⁵ have discussed modifications of this latter term so that a uniform parameter set can be developed for all baryon calculations. Such a consistent quark model was used by Kalman, Hall, and Misra⁶ and by Kalman and Misra⁷ to examine baryoniums. A more interesting application is to mesons. Recently Kalman and Mukerji⁸ successfully applied the basic Isgur-Karl model to a study of the low-lying S states of charmonium. It is the purpose of this paper to present a full calculation of the masses of all of the low-lying states of the ψ and Υ systems.

II CONSISTENT MODEL

The model employs a Hamiltonian of the form

$$H = 2m_Q - (H_0 + H_{\text{HP}} + H_{\text{SO}}) \sum_i \Lambda_i^a \Lambda_i^{a*}, \quad (2.1)$$

where m_Q is the mass of the c quark for the ψ system and of the b quark for the Υ system, also

$$H_0 = \sum_i P_i^2 / 2m_Q - V - \left| \sum_i P_i \right|^2 / 4m_Q, \quad (2.2a)$$

$$H_{\text{HP}} = \frac{4\alpha_s}{3m_Q^2} \left[\frac{8\pi}{3} (\vec{S}_1 \cdot \vec{S}_2) \delta^3(\vec{r}) + \frac{1}{r^3} \left| \frac{3(\vec{S}_1 \cdot \vec{r})(\vec{S}_2 \cdot \vec{r})}{r^2} - \vec{S}_1 \cdot \vec{S}_2 \right| \right], \quad (2.2b)$$

$$H_{\text{SO}} = H_{\text{SO}1G} + H_{\text{SO}HO}, \quad (2.2c)$$

$$H_{\text{SO}1G} = \frac{4\alpha_s}{3m_Q^2 r} (\vec{S}_1 \cdot \vec{r} \times \vec{P}_1 - \vec{S}_2 \cdot \vec{r} \times \vec{P}_2 - 2\vec{S}_1 \cdot \vec{r} \times \vec{P}_2 - 2\vec{S}_2 \cdot \vec{r} \times \vec{P}_1), \quad (2.2d)$$

$$H_{\text{SO}HO} = -\frac{2K}{m_Q^2} (\vec{S}_1 \cdot \vec{r} \times \vec{P}_1 - \vec{S}_2 \cdot \vec{r} \times \vec{P}_2), \quad (2.2e)$$

where \vec{r} is the interquark distance and \vec{P}_i , \vec{S}_i , and Λ_i^a ($= \Lambda_i^{a*}$) are the momenta, spins, and color vectors of the quark (antiquark). Finally

$$V = \left[\frac{1}{2} kr^2 - U(r) \right], \quad (2.2f)$$

where $U(r)$ is some unknown potential which incorporates an attractive potential at short range (a Coulomb-type piece derived from QCD) and deviations from the harmonic-oscillator interaction at large distances.

In applications to the baryons, the spin-orbit force is neglected from the beginning. This is based on calculations by Isgur and Karl² which indicate "that spin-orbit forces, if present at all, are at a level much reduced over naive expectations" Isgur and

Karl² suggest that this result is due in part to a cancellation between that part of the spin-orbit interaction arising from one-gluon exchange [Eq. (2.2d)] and that arising from the harmonic potential [Eq. (2.2e)]. This suggestion is considered in detail by Schnitzer.¹⁰ He notes that the sum of the two spin-orbit terms [Eq. (2.2c)] depends on $\langle r \rangle_{\text{hadron}}$. "Since $\langle r \rangle_{\text{baryons}}$ is somewhat larger than $\langle r \rangle_{\text{mesons}}$, one also understands why the coefficient of $L \cdot S$ is absent in the Isgur-Karl model of baryons, is weakly attractive for ordinary mesons, and more strongly attractive for charmonium." In view of Schnitzer's findings a spin-orbit term has been included in this consistent model for mesons although it was disregarded in the corresponding model for baryons.

The wave functions for the low-lying meson states are as follows

$$\psi_{000} = \frac{\beta^{3/2}}{\pi^{3/4}} \exp(-\frac{1}{2}\beta^2 r^2), \quad (2.3)$$

$$\psi_{11m} = (\frac{2}{\pi})^{1/2} \frac{2\beta^{5/2}}{\pi^{1/4}} r \exp(-\frac{1}{2}\beta^2 r^2) Y_{1m}(\theta, \phi), \quad (2.4)$$

$$\psi_{200} = (\frac{2}{\pi})^{1/2} \frac{\beta^{7/2}}{\pi^{3/4}} (\frac{1}{2}\beta^2 - r^2) \exp(-\frac{1}{2}\beta^2 r^2), \quad (2.5)$$

$$\psi_{22m} = \frac{4\beta^{7/2}}{\sqrt{13}\pi^{1/4}} \beta^2 r^2 \exp(-\frac{1}{2}\beta^2 r^2) Y_{2m}(\theta, \phi), \quad (2.6)$$

where

$$\beta^4 = km_Q \quad (2.7)$$

The contribution of the harmonic-oscillator potential to the energy of the state is given by

$$E_0 = (n + \frac{1}{2}) \omega_Q, \quad (2.8)$$

where

$$\omega_Q^2 = (4k)/m_Q \quad (2.9)$$

Calculations of the nonharmonic part of the potential for different values of β [Eq. (2.7)] have been discussed by Kalman, Hall, and Misra.⁷ Based on this work,¹¹ we set

$$a(t) = (\beta^2 t^{1/2}/\pi^{3/2}) \times \int d^3r U(r) \exp(-t\beta^2 r^2), \quad (2.10a)$$

$$b(t) = (\beta^4 t^{3/2}/\pi^{3/2}) \times \int d^3r U(r) r^2 \exp(-t\beta^2 r^2), \quad (2.10b)$$

$$c(t) = (\beta^2 t^{1/2}/\pi^{3/2}) \times \int d^3r U(r) r^4 \exp(-t\beta^2 r^2). \quad (2.10c)$$

For charmonium we set $t=1$ and use $a=a(1)$, $b=b(1)$, and $c=c(1)$ as three of the basic parameters needed to be set from experimental data. For the Υ system we use the quadratic approximation

$$a(t) = A + Bt + Ct^2, \quad (2.11a)$$

$$b(t) = (3A + Bt - Ct^2)/2, \quad (2.11b)$$

and

$$c(t) = (15A + 3Bt - Ct^2)/4 \quad (2.11c)$$

The values of A , B , and C are obtained from a , b , and c by setting $t=1$ in Eqs. (2.11). Thus the parameters for the Υ system are derived from those of the charmonium system. It then follows from Eqs. (2.1), (2.3)–(2.6), (2.8), and (2.10) that the total contribution to the energy, excluding mixing, hyperfine, and spin-orbit effects is then

$$E_0(S) = 2m_Q + \frac{1}{2}\omega_Q + a(t), \quad (2.12)$$

$$E_0(P) = 2m_Q + \frac{1}{2}\omega_Q + \frac{1}{2}b(t), \quad (2.13)$$

$$E_0(S') = 2m_Q + \frac{1}{2}\omega_Q + \frac{1}{2}a(t) - 2b(t) + \frac{1}{2}c(t), \quad (2.14)$$

$$E_0(D) = 2m_Q + \frac{1}{2}\omega_Q + \frac{4}{11}c(t), \quad (2.15)$$

where $t=1$ for the charmonium system and

$$t = (m_b/m_c)^{1/2} \quad (2.16)$$

for the Υ system.

In addition to mixing caused by the hyperfine interaction, the nonharmonic potential U itself has an off-diagonal contribution

$$U_0 = \langle S | U | S' \rangle = \langle S' | U | S \rangle = (\frac{1}{2})^{1/2} a(t) - (\frac{1}{2})^{1/2} b(t) \quad (2.17)$$

The quark and antiquark also interact via gluon exchange giving rise to a color-magnetic force [Eq. (2.2b)]. For the S states, there is no spin-orbit or tensor term [second term in Eq. (2.2b)]. The only contribution is the Fermi contact term [first term in Eq. (2.2b)]. This interaction not only splits (ψ, η_c) , (Υ, η_b) , (ψ', η'_c) , and (Υ', η'_b) but also $^3(\psi, \psi')$, (Υ, Υ') , and (η_b, η'_b) . Evaluating this interaction using Eqs. (2.2b), (2.3), and (2.5) for ψ, ψ' or Υ, Υ' yields the mixing matrix

$$\begin{pmatrix} E_0(S) + \frac{2^{3/2}}{3} \delta_Q & U_0 + \frac{2}{\sqrt{3}} \delta_Q \\ U_0 + \frac{2}{\sqrt{3}} \delta_Q & E_0(S') + \sqrt{2} \delta_Q \end{pmatrix} \quad (2.18)$$

where $E_0(S)$, $E_0(S')$, and U_0 are given by Eqs (2.12), (2.14), and (2.17), respectively,

$$\delta_c = 4\alpha_s \beta^2 / 3\sqrt{2} \pi m_c^2 \quad (2.19)$$

and

$$\delta_b = (m_c/m_b)^{1/4} \delta_c \quad (2.20)$$

Similarly for (η_c, η_c') and (η_b, η_b') the corresponding

mixing matrix is

$$\begin{pmatrix} E_0(S) - 2^{1/2} \delta_Q & U_0 - 2\sqrt{3} \delta_Q \\ U_0 - 2\sqrt{3} \delta_Q & E_0(S') - 3\sqrt{2} \delta_Q \end{pmatrix} \quad (2.21)$$

The P and D states, on the other hand, have no contributions from the Fermi contact term. Following Isgur and Karl,² the tensor term is easily evaluated from the identity

$$\begin{aligned} \langle LSJ | r^{-1} (\vec{S}_1 \cdot \vec{r} \vec{S}_2 \cdot \vec{r} - \vec{S}_1 \cdot \vec{S}_2) | L'S'J \rangle &= (-)^{J-L-S} [(2L+1)(2S+1)]^{1/2} W(L, L, S, S', 2J) \\ &\times \langle L \pm \frac{1}{2} | \vec{r}^{-1} \vec{r} \cdot \vec{r} | L' \rangle \langle S \pm \frac{1}{2} | \vec{S}_1 \cdot \vec{S}_2 | S' \rangle, \end{aligned} \quad (2.22)$$

where W is a Racah coefficient and the last two factors are the reduced matrix elements of the tensors whose components are displayed. Thus applying Eqs (2.2) and (2.6) to Eq (2.22) yields

$$\langle {}^1P_1 | H_{\text{tens}} | {}^1P_1 \rangle = 0, \quad (2.23)$$

$$\langle {}^1P_0 | H_{\text{tens}} | {}^1P_0 \rangle = -\frac{4\sqrt{2}}{3} \delta_Q, \quad (2.24)$$

$$\langle {}^3P_1 | H_{\text{tens}} | {}^3P_1 \rangle = \frac{2\sqrt{2}}{3} \delta_Q, \quad (2.25)$$

$$\langle {}^3P_0 | H_{\text{tens}} | {}^3P_0 \rangle = -\frac{2\sqrt{2}}{15} \delta_Q, \quad (2.26)$$

$$\langle {}^1D_2 | H_{\text{tens}} | {}^1D_2 \rangle = 0, \quad (2.27)$$

$$\langle {}^3D_1 | H_{\text{tens}} | {}^3D_1 \rangle = -\frac{4\sqrt{2}}{15} \delta_Q. \quad (2.28)$$

$$\langle LSJM | \vec{L} \cdot \vec{S} | L'SJM \rangle = \frac{1}{2} [J(J+1) - L(L+1) - S(S+1)] \delta_{JJ} \delta_{LL} \delta_{MM}, \quad (2.33)$$

the spin-orbit contribution to the P and D states calculated from Eqs (2.2b), (2.4), and (2.6) is

$$\langle {}^1P_1 | H_{\text{SO}} | {}^1P_1 \rangle = 0, \quad (2.34)$$

$$\langle {}^3P_0 | H_{\text{SO}} | {}^3P_0 \rangle = -4\sqrt{2} \delta_Q + \omega_Q^2/m_Q, \quad (2.35)$$

$$\langle {}^3P_1 | H_{\text{SO}} | {}^3P_1 \rangle = -2\sqrt{2} \delta_Q + \omega_Q^2/2m_Q, \quad (2.36)$$

$$\langle {}^3P_2 | H_{\text{SO}} | {}^3P_2 \rangle = +2\sqrt{2} \delta_Q - \omega_Q^2/2m_Q, \quad (2.37)$$

$$\langle {}^1D_2 | H_{\text{SO}} | {}^1D_2 \rangle = 0, \quad (2.38)$$

$$\langle {}^3D_1 | H_{\text{SO}} | {}^3D_1 \rangle = -\frac{12\sqrt{2}}{5} \delta_Q + 3\omega_Q^2/2m_Q. \quad (2.39)$$

$$\langle {}^3D_2 | H_{\text{SO}} | {}^3D_2 \rangle = -\frac{4\sqrt{2}}{5} \delta_Q - \omega_Q^2/2m_Q, \quad (2.40)$$

$$\langle {}^3D_3 | H_{\text{SO}} | {}^3D_3 \rangle = \frac{8\sqrt{2}}{5} \delta_Q - \omega_Q^2/m_Q, \quad (2.41)$$

III CALCULATIONS

Examination of the previous section shows that there are seven parameters to be calculated, namely, ω , a , b , c , b_c , m_c , and m_b . All but the last one can be calculated from the charmonium sector. The 1P_1 , 3D_2 , and 3D_3 states of charmonium have not yet been observed and are predicted in this paper. The 3D_1 state is just above threshold for disintegration by strong-interaction pair production into charmed

TABLE I Masses of the low-lying states of ψ and Υ systems in MeV. Input parameters are underlined.

ψ				Υ			
State	Experiment	Calculation	Deviation (%)	State	Experiment	Calculation	Deviation (%)
ψ	<u>3097</u>	3096.2	-0.027	Υ	<u>9440</u>	9441.6	0.018
ψ'	<u>3685</u>	3684.2	-0.021	Υ'	10000	9998.2	-0.018
η_c	<u>2284</u>	2984.8	0.025	η_b		9369.3	
η_c'	<u>3592</u>	3592.8	0.023	η_b'		9996.8	
1P_1		3520.8		1P_1		10178.9	
3P_0	<u>3414</u>	3413.1	-0.026	3P_0		10130.6	
3P_1	<u>3507</u>	3507.7	0.021	3P_1		10169.5	
3P_2	<u>3551</u>	3550.1	-0.024	3P_2		10194.1	
1D_2		3838.2		1D_2		10298.2	
3D_1	<u>3768</u>	3840.9	1.94	3D_1		10285.1	
3D_2		<u>3849.5</u>		3D_2		10277.7	
3D_3		3829.3		3D_3		10304.1	

mesons. The mass of this state is presumably affected by this decay and is thus not suitable for fitting to the parameters. This leaves ψ (3S_1), ψ' (3S_1), η_c (1S_0), η_c' (1S_0), $\chi(3415)$ (3P_0), $\chi(3510)$ (3P_1), $\chi(3550)$ (3P_2). From Eqs. (2.22) and (2.33), it is clear that once two of the P states are fit to the parameters, the value of the third state is obtained in a model-independent manner. The values $\omega = 390.5$ MeV, $a = -3004.9$ MeV, $b = -4430.3$ MeV, $c = -11349.9$ MeV, $\delta = 21.63$ MeV, and $m_c = 2749.0$ MeV were obtained by brute-force substitution until the masses of ψ , ψ' , η_c , η_c' , $\chi(3415)$, and $\chi(3510)$ corresponded to the experimental values within approximately 0.02% error (< 1 MeV). The corresponding predicted values of the masses of the 1P_1 , 3D_1 , 3D_2 , and 3D_3 states are found in Table I. Note that the mass of $\psi(3770)$ (3D_1) differs from the experimental value by 1.9%. As noted earlier, this is not a test of the model since there are undoubtedly contributions to this mass from the strong decay of this state. The value of m_b is obtained by fitting to Υ (3S_1). For display purposes it was decided to use the value $m_b = 6188.6$ MeV which equalizes the error between Υ (3S_1) and Υ' (3S_1). With this single parameter and those already obtained for the charmonium system, the masses of the entire Υ spectrum up to $n=2$ are obtained. The results are given in Table I. Finally, for all states mixed by the nonharmonic U term and/or the hyperfine interaction, the composition of the states after mixing is as follows:

$$|\psi\rangle = 0.9974 |^3S_1\rangle - 0.0639 |^3S_1'\rangle + 0.0275 |^3D_1\rangle, \quad (3.1)$$

$$|\psi'\rangle = 0.0649 |^3S_1\rangle + 0.9966 |^3S_1'\rangle + 0.0508 |^3D_1\rangle, \quad (3.2)$$

$$|\eta_c\rangle = 0.9725 |^1S_0\rangle - 0.2330 |^1S_0'\rangle, \quad (3.3)$$

$$|\eta_c'\rangle = 0.2330 |^1S_0\rangle + 0.9725 |^1S_0'\rangle, \quad (3.4)$$

$$|\Upsilon\rangle = 0.7413 |^3S_1\rangle - 0.6711 |^3S_1'\rangle + 0.0142 |^3D_1\rangle, \quad (3.5)$$

$$|\Upsilon'\rangle = 0.6712 |^3S_1\rangle + 0.7413 |^3S_1'\rangle - 0.0016 |^3D_1\rangle, \quad (3.6)$$

$$|\eta_b\rangle = 0.7294 |^1S_0\rangle - 0.6840 |^1S_0'\rangle, \quad (3.7)$$

$$|\eta_b'\rangle = 0.6840 |^1S_0\rangle + 0.7294 |^1S_0'\rangle, \quad (3.8)$$

IV DISCUSSION OF THE RESULTS

Two interesting features emerge from the results. First of all, the values of the masses of the Υ and Υ' states are obtained using the potential derived from the charmonium spectrum. The only parameter used is the mass of the b quark. Thus the results are consistent with flavor independence of the potential. Second, the composition of the states as given in Eqs. (3.1)–(3.8) is very different in the charmonium and Υ systems. In the charmonium system the states are essentially unmixed, but in the Υ system both states contain almost equal mixtures of S and S' . In both systems there is very little admixture of D states. Since the 3D_1 state in the Υ system is below threshold for strong pair production of

charmed-mesons, a determination of the experimental values of the mass of this state would test the hypothesis that the roughly 2% deviation from the known mass of the corresponding charmonium state is indeed due to its decay properties.

ACKNOWLEDGMENT

The authors are grateful to the Natural Sciences and Engineering Research Council of Canada for partial financial support (Grant No. A0358).

¹A. De Rújula, H. Georgi, and S. L. Glashow, Phys. Rev. D **12**, 147 (1975).

²N. Isgur and G. Karl, Phys. Lett. **72B**, 109 (1977); **74B**, 353 (1978); Phys. Rev. D **16**, 4187 (1978).

³N. Isgur and G. Karl, Phys. Rev. D **19**, 2653 (1979).

⁴N. Isgur and G. Karl, Phys. Rev. D **21**, 3175 (1980).

⁵C. S. Kalman and R. L. Hall, Phys. Rev. D **25**, 217 (1982).

⁶C. S. Kalman, Phys. Rev. D **26**, 2326 (1982).

⁷C. S. Kalman, R. L. Hall, and S. K. Misra, Phys. Rev. D **21**, 1908 (1980).

⁸C. S. Kalman and S. K. Misra, Phys. Rev. D **26**, 233 (1982).

⁹C. S. Kalman and N. Mukerji, Phys. Rev. D **26**, 3264 (1982).

¹⁰H. J. Schnitzer, Brandeis University report, 1981 (unpublished).

¹¹The notation is somewhat different here than in Ref. 7.

APPENDIX G

Formulation of spin-related expressions.

In QED the field states are given by

$$F^{\mu\nu} = \partial^\mu A^\nu - \partial^\nu A^\mu \quad (G.1)$$

where $F^{\mu\nu}$ is the single field strength which replaces the electric (\vec{E}) and magnetic (\vec{B}) fields of ordinary non-relativistic electro-dynamics; where A^μ, A^ν are electromagnetic 4-vector potentials; and

$$\partial^\mu = \frac{\partial}{\partial x^\mu}$$

In QCD we correspondingly define the field strength

$$G_k^{\mu\nu} = \partial^\mu A_k^\nu - \partial^\nu A_k^\mu + \alpha_s f_{klm} A_l^\mu A_m^\nu \quad (G.2)$$

which comes from the non-Abelian gauge field theory, where α_s is the strong interaction coupling constant, f_{klm} are the SU(3) structure constants, similar to the SU(2) structure constants ϵ_{ijk} ; and where the new index k refers to the eight coloured gluons of QCD in place of the single colourless photon of QED.

There are 8 conserved colour-charges in QCD:

$$F_k^C = \int^\infty d^3x \left\{ j_k^0(x) + f_{klm} G_l^{0\nu} A_m^\nu \right\} \quad (G.3)$$

where the first term in the integrand is the current density due to the quark charge and the second term is the charge contribution of the gluon; where the F_k^C matrices obey the commutation relation

$$[F_i^C, F_j^C] = i f_{ijk} F_k^C \quad (G.4)$$

and where F_k^C is related to the 8 Gell-Mann SU(3) matrices λ_k

$$F_k^C = \frac{1}{2} \lambda_k \quad (G.5)$$

The meson colour wave functions are

$$\begin{aligned} \psi^C &= \frac{1}{\sqrt{3}} \delta^{ij} | \bar{q}_i q_j \rangle \\ &= \frac{1}{\sqrt{3}} (| \bar{q}_R q_R \rangle + | \bar{q}_B q_B \rangle + | \bar{q}_G q_G \rangle) \end{aligned} \quad (G.6)$$

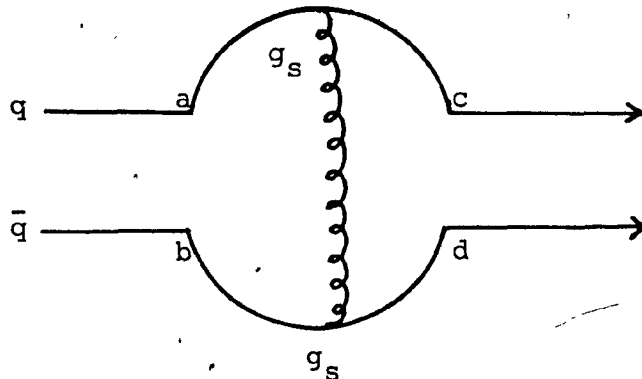


Fig. 10

Quark and Antiquark Coupling in a Meson with Gluon Transfer

When a quark and antiquark couple through a gluon g_s being emitted by one and absorbed by the other (Fig. 10) the coupling is given by

$$g^2 = \sum_{ijabcd} \frac{\delta_{ab}}{\sqrt{3}} \left(\frac{g_s \lambda_{ab}^i}{2} \right) \left(\frac{g_s \lambda_{bd}^j}{2} \right) \frac{\delta_{cd}}{\sqrt{3}}$$

$$= -\frac{4}{3} g_s^2 = -\frac{4}{3} \alpha_s \quad (\text{G.7})$$

We can now write the QCD Lagrangian density for quark-antiquark forces

$$\mathcal{L}_{\text{QCD}} = -\frac{1}{4} G_k^{\mu\nu} G_k^{\mu\nu} - \bar{q} \left[i\gamma_\mu D^\mu - m \right] q \quad (\text{G.8})$$

where $G_k^{\mu\nu}$ has been defined in (5.2), q, \bar{q} are the spin $\frac{1}{2}$ fermion fields of the quark, antiquark, the matrices γ_μ are the usual matrices of relativistic quantum mechanics. Also, D^μ is the covariant derivative

$$D^\mu = \frac{\partial}{\partial x_\mu} + i g_s \frac{\lambda_k}{2} A_k^\mu, \quad (\text{G.9})$$

and m is the mass of the quark (antiquark).

The QCD Lagrangian density is similar to the QED Lagrangian density

$$\mathcal{L}_{\text{QED}} = -\frac{1}{4} F^{\mu\nu} F^{\mu\nu} = \frac{1}{2} (\vec{E}^2 - \vec{B}^2) \quad (\text{G.10})$$

To study the bound state in a meson we can use the Bethe-Salpeter²² (B-S) equation of relativistic quantum field theory. The scattering amplitude in a quark-antiquark scattering process is given by the matrix element⁴

$$\phi_{ab}(\vec{x}_1, \vec{x}_2) = \langle 0 | T \{ q_a(\vec{x}_1), \bar{q}_b(\vec{x}_2) \} | \text{MESON} \rangle \quad (\text{G.11})$$

which is the B-S amplitude of a meson, where $q_a(\vec{x}_1)$, $\bar{q}_b(\vec{x}_2)$ are the field operators of a quark and antiquark respectively, T is the time-ordered product, $|0\rangle$ the vacuum and $|\text{MESON}\rangle$, a meson state which is a quark-antiquark bound state.

In momentum-space representation, the Fourier transform of the scattering amplitude⁴ is

$$\chi_{ab}(\vec{p}_1, \vec{p}_2) = \frac{1}{(2\pi)^4} \int d^4x_1 d^4x_2 \exp[i(\vec{p}_1 \vec{x}_1 + \vec{p}_2 \vec{x}_2)] \times \phi_{ab}(\vec{x}_1, \vec{x}_2) \quad (\text{G.12})$$

We can consider the meson as being created in a quark-antiquark scattering process. The inverse propagator for a quark and antiquark ($\not{p} \mp m_q$) is displayed in Figure 11.⁴

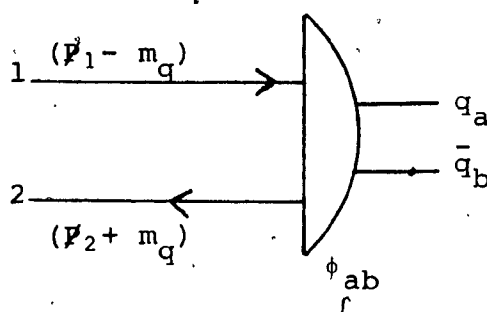


Fig. 11

Inverse Propagator of Quark-Antiquark

In Figure 11, $\mathcal{P}_1, \mathcal{P}_2$ in a time-ordered scattering process are obtained from Feynman diagrams, where $\mathcal{P}_\mu = -i\gamma_\mu P_\mu$. The scattering process can also be represented by a two quark, two antiquark scattering process as shown in Figure 12.

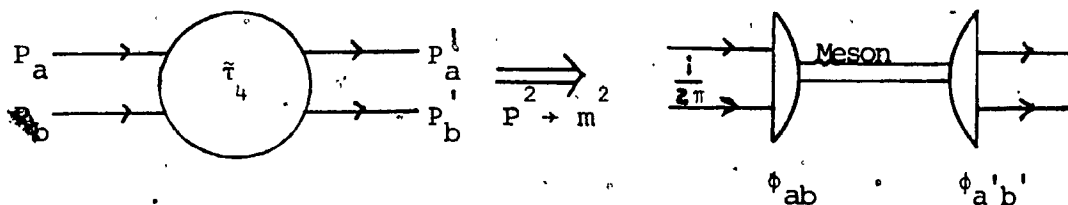


Fig. 12

Graphical Representation of B-S Scattering Amplitude in a Two-quark, Two-antiquark Scattering Process

In the diagram (Fig. 12) \tilde{g}_4 is the two quark - two antiquark Green's function. The Fourier transform of the two particle B-S kernel G_{ab} in the configuration space B-S equation can be written in the limit $P^2 \rightarrow M^2$ as $\tilde{G}_{ab}(p_1, p_2, p'_1, p'_2)$ which is also a Green's function. We then have the propagator for the meson

$$\begin{aligned}
 & (\mathcal{P}_1 - m_q) \chi_{ab}(\mathcal{P}_1, -\mathcal{P}_2) (\mathcal{P}_2 + m_q) = \\
 & \int d^4 p_1 d^4 p_2 \tilde{G}_{ab}(p_1, p_2, p'_1, p'_2) \chi_{ab}(p'_1, p'_2) \quad (G.13)
 \end{aligned}$$

If the scattering process is done with large transfer of momentum, we are in the region of asymptotic freedom which

can be approximated by one-gluon exchange. The use of the Coulomb gauge is justifiable.

If the process is considered instantaneous, the Coulomb potential for the spin-independent part of the B-S kernel has the form⁴:

$$G_{ab}^C = -i \delta(t) \gamma_0^a \gamma_0^b \frac{4\alpha_s}{3}, \quad (G.14)$$

and in this non-retardation limit the spin-dependent part of the B-S kernel has the form²³:

$$G_{ab}^{C,S} = i\delta(t) \gamma_0^a \gamma_0^b \frac{2\alpha_s}{3} \left[\vec{\alpha}^a \cdot \vec{\alpha}^b + \frac{(\vec{\alpha}^a \cdot \vec{x}_a)(\vec{\alpha}^b \cdot \vec{x}_b)}{r^2} \right] \quad (G.15)$$

where $\vec{\alpha}^a, \vec{\alpha}^b$ are the Dirac α matrices.

The objective of the formulation in this section was to obtain equation (G.15) which is the part of the B-S kernel which leads to spin-spin and spin-orbit interactions due to the colour magnetic moments of the quarks. The instantaneous or non-retardation limit is justifiable where the situation permits us to consider the scattering process non-relativistically.

In configuration space this three dimensional B-S amplitude⁴ may be written as

$$\psi_{ab}(x) = \frac{1}{(2\pi)^3} \int d^3q e^{i\vec{q} \cdot \vec{x}} \int dq_0 \chi_{ab}(E, q) \quad (G.16)$$

For heavy quarks, in the non-relativistic limit, if we neglect small components, ψ_{ab} is a solution of the Breit equation²⁴

$$H_B \psi_{ab}(\vec{x}) = E \psi_{ab}(\vec{x}) \quad (G.17)$$

where H_B is the Breit Hamiltonian²⁴

$$H_B = H_a + H_b - U(\vec{x}) \quad (G.18)$$

where H_a , H_b are the Dirac Hamiltonians for the quark and antiquark and $U(\vec{x})$ is given by⁴

$$\begin{aligned} U(\vec{x}) &= -2\pi i \int d^3k e^{-i\vec{k}\cdot\vec{x}} \gamma_0^a G_{ab}(-\vec{k}^2) \gamma_0^b \\ &= V_{SI}(r) + V_S(\vec{x}) \end{aligned} \quad (G.19)$$

where V_{SI} is the spin-independent part such as a Coulomb interaction and V_S is the spin dependent part.

The Dirac Hamiltonian is

$$H = \alpha \cdot (\vec{p} - q\vec{A}) + \beta m + q\phi \quad (G.20)$$

where m , \vec{p} and q are the rest mass, momentum and charge of a free Dirac particle, α and β are the usual four-by-four (4 x 4) Dirac matrices, \vec{A} is the vector potential of the external magnetic field and ϕ the scalar potential within which the particle is moving. In the non-relativistic

limit we may use the reduced Dirac Hamiltonian by retaining only the leading terms in a power series expansion of the Hamiltonian in powers of v/c or inverse quark masses. To obtain a power series in the inverse quark mass, we perform a Foldy-Wouthuysen²⁵ transformation.

In the Dirac equation

$$i \frac{\partial \psi}{\partial t} = H \psi \quad (G.21)$$

a unitary transformation is performed on ψ ,

$$\psi' = e^{iS} \psi \quad (G.22)$$

where the hermitian operator S is the generator of the unitary transformation. The purpose of the unitary transformation is to reduce the coefficients of the α -dependent terms in H by as high a power of $1/m$ as desired.

We now have

$$i \frac{\partial \psi'}{\partial t} = H' \psi' \quad (G.23)$$

where

$$H' = e^{iS} H e^{-iS} \quad (G.24)$$

Expanding, we obtain, for the one particle case

$$H' = H + [iS, H] + \frac{1}{2} [iS, [iS, H]] + \dots \quad (G.25)$$

where the first term of S is given by

$$S = -i\gamma^0 \vec{\alpha} \vec{q} / 2m \quad (G.26)$$

For the generalisation of this transformation to the two particle case²³, we have for the Breit Hamiltonian

$$H_B = \beta^a m_a + \beta^b m_b + V_{SI}(r) + \vec{\alpha}^a \vec{q} - \vec{\alpha}^b \vec{q} + V_S(\vec{x}) \quad (G.27)$$

and the transformed Hamiltonian is

$$\begin{aligned} H' = & \beta^a m_a + \beta^b m_b + V_{SI}(r) + \frac{\beta^a}{2m_a} (\vec{\alpha}^a \vec{q})^2 + \frac{\beta^b}{2m_b} (\vec{\alpha}^b \vec{q})^2 \\ & - \frac{\beta^a}{8m_a^3} (\vec{\alpha}^a \vec{q})^4 - \frac{\beta^b}{8m_b^3} (\vec{\alpha}^b \vec{q})^4 \\ & + \frac{1}{8m_a^2} \left[\left[\vec{\alpha}^a \vec{q}, V_{SI}(\vec{x}) \right], \vec{\alpha}^a \vec{q} \right] \\ & + \frac{1}{8m_b^2} \left[\left[\vec{\alpha}^b \vec{q}, V_{SI}(\vec{x}) \right], \vec{\alpha}^b \vec{q} \right] \\ & + \frac{\beta^a \beta^b}{4m_a m_b} \left[\left[\vec{\alpha}^a \vec{q}, V_S(r) \right]_+, \vec{\alpha}^b \vec{q} \right]_+ \\ & + \frac{\beta^a m_a - \beta^b m_b}{2(m_a^2 - m_b^2)} \left[V_S(\vec{x}) \right]^2 + \dots \end{aligned} \quad (G.28)$$

It is important to note that in (G.28) the potential has been generalised to replace the Coulomb potential given in equation (G.14). The spin-independent potential here is

$$V_{SI}(r) = V(r) + S(r) \quad (G.29)$$

where $V(r)$ is a general vector exchange potential replacing equation (G.14) and $S(r)$ is an arbitrary spin-independent scalar potential. For a one-gluon exchange we have the Coulomb potential⁴

$$V(r) = -\frac{4\alpha_s}{3r} \quad (G.30)$$

For the spin-dependent part of the B-S kernel, we obtain, in replacement of equation (G.15)

$$V_S(\vec{x}) = -\frac{1}{2} V(r) \left[\frac{\vec{a} \cdot \vec{b}}{\alpha^2} + \frac{(\vec{a} \cdot \vec{x})(\vec{b} \cdot \vec{x})}{r^2} \right] \quad (G.31)$$

In equation (G.28) if the eigenvalues of β^i are inserted, as well as the 4×4 matrices α^i , we obtain the non-relativistic expansion of the Fermi-Breit Hamiltonian⁴

$$H_{FB} = \sum_i \left(m_i + \frac{\vec{p}_i^2}{2m_i} \right) + V_{SI}(r) + H_{kin} + H_{LL} + H_D + H_{SS} + H_{LS} + H_T \quad (G.32)$$

where H_{kin} is the relativistic correction of the kinetic energy;

H_{LL} is the orbit-orbit interaction;

H_D is the Darwin term;

H_{SS} is the spin-spin hyperfine interaction;

H_{LS} is the fine structure spin-orbit term; and

H_T is the tensor term.

Our concern is with the three last terms:

$$H_{SS} = \frac{\vec{\sigma}^a \cdot \vec{\sigma}^b}{6m_a m_b} \nabla^2 V(r) \quad (G.33)$$

where $\vec{\sigma}^a$, $\vec{\sigma}^b$ are the appropriate Pauli matrices from $\vec{\sigma}^a$, $\vec{\sigma}^b$.

Equation (G.33) is the form for the spin-spin term for a vector potential. In particular, for the Coulomb case, by using Poisson's equation we have

$$\nabla^2 \left(\frac{1}{r} \right) = -4\pi \delta^3(r) \quad (G.34)$$

which is a contact interaction and gives rise to the Fermi contact term. Even for more general potentials which vanish at $r \rightarrow \infty$, this is a short range interaction. For a scalar potential the spin-spin part is zero - there is no contribution from the confinement potential to H_{SS} .

The spin-orbit term is

$$H_{LS} = \frac{1}{4r} \frac{d}{dr} (V - \frac{S}{3}) \left\{ \frac{1}{m_a^2} (\vec{\sigma}^a \cdot \vec{x} \times \vec{p}_a) - \frac{1}{m_b^2} (\vec{\sigma}^b \cdot \vec{x} \times \vec{p}_b) - \frac{2}{m_a m_b} [(\vec{\sigma}^a \cdot \vec{x} \times \vec{p}_b) - (\vec{\sigma}^b \cdot \vec{x} \times \vec{p}_a)] \right\} \quad (G.35)$$

Written in terms of $\vec{L} \cdot \vec{S}$, using $\vec{S} = (\vec{\sigma}^a + \vec{\sigma}^b)/2$, we obtain for the four vector

$$H_{LS} = \frac{3}{2m_q^2} \frac{1}{r} \frac{dV}{dr} (\vec{L} \cdot \vec{S}) \quad (G.36)$$

and for the four scalar (per quark)

$$H_{LS} = - \frac{1}{2m_q^2} \frac{1}{r} \frac{dV}{dr} (\vec{L} \cdot \vec{S}) \quad (G.37)$$

The tensor part of the hyperfine interaction is

$$H_T = \frac{1}{12 m_a m_b} S_{ab} \left\{ \frac{1}{r} \frac{dV(r)}{dr} - \frac{d^2 V(r)}{dr^2} \right\} \quad (G.38)$$

where S_{ab} is obtained from $V_S(\vec{x})$ in (G.31)

$$S_{ab} = \left\{ \frac{3 (\vec{\sigma}^a \cdot \vec{x}) (\vec{\sigma}^b \cdot \vec{x})}{r^2} - \vec{\sigma}^a \cdot \vec{\sigma}^b \right\} \quad (G.39)$$